Triggered release of liposome contents by the divalent anion $B_{12}H_{11}SH(2-)$: Biochemical studies

Dissertation
zur Erlangung des Doktorgrades der Naturwissenschaften
- Dr. rer. nat. -

vorgelegt dem Promotionsausschuss
des Fachbereichs 2 (Biologie/Chemie) der Universität Bremen

von
Doaa Elsayed Mohammed Osman Awad

Universität Bremen 2006

Tag des öffentlichen Kolloqiums

05.12.2006

Gutachter der Dissertation

1. Gutachter: Prof. Dr. Detlef Gabel

2. Gutachter: Prof. Dr. Mathias Winterhalter

Acknowledgements

My deepest gratitude goes to my supervisor Prof. Detlef Gabel for his help and support. The long discussions with him have made great impact on me.

I am grateful to Prof. Mathias Winterhalter, Prof. Manfred Radmacher and Dr. Monika Fritz for reviewing the thesis.

I wish to express my gratitude to Renate and Ulfert Alberts who took me under their wings on my arrival at Bremen.

My parents are warmly thanked. Without their support, this work would have been much harder.

It has been a great pleasure to work with the whole working group. They are all great people. I thank all of them.

List of abbreviations

APr	Acryloylpyrrolidine
B-6-14	S-(N,N-(2-dimyristoyloxyethyl)-acetamido)-thioundecahydro-closo-dodecaborate
B-6-16	S-(N,N-(2-dipalmitoyloxyethyl)-acetamido)-thioundecahydro-closo-dodecaborate
BChl	Bacteriochlorophyll
BNCT	Boron neutron capture therapy
BSH	Mercaptoundecahydrododecaborate ($Na_2B_{12}H_{11}SH$)
CPP	cell-penetrating peptide
Cryo-TEM	Cryo-transmission electron microscopy
DSC	Differential scanning calorimetry
DHC	Dihydrocholesterol
DLPC	Dilauroylphosphatidylcholine
DMPC	Dimyristoylphosphatidylcholine
DODAB	Dioctadecyldimethylammonium bromide
DOPC	Dioleoylphosphatidylcholine
DOPE	Dioleoylphosphatidylethanolamine
1,2-di-O-SPC	1,2-di-O-stearoylphosphocholine
DPPC	Dipalmitoylphosphatidylcholine
DPPE	Dipalmitoylphosphatidylethanolamine
DPP1sCho	Diplasmenylcholine
ECM	Extracellular matrix
EGF	Epidermal growth factor
FA	Folic acid
FR	Folate receptor
FRET	Fluorescence resonance energy transfer
FTL	folate-targeted liposome
GdDTPA	Gadolinium diethyltriamine penta-acetic acid
H_{II}	Inverted hexagonal phase
HA	Hyaluronic acid
HAL	Hyaluronic acid-modified liposome

ILA	Interlamellar attachment
ITC	Isothermal titration calorimetry
L_α	Lamellar phase
LCST	Lower critical solution temperature
LysoPPC	Palmitoyl-2-hydroxy-sn-glycero-3-phosphocholine
MMCA	Macromolecular contrast agent
MPPC	Monopalmitoylphosphatidylcholine
NIPAM	N-isopropylacrylamide
NTL	Nontargeted liposome
PA	Palmitic acid
PC	Phosphatidylcholine
PLA_2	Phospholipase A_2
PE	Phosphatidylethanolamine
PS	Phosphatidylserine
PEG	Poly-(ethylene glycol)
Q_{II}	Cubic phase
TAT	trans-activating transcriptional activator
TMC	Transmonolayer contact
WSA	Water soluble acridine

1. Introduction

1.1. Boron neutron capture therapy (BNCT)

BNCT was established as a radiation therapy based on the nuclear reaction between the ^{10}B nucleus and low-energy (0.025 electron volt) or thermal neutrons. At exposure to thermal neutrons, the ^{10}B nucleus was able to disintegrate into highly energetic and short-ranged alpha (^{4}He) and lithium (^{7}Li) particles with 2.79 million electron volts of energy (Taylor 1935) making them very deadly to the cell in which they were originated. The therapeutic potential of this reaction was recognized by Locher (Locher 1936).

Because of the short pathways of these heavy particles, a range of about one cell diameter (Gabel 1987), they were able to destroy tumor cells in which ^{10}B was localized without affecting the surrounding tissue.

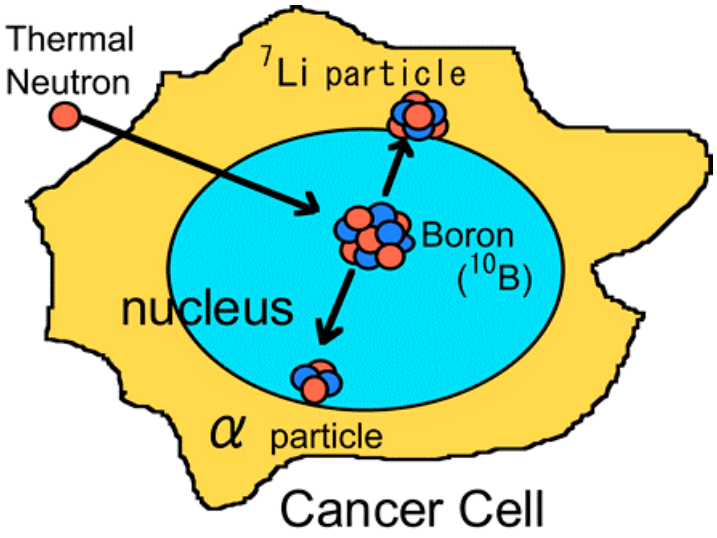

Figure 1 The BNCT cell-killing mechanism (www.osaka-med.ac.jp).

For a successful treatment, accumulation of ^{10}B in tumor to a larger extent than in the surrounding healthy tissue was necessary in order to destroy tumor cells while minimizing damage to healthy tissues (Barth 1990a 1990b, Barth 1992). Moreover, the localization of ^{10}B on a subcellular level had a great influence on the biological effectiveness of BNCT (Gabel 1987). Gabel et al. found that the Relative Local Efficiency (RLE), which indicated the effectiveness of a given intracellular boron concentration to produce cell death, in relation to a uniform distribution throughout the cell was six times higher for boron localization in the nucleus.

1.2. Mercaptoundecahydrododecaborate (BSH: $Na_2B_{12}H_{11}SH$)

A major effort was directed toward the synthesis of boron-containing compounds with greater selectivity for neoplastic cells compared with normal cells (Hawthorne 1993, Soloway 1998), but only BSH and 4-dihydroxyborylphenylalanine (BPA) represented promising boron carriers for the BNCT and are characterized by the absence of toxic side effects. As the tumor-localizing properties of BSH had been evaluated, it was found that its tumor/blood ratios ranged from 1.4 to 20. In addition, it has been established that BSH was sufficiently nontoxic (LD_{50} 73 $\pm$ 4 mg of boron per kg body weight in male CD1 Swiss mice by intraperitoneal injection) (Soloway 1967). As a result of these studies, BSH has been used by Hatanaka in BNCT (Hatanaka 1975).

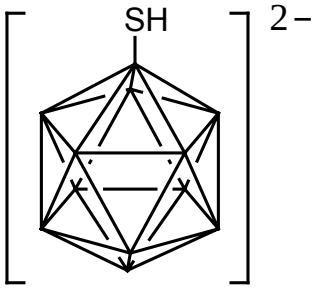

Figure 2 Mercaptoundecahydrododecaborate (BSH). Boron carrier for BNCT. Each corner represents a B-H group, except the corner connected to the mercapto group, which represents a boron atom.

1.2.1. Administration of BSH

BSH has been administered on the night before neutron irradiation. About 50 mg ^{10}B/kg body weight (BSH has a boron weight percentage of 53%) has been dissolved in distilled water to make an isotonic solution and then diluted with an equal volume of physiological saline. An infusion pump has been used for continuous intraarterial infusion. On the following morning, the patient has been transported to the reactor by ambulance (Amano 1986). It has been predicted that infusion of BSH at a rate that would deliver about 135 mg ^{10}B/kg body weight/day could result in more favorable concentrations of ^{10}B in tumor than those from the 1- to 2-hours infusions (Finkel 1989). Moreover, very slow intraperitoneal infusion of $Na_2B_{12}H_{11}SH$ or its dimer $Na_4B_{24}H_{22}S_2$ into melanoma-bearing mice yielded higher boron concentrations in the tumor than did rapid injection (Slatkin 1986).

1.2.2. Binding and distribution of BSH in tumor tissue

Amano was the first to describe the localization of BSH on a subcellular level (Amano 1986). He estimated the boron distribution in tumors from patients who had infused with BSH. He found that the boron was accumulated around and in the nuclei adjacent to the nuclear membrane.

Finkel et al. examined the postmortem distribution of ^{10}B after slow intravenous infusion of BSH into a terminally ill patient with malignant astrocytoma. In this patient, ^{10}B concentrations in the tumor were in the range of 2 to 6 µg/g after 25 hours of continuous intravenous infusion of BSH in a total dose of 13.5 mg ^{10}B/kg body weight (Finkel 1989). Accordingly, the authors concluded that patients should be infused with about tenfold more BSH than was infused in this patient since the minimum ^{10}B concentration needed in tumor to produce successful therapy was ~35 µg/g tumor (Fairchild 1985).

BSH distribution has been investigated in glioma tissue obtained from patients which had received BSH (Haselsberger 1994). Haselsberger and his coworkers could detect ^{10}B only in the nuclei but they did not exclude the possibility of accumulations below the detection limit in other cell compartments and/or in the extracellular space.

Consistent with the above-mentioned information, Neumann and his group found that BSH was strongly associated with extracellular structures, the cell membrane and the electron dense regions within the nucleus of glioblastoma multiform tissue sections of patients having received BSH prior to surgery (Neumann 2002).

BSH has also been detected in the cytoplasm and in nuclei of glioma tissue using immunohistochemistry (Otersen1997). Otersen et al. observed a strong and persistent binding of BSH to tumor tissue, whereas in healthy brain tissue all boron was excluded. The results of Otersen et al. were in a good agreement with those reported by other groups (Ceberg 1995, Stragliotto 1995).

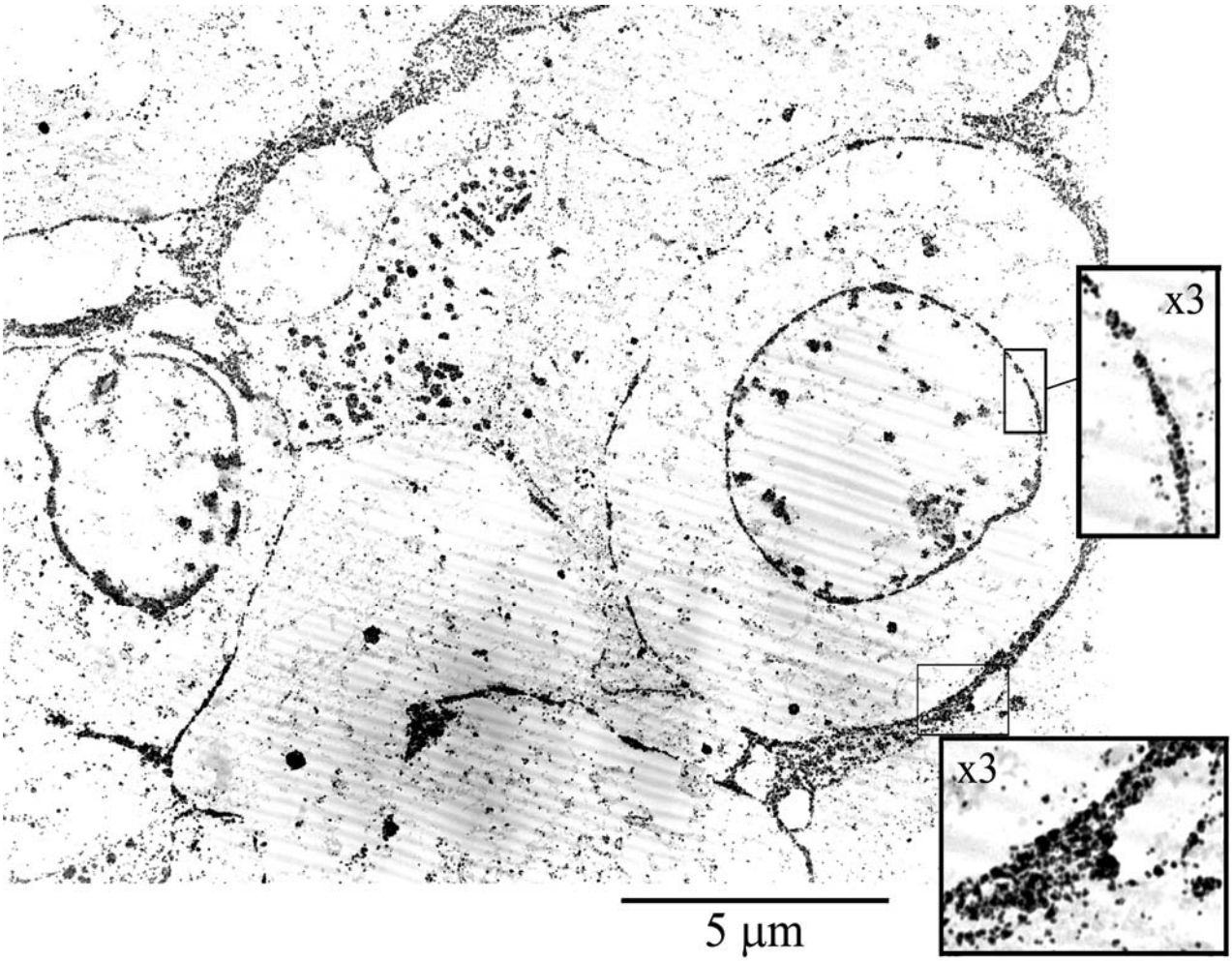

Figure 3 Electron microscopic photograph of a tissue section from BSH-infused patient. Black structures are stained for BSH. Insets are shown with a three times higher magnification. Staining of cell and nuclear membrane is prominent. Most BSH is located in intercellular space near the cell membranes (Neumann 2002).

1.2.3. Interaction of BSH with phosphatidylcholine

The strong binding of the doubly negatively charged BSH ions to the cells in human tumor tissue and its presence within cells and cell nuclei were unexpected. Kageji et al. (Kageji 1998) proposed a mechanism of boron uptake into malignant glioma cells. They suggested that BSH could pass through the disrupted blood brain barrier easily and could come into contact with tumor cells; there, BSH could bind on the extracellular surface of plasma membrane to choline residues, which were evidenced to increase abnormally in tumor tissue (Fulham 1992, Ott 1993). After binding to the plasma membrane, boron with choline residues might be internalized into the cell by endocytic pathways (Kageji 1998). The hypothesis of Kageji et al. was supported by

the investigations of Lutz et al. which showed an interaction of BSH with the choline headgroups of phosphatidylcholine (PC) (Lutz 2000).

1.2.4. Pharmacokinetics of BSH

The pharmacokinetic properties of BSH have been evaluated by several groups. Haritz and his group observed no toxic side effects when 50 mg BSH/kg body weight has been infused with a maximum speed of 1 mg BSH/min. The investigations of feces revealed a significant boron excretion through an entero-hepatic pathway, in addition to the urinary excretion (Haritz 1994).

When Gabel et al. had evaluated the pharmacokinetic features of BSH in two different populations of patients, they found no difference in the pharmacokinetic parameters for the various dosage ranges studied (12-33; 40-66; 75 mg BSH/kg). Consequently, a dose-independent (linear) disposition of BSH was assumed (Gabel 1997). It was noteworthy that following the one-hour infusion of BSH, blood levels declined in a biexponential fashion. According to the terminal half-life (approximately 72 hours), the authors advised multiple BSH administrations in order to obtain higher BSH concentrations in the tumor.

The pharmacokinetic studies of Kageji et al. revealed that BSH could move easily from blood to the peripheral organs and was retained there for a long time with slow elimination (Kageji 1997). Although BSH after intraarterial infusion moved into the peripheral organs more easily than after intravenous infusion, the authors recommended intravenous infusion since it was safer, and resulted in sufficient boron concentration in tumor. No major toxic side effects were observed with the amounts of BSH used (maximum 86 mg ^{10}B/kg). It has also been observed that boron uptake in malignant glioma was about three times higher than in low grade glioma. Tumor/blood ratio was above one in 75% and above two in 44% of the malignant glioma patients. Additionally, Kageji and his group found a good correlation between boron uptake and time interval from BSH infusion, and irradiation around 15-20 hours after BSH infusion was assumed to be optimal. More recent studies also demonstrated that neutron irradiation was optimal around 12-19 hours after the infusion had been started (Kageji 2001).

1.3. Liposomes

Liposomes (phospholipid vesicles) were first described by Bangham et al. (Bangham 1965). They have shown that aqueous suspensions of phospholipids, composed of concentric bimolecular lamellae, shared many of the dimensional, structural and functional properties of membranes. The properties of liposomes have been further described (Sessa 1968). It was confirmed that aqueous solutes were trapped in aqueous compartments between a series of lipid bilayers. Sessa and Weissmann also showed that liposomes constituted a valuable model system of biological membranes since they exhibited many of their properties such as the capability of ion discrimination, the osmotic swelling, and the response to a variety of physiologic and pharmacologic agents.

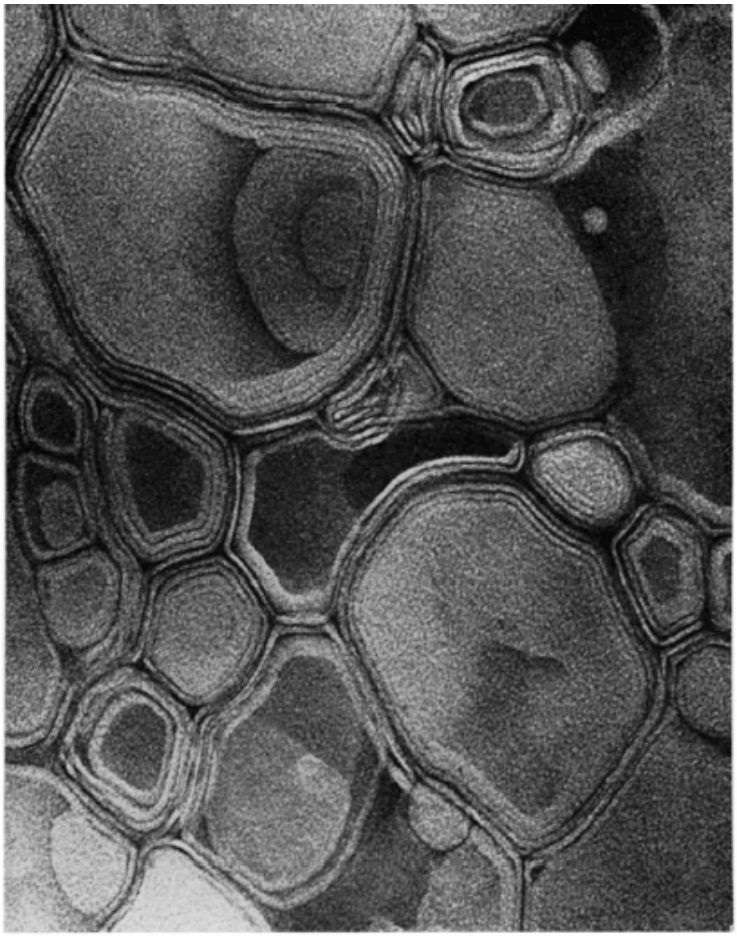

Figure 4 Electron micrograph of liposomes, showing concentric lipid bilayers separated by electron-opaque aqueous layers (Sessa 1968).

1.3.1. Phospholipids

Phospholipids are amphipathic molecules. They contain both a hydrophilic, called the polar headgroup, and a hydrophobic moiety. The overall shape of a phospholipid

such as PC is rectangular. The two fatty acid chains are approximately parallel to one another, whereas the phosphorylcholine moiety points in the opposite direction. Phospholipids, when dispersed in water, tend to protect their hydrophobic tails from contact with water. These preferences could be satisfied by formation of either a micelle or a lipid bilayer. The favored structure for most phospholipids in aqueous media is a lipid bilayer rather than a micelle. The reason is that their two fatty acyl chains are too bulky to fit into the interior of a micelle. Hydrophobic interactions are the major driving force for the formation of lipid bilayers. Furthermore, the van der Waals attractive forces between the hydrocarbon tails favor close packing of the tails. Additionally, there are electrostatic and hydrogen bonding attractions between the polar headgroups and water molecules (Stryer 1975).

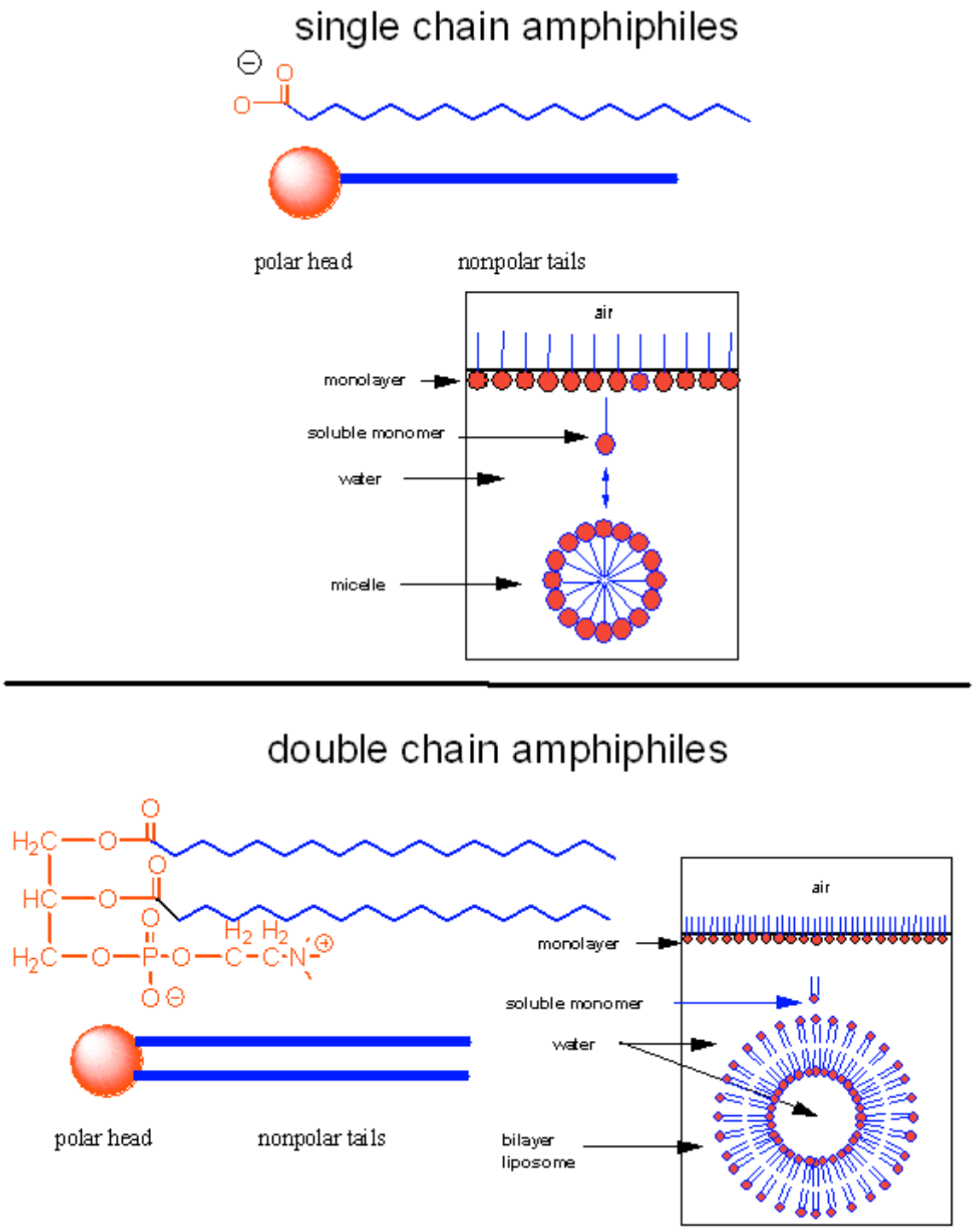

Figure 5 Structures of single and double chain amphiphiles in water, micelles and bilayers (www.employees.csbsju.edu).

1.3.2. Preparation of liposomes

The term liposome has originally been used by Bangham et al. to describe aqueous dispersions of multilamellar vesicles produced by mechanical agitation of a dry lipid

film in presence of an aqueous medium (Bangham 1965). Sessa and Weissmann have assumed during their work that multilamellar systems provided a less suitable model for some kinds of study than monolayer and bilayer systems (Sessa 1968). Since then, a large number of subclasses of liposomes has been produced (New 1990). Small unilamellar vesicles have been prepared by sonication or French press techniques, large unilamellar vesicles via dilution from organic solvents, detergent dialysis or extrusion of multilamellar vesicles.

Extrusion is a popular method of unilamellar liposomes preparation where multilamellar lipid suspension can be forced through small pores in polycarbonate filter membranes to yield particles having a diameter near the pore size of the filter used (Hope 1985). Hope and coworkers demonstrated that multiple passes were required to reduce the size and multilamellarity of extruded vesicles and that their size depended on the pore size of the membrane filters. Additionally, Mayer et al. proved that the unilamellarity and trapping efficiencies of these vesicles were significantly enhanced by freezing and thawing the multilamellar vesicles prior to extrusion and accordingly recommended them to be an appropriate system for targeting protocols (Mayer 1985, Mayer 1986).

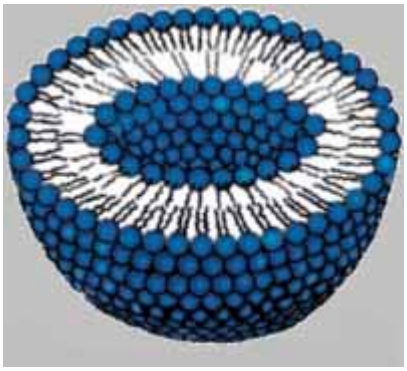

Figure 6 A schematic diagram of a conventional unilamellar liposome (www.livonlabs.com).

1.3.3. Physical properties of lipid-bilayer membranes

The use of liposomes as model systems or in drug research required insight into their physical properties (Düzgüneş 1981, Mouritsen 1998).

1.3.3.1. Geometric packing constraints in egg phosphatidylcholine vesicles

When the physical characteristics of unilamellar PC vesicles had been studied and various physical parameters had been established, an average surface area per

hydrophilic group of PC of 60 Å^{22} and a bilayer thickness of 40 Å were considered in the calculations (Huang 1969). Further investigations of Huang and Mason revealed that PC molecules of the inner and outer monolayers had different geometry, and the vesicle bilayer had an asymmetrical interface through its center (Huang 1978).

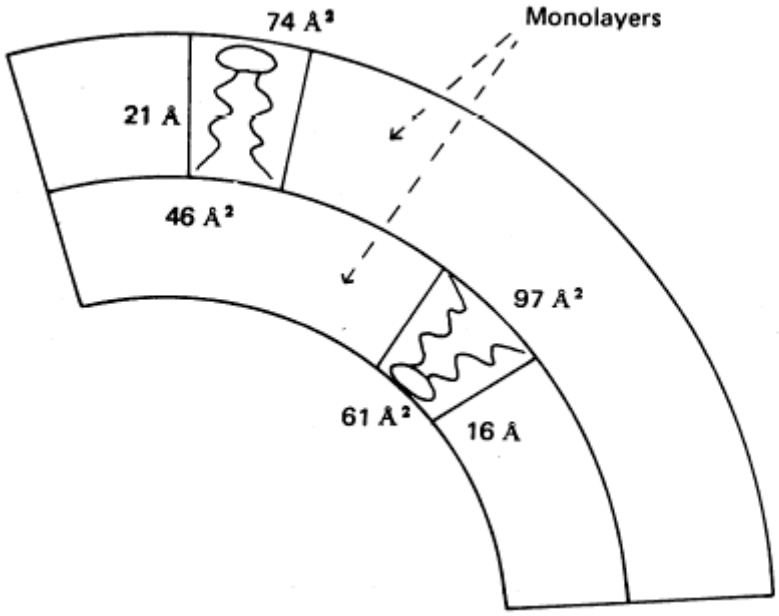

Figure 7 Vesicle bilayer cross section showing the packing geometry of lipids within the inner and outer vesicle monolayers (Huang 1978).

As shown in Figure 7, the effective surface area available to the PC's polar headgroup was greater on the outer monolayer surface than on the surface of the inner monolayer. In contrast, the effective cross-sectional area available to the PC's acyl chains was greater within the inner monolayer than within the outer monolayer. These conformational differences were caused by the higher degree of surface curvature of the inner monolayer relative to the outer monolayer in the small vesicle with a diameter of approximately 200 Å (20 nm).

1.3.3.2. Induction of fusion in phospholipid membranes

DNA-induced fusion of unilamellar cationic liposomes was investigated (Huebner 1999). Aggregation and flattening of the bilayers at the contact regions of adjacent vesicles were demonstrated. It was assumed that DNA adsorbed to the oppositely charged lipid bilayer acting as a molecular glue enforcing close apposition of neighboring vesicle membranes. The authors also observed a stack of tightly associated, alternating sheets of DNA and lipid bilayers built around a single central vesicle. Formation of such structures was explained by a mechanism that involved

rupture of an approaching vesicle followed by adsorption of its membrane to a template vesicle or a lipid-DNA complex (Huebner 1999).

When thermodynamics of cationic lipid-DNA complex formation were studied, it was observed that the heat of interaction was endothermic. The energetic driving force for DNA-liposomes association was presumed to be due to an increase in entropy resulting from release of counter ions and water (Kennedy 2000, Pozharski 2002).

Interaction of Ca^{2+} and Mg^{2+} with phosphatidylserine (PS) vesicles was found to induce aggregation, release of vesicle contents and fusion. Addition of either cation produced complexes with a stoichiometry of 1:2 cation/PS. Ca^{2+} induced formation of an anhydrous complex of closely apposed membranes with highly ordered crystalline acyl chains and a very high transition temperature (> 100°C). By contrast, Mg^{2+} led to little fusion and produced a more hydrated complex (Portis 1979).

Effect of Ca^{2+} and Mg^{2+} on membrane fusion was further investigated using mixed phospholipid vesicles (Düzgüneş 1981). The rate and extent of fusion induced by Ca^{2+} in PS/PC vesicles were lower compared to those in pure PS vesicles. Presence of 50% PC completely inhibited fusion. However, the fusogenic capacity of Mg^{2+} was abolished by the presence of 10% PC. When phosphatidylethanolamine (PE) was mixed with PS, rapid fusion could be induced by Ca^{2+}. The authors suggested that the role of phospholipids in membrane fusion was related to their ability to form dehydrated intermembrane complexes with divalent cations.

Fusion was found to be largely influenced by the hydration properties of the polar groups (Rand 1988). It was demonstrated that PS vesicles could achieve close opposition because of their low degrees of hydration, whereas PC was evidenced to be more hydrated and accordingly had more electrostatic repulsion.

Kozlov and Markin proposed that charges of the external monolayers of the contacting negatively charged PS membranes together with adsorbed Ca^{2+} ions formed a lattice of alternating opposite charges of the chess-board type (Kozlov 1984). The strong electric attraction between these molecules was responsible for the considerable increase in the transition temperature (> 100°C) as compared to that in the remaining part of the bilayer. Furthermore, it was assumed that the molecules sited in the contact region went into the crystalline state since they were in the liquid state at too high temperature. After a crystalline region had been formed, it was presumed that the events further proceeded as follows. The parts of the membranes, adjacent to the contact region were attracted due to the interaction

between the lattices of alternating charges. Due to this, the contact region became enlarged. That is, it acted as a sort of a “zipper” “clasping” the liposomes to each other. When the contact area reached approximately a fifth part of the area of the external monolayer, the external monolayers of the interacting membranes became disrupted, giving rise to a hydrophobic hole. Further evolution of this hole should result in disruption of the second monolayer of the membrane leading to efflux of the liposome contents (Kozlov 1984).

1.3.3.2.1. Stalk mechanism of membrane fusion

According to the theory developed by Kozlov et al. (Kozlov 1989), the fusion process should include the following principal steps:

1. Nucleation of a monolayer stalk connecting the outer monolayers of interacting membranes.
2. Expansion of the stalk and formation of a separating bilayer between the inner volumes of the liposomes.
3. Formation and evolution of an inverted pore in the separating bilayer leading to a complete fusion process.

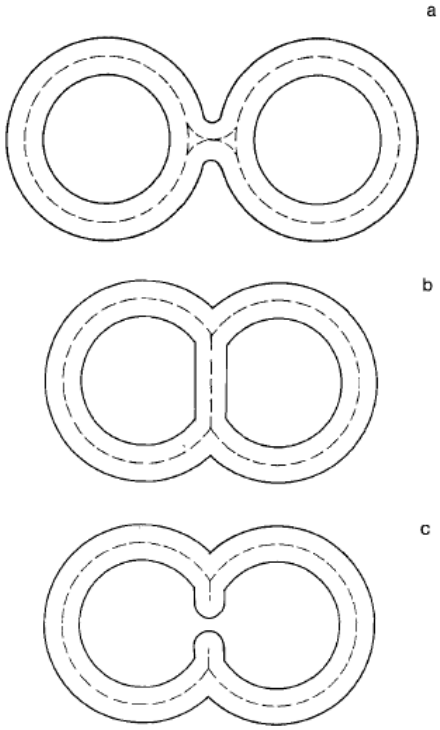

Figure 8 Stalk mechanism of membrane fusion. (a) Stalk formation, (b) Stalk expansion and contact bilayer formation, (c) formation of a pore in a separating bilayer (Kozlov 1989).

It should be mentioned that the edge of an inverted pore was formed by a lipid monolayer (Figure 9), whereas a contact between the liposomal aqueous compartment and hydrophobic lipid tails took place in the edge region of a hydrophobic pore.

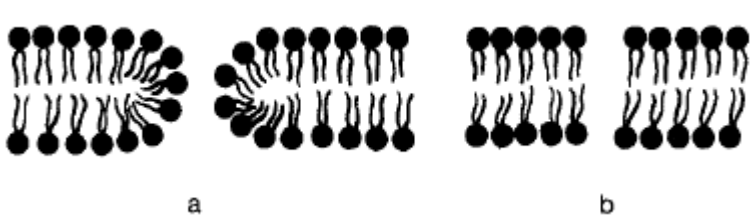

Figure 9 Molecular structure of a pore in lipid bilayer. (a) inverted pore, (b) hydrophobic pore (Kozlov 1989).

Fusion of PS liposomes in the presence of Ca^{2+} can be further explained by changes in the monolayer curvature in addition to the electrostatic effects explained above. Without Ca^{2+}, the vesicle monolayers have a positive spontaneous curvature. Addition of Ca^{2+} to the system results in neutralization of the negative charges of the outer monolayers and accordingly compensation of the electrostatic repulsion between the polar heads. As a result, the area of the monolayer in the region of polar heads tends to contract and the spontaneous curvature of the monolayer becomes negative. Because Ca^{2+} can not penetrate into PS liposomes, the inner monolayer has an opposite spontaneous curvature, a circumstance favorable for fusion.

Additionally, Ca^{2+}-induced dehydration of PS monolayers leads to a significant change in their spontaneous curvature. It is noteworthy that the change in spontaneous curvature induced by dehydration occurrs in the same direction as the change caused by electrical effects (towards negative values) (Kozlov 1989).

1.3.3.2.2. The modified stalk theory of membrane fusion and inverted phase formation

It was reported that the stalk and the transmonolayer contact (TMC) could mediate transitions between lamellar (L_α), inverted hexagonal (H_{II}) and inverted cubic (Q_{II}) phases (Siegel 1999). These predictions were supported by studies of the mechanism of these transitions (Siegel 1997). Moreover, the stalks and TMCs were demonstrated to be the lowest energy structures to form between apposed membranes.

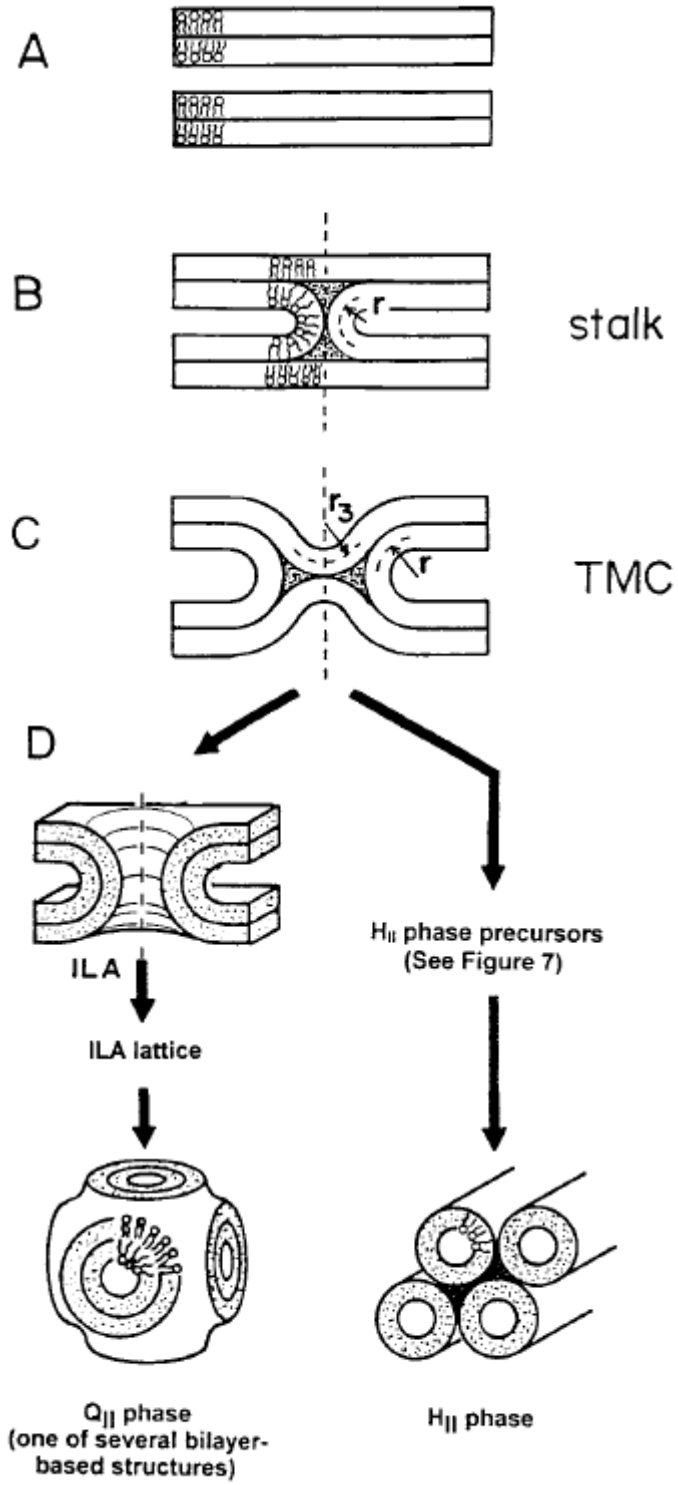

Figure 10 The modified stalk mechanism. (A) Planar L_α phase bilayer. (B) Stalk. The stalk is cylindrically symmetric around the dashed vertical axis and is formed only from lipids in the apposed monolayers. (C) trans monolayer contact (TMC) or hemifusion intermediate. (D) Left: Rupture of the diaphragm of the TMC producing a fusion pore, also termed an interlamellar attachment (ILA) (Siegel 1997).

The stalk was evidenced to be the first fusion intermediate. A TMC was then formed by radial expansion of the exterior monolayers of the stalk which pinched inward to form a single bilayer diaphragm at the center of the TMC. A TMC could reduce its energy by diaphragm rupture producing an ILA.

Accumulation of ILAs in sufficient numbers led to formation of ILA lattices which were intermediates in Q_{II} phase formation. For systems near the $L\alpha/H_{II}$ phase boundry, TMCs could assemble into H_{II} precursors as illustrated in Figure 11 (Siegel 1997).

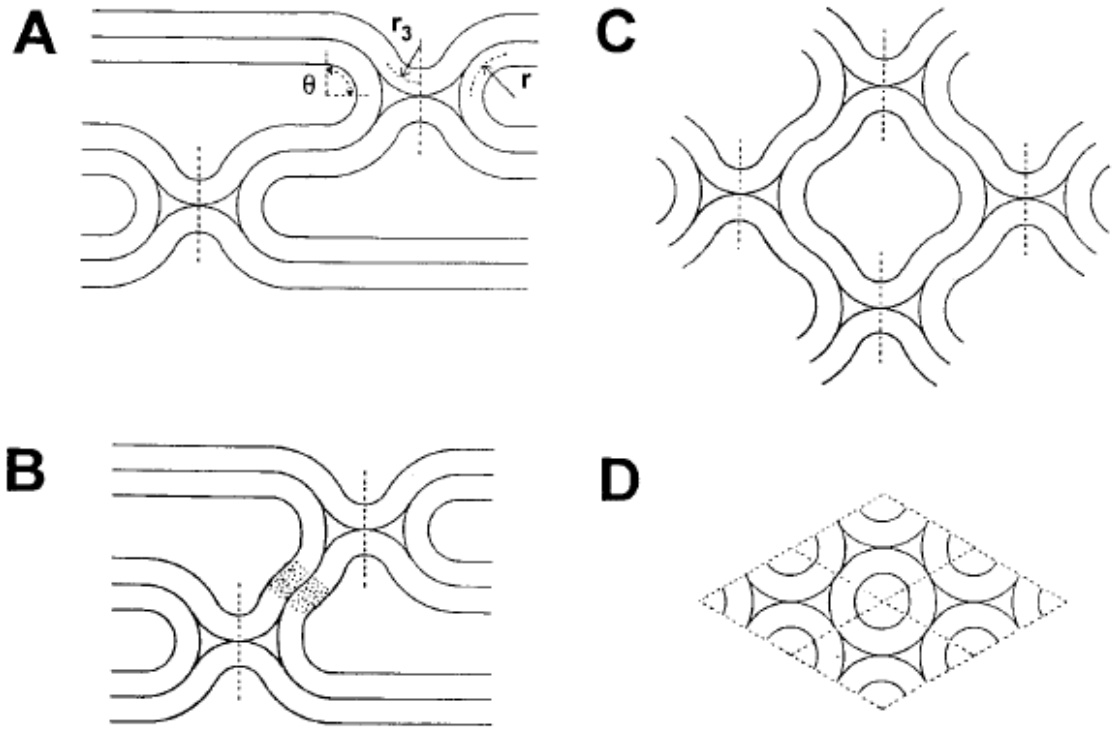

Figure 11 TMC aggregation into H_{II} phase precursors. (A) isolated TMCs within a set of apposed bilayers. r is the marginal radius, r_3 is the dimple radius of curvature and θ is the marginal angle. (B) Side-to-side aggregation of two TMCs. (C) An aggregate with body-centered cubic or primitive tetragonal symmetry. (D) Cross section of a bundle of H_{II} phase tubes (Siegel 1997).

1.3.3.3. Phase behavior of lipid bilayers

As the phase behavior of unilamellar vesicles of dilauroylphosphatidylcholine/dipalmitoylphosphatidylcholine (DLPC/DPPC) had been mapped, coexisting ordered and fluid phase domains were visualized (Korlach 1999). Furthermore, it was demonstrated that ordered phase domains were exactly

superimposed in the apposing monolayers. In addition, cholesterol was found to increase the fluid fractional area of the coexisting phase domains which was accompanied by a decrease in the diffusion coefficient in the fluid phase.

1.3.4. Liposomal drug formulations

The unilamellar liposomes exhibiting high trapping efficiencies and controlled lamellarity would appear to have significant advantages for packaging and delivering biologically active agents in vivo (Mayer 1986).

Liposomes were recommended as drug delivery systems to improve the unfavorable properties of many free drugs such as the poor solubility, rapid metabolism, instability under physiological conditions or inappropriate biodistribution (Allen 2004, Leonetti 2004).

Many of the drug delivery approaches take advantage of the unique pathophysiology of tumor vasculature. That is, the enhanced permeability of tumor blood vessels and the decreased rate of clearance caused by the lack of functional lymphatic vessels resulted in the increased accumulation of macromolecules in tumors after intravenous administration (Pathak 2005, Dreher 2006).

1.3.5. Steric stabilization of liposomes

Most lipid vesicles failed to stay in blood for more than few hours, owing to the opsonic activity of the plasma components and to the liposome removal by the cells of the mononuclear-phagocytic systems (Blume 1990).

Studies of Gabizon and Papahadjopoulos revealed that a change in liposome composition from (phosphatidylglycerol/PC/cholesterol) to (monosialoganglioside /distearoylphosphatidylcholine (DSPC)/cholesterol) showed a 25-fold increase in liposome concentration in the tumor. Concomitantly, there was a decrease by a factor of 4 of the recovered dose localizing in the liver and spleen. The most favorable results were obtained with liposomes containing a small molar fraction of a negatively charged glycolipid, such as monosialoganglioside which gave rise to a steric surface barrier. The authors proposed that tumors were accessible to liposomes due to diminished liposomal uptake by the reticuloendothelial system and explained their accumulation in tumors by an endocytic uptake or binding of liposomes by capillary endothelial cells (Gabizon 1988).

Blume and Cevc mentioned that cholesterol-containing vesicles might be unsuitable for certain applications, for example in patients with a high risk of hypercholesterimia.

Moreover, cholesterol-rich vesicles were difficult to prepare in large quantities. In addition, sugar-containing liposomes could be immunologically dangerous. Although the natural glycolipids should be non-immunogenic, but upon their incorporation into liposomes at high concentrations and in combinations not encountered in the living systems, they might become immunogenic (Blume 1990).

Blume and Cevc have presented lipidic carriers suitable for the sustained drug release in vivo. The authors recognized that the lipid charge was the main determinant of the vesicle uptake. They have also confirmed that the sterical surface-protection slowed down the adsorption of macromolecules from the blood onto vesicular surface and suppressed the elimination of the drug-carrying system from the blood by the phagocytes.

Liposomes prepared from DSPC containing 10% distearoylphosphatidylethanol-amine-conjugated poly-(ethylene glycol5000) (DSPE-PEG5000) stayed in blood and avoided liver and spleen for many hours. Resistance of DSPC/DSPE-PEG vesicles to phagocytosis was due to presence of the sterical surface-barriers on the vesicles created by the PEG residues attached to PE. This resulted in a limited accessibility of the binding sites for the blood macromolecules. Also important was the finding that the permeability of the encapsulated model-drug carboxyfluorescein (CF) from the DSPE-PEG-containing liposomes was by approximately a factor of two less than for pure DSPC liposomes (Blume 1990). The mechanism of this effect was investigated (Silvander 2000). What has been confirmed was that the PEG lipids increased the packing order both in the hydrocarbon moiety and at the water/hydrocarbon interface of liposomes.

Steric stabilization effect of DSPE-PEG was further investigated (Du 1997). Monolayers of dipalmitoylphosphatidylethanolamine (DPPE) mixed with various mole percentages of DSPE-PEG (PEG, MW 750-5000) were deposited on DPPE-coated glass surfaces. A closer simulation of PEG-liposome surfaces was a lipid monolayer on a solid support, with PEG on the water-facing surface. PEG moieties protruded from the surface, while the hydrophobic tails of these molecules were anchored into the surface monolayer. Du et al. established a relationship between covered lipid surface area by PEG and the inhibition of protein adsorption as well as cell adhesion. They found that, increasing percentages of DSPE-PEG in the supported lipid surfaces increasingly inhibited the adsorption of bovine serum albumin, laminin and

fibronectin. Increasing percentages of DSPE-PEG also inhibited the adhesion of erythrocytes, lymphocytes and macrophages to these supported lipid surfaces.

It has been also assumed that PEG attracted water to the liposomes surface, presenting a barrier to the adherence of protein opsonins. The hydrophilic barrier also retarded disintegration of the liposomes through exchange and/or transfer of liposomal phospholipids to high density lipoproteins (Allen 1998).

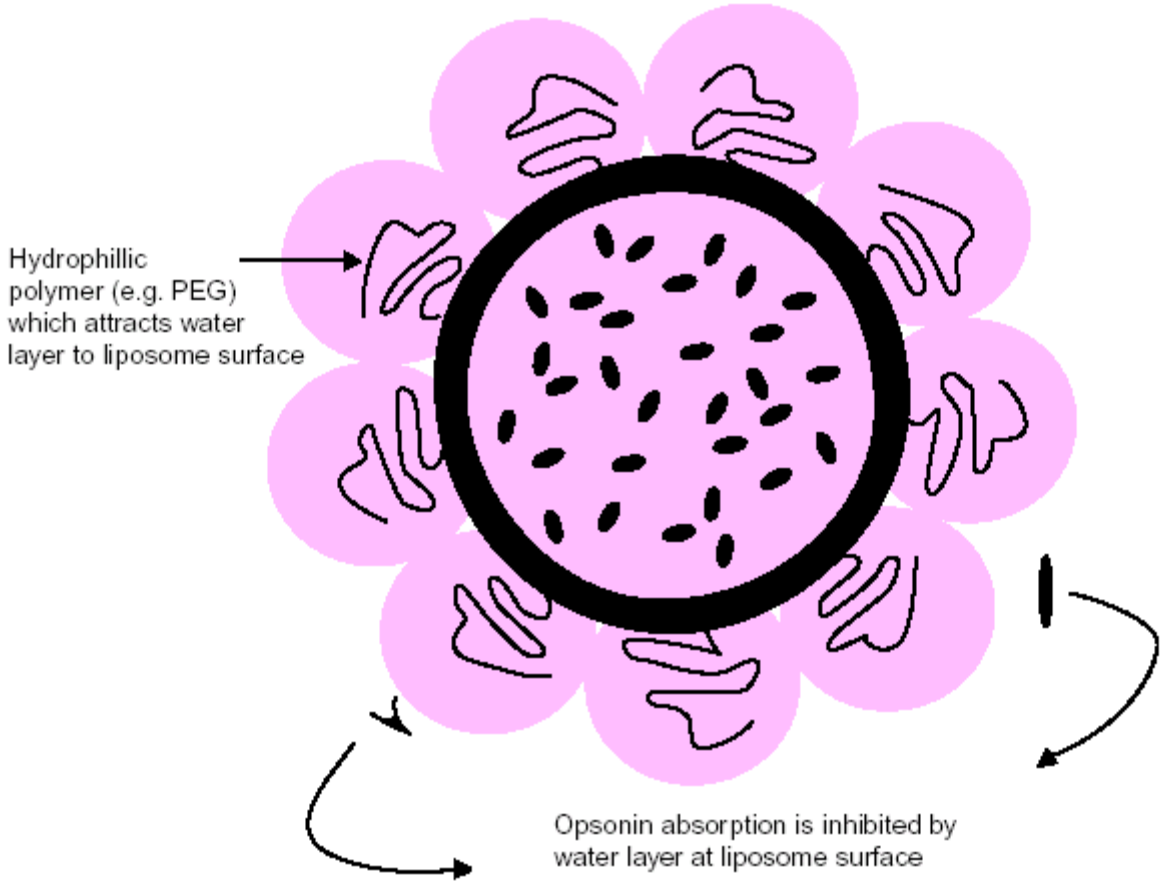

Figure 12 A schematic diagram depicting a drug-containing liposome with a surface coating of PEG (Allen 1998).

As the adsorption of human serum albumin to DPPC bilayer membranes containing DPPE-PEG had been studied as a function of content and headgroup size of the polymer lipid, two regimes of grafted polymer behavior were defined (Bartucci 2002). At low grafting concentrations the polymer chains were in the mushroom regime, whereas at high grafting concentrations the chains interacted laterally forming extended brushes. The authors detected conversion between the two regimes at mole fractions ~ 0.04, 0.01-0.02, 0.005-0.01 for DPPE-PEG with mean PEG molecular masses of 350, 2000 and 5000 Da, respectively. It has been also observed that the protein absorption was strongly attenuated by the steric stabilization exerted

by the polymer lipid in the mushroom regime, and was completely eliminated in the high-density brush regime.

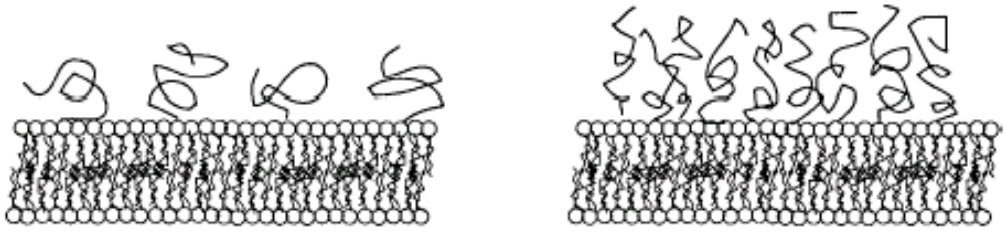

Figure 13 A schematic view of the mushroom regime (left) and the brush regime (right) of polymer coils (Silvander 2002).

The lateral repulsion at high surface concentrations of the polymer lipid was one reason presumed to affect the structural properties of the liposome and eventually lead to its disruption (Silvander 2002). As expected from the lateral repulsion between the attached PEG polymer coils there has been a maximum amount of PEG lipid that has been included before structural destabilization took place (Edwards 1997, Johnsson 2003).

The effect of DPPE-PEG2000 on aggregate structure of various liposomal formulations was studied using cryo-transmission electron microscopy (cryo-TEM) (Edwards 1997). The micrographs showed that incorporation of more than 10 mol% PEG lipid into egg PC or DSPC liposomes resulted in formation of a large fraction of open bilayer discs. At higher concentration of PEG lipid (>20 mol%), the discs disappeared and the threadlike micelles converted into globular micelles. It was also found that a decrease in phospholipid chain length decreased the amount of PEG lipid needed to induce micelle formation, whereas phospholipid saturation or the presence of cholesterol had little or no effect (Edwards 1997). Similar results were obtained as the aggregate structure of mixtures of PEG lipids and DPPC or DSPC had been further investigated (Johnsson 2003). But formation of disk-like micelles occurred at low PEG lipid concentrations (<5 mol%) in mixtures of DPPC or DSPC.

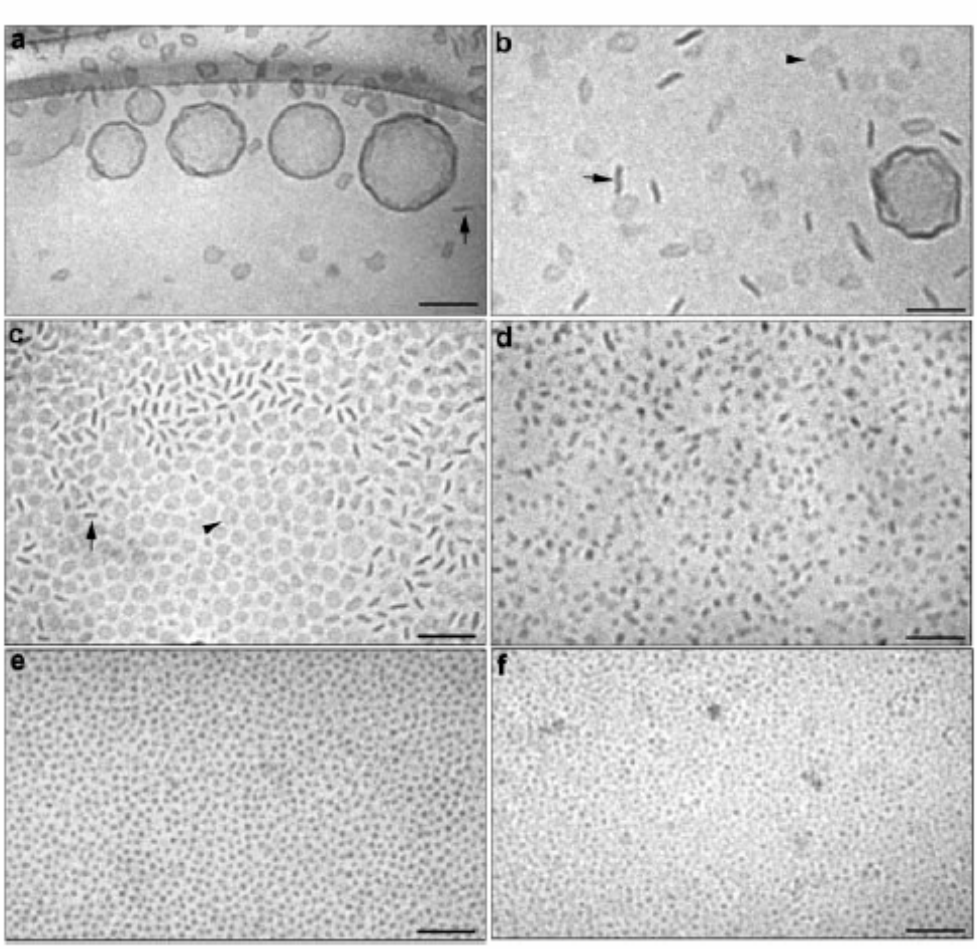

Figure 14 Cryo-TEM images of DPPC dispersions containing DPPE-PEG 2000 in concentrations of (a) 4.5 mol%, (b) 9.5 mol%, (c) 19.5 mol%, (d) 30.2 mol%, (e) 49.7 mol%, (f) 68 mol%. The arrowheads in b and c denote disks observed edge-on and face-on, respectively. Bar, 100 nm (Johnsson 2003).

As shown in Figure 14 c (19.5 mol% PEG), the strongly dominating structure were relatively small disks. Increasing the PEG lipid concentration resulted in complete disappearance of the liposomes and a significant decrease in size of the disk-like micelles. The progressive size decrease continued at higher PEG lipid concentrations and the shape of the micelles approached spherical micelles.

The liposomes undergoing this transformation lost their encapsulation ability and consequently lost their value as vehicles for delivery of water-soluble drugs. Therefore, the obtained results are of great importance for a design of successful liposomal delivery system.

1.3.6. Accumulation of liposomes in tumors (The concept of enhanced permeability and retention EPR)

It was remarkable that the antitumor effect of a macromolecular drug carrier coupled to a drug depended on its accumulation, as well as its distribution within the tumor. The mechanism of liposome accumulation in tumors and their detailed localization remained unclear. However, the accumulation of liposomes in tumor tissue could be due to extravasation (to enter tumor tissue from the vasculature) through leaky endothelium of tumor tissues possessing increased vascular permeability coupled with an impaired lymphatic drainage (Muggia 1999, Pathak 2005, Dreher 2006).

1.3.6.1. Tumor vascular permeability, accumulation and penetration of macromolecular drug carriers

Dreher et al. investigated how molecular weight influences the accumulation of a model macromolecular drug carrier, dextran covalently linked to a fluorophore, in tumors. They also quantified penetration of such macromolecular drug carriers from the vascular surface into the tumor interstitium. It was found that dextrans of 3.3 and 10 kDa penetrated deeply (greater than 35 μm) and homogeneously into tumor tissue from the vessel wall. Dextrans with molecular weights between 40 and 70 kDa had the highest accumulation in solid tumors but were largely concentrated near the vascular surface. This higher concentration in the vicinity of the vascular surface, where cancer cells proliferate more rapidly compared with those located further away from the vascular surface might lead to a greater overall therapeutic efficacy of therapeutic agents. Additionally, if the drug carrier was larger than 10 kDa and hence localized near the vascular surface, then the drug itself could be released from its carrier so that the drug could penetrate much deeper into tumor tissue (Dreher 2006).

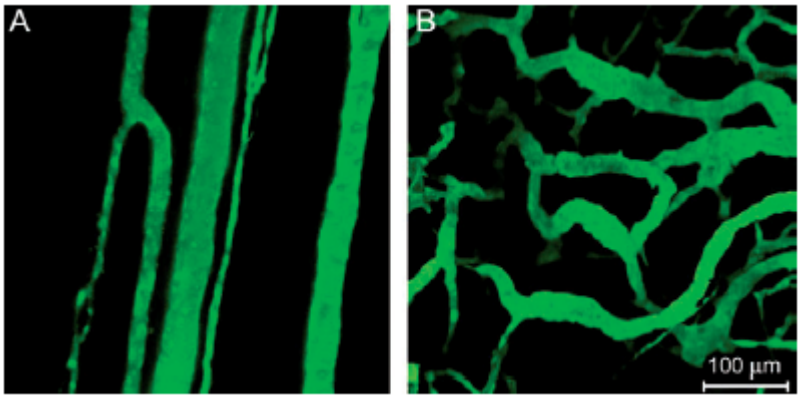

Figure 15 Normal and tumor vasculature. (A) Normal vasculature; normal vessels are aligned parallel to one another, (B) Tumor vasculature ; tumor vessels have a chaotic geometry with vessels that are dilated and have uneven diameters. Scale bar = 100 µm (Dreher 2006).

1.3.6.2. Characterizing extravascular fluid transport of macromolecules in the tumor interstitium

Delivery and interstitial transport of macromolecules through the extracellular matrix (ECM) and supporting stroma of a tumor have been determined (Pathak 2005). Albumin-gadolinium diethyltriamine penta-acetic acid (albumin-GdDTPA) was used as a macromolecular contrast agent (MMCA) in the magnetic resonance experiments. Delivery of MMCA through the vasculature and its transport within the tumor interstitium were characterized. Tumor was modeled to consist of (i) the intravascular space, (ii) the perivascular region of the tumor interstitium that the MMCA initially extravasated into and (iii) the interstitium within which slow macromolecular transport events, such as convective and lymphatic drain occurred. The results showed that clearance of macromolecules through the interstitial matrix was not efficient. A few lymphatic vessels were detected in these tumors but they were primarily collapsed and tenuous suggesting that lymphatic drainage played a minimal role and that the bulk of drainage was due to convective transport.

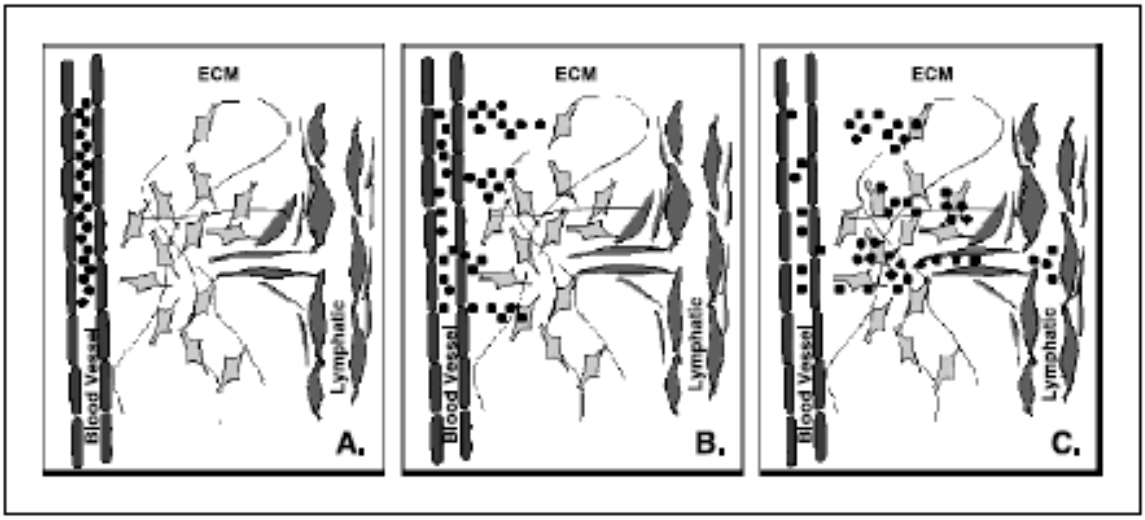

Figure 16 Schematic illustrating compartmentalization of the macromolecular contrast agent albumin-GdDTPA. (A) during the early phase (the first 31 minutes of the magnetic resonance experiment), the MMCA is confined to the vascular space, immediately followed by (B) extravasation from the hyper-permeable tumor vessels into the extravascular space, from which (C) it is cleared by convection and/or tumoral lymphatics, if present (Pathak 2005).

1.3.7. Liposome-encapsulated doxorubicin

Doxorubicin, an anthracycline antibiotic active against a wide range of tumors, has been in use for the treatment of human malignancies since long time (Barlow 1973, Zocchi 1989). Liposomal doxorubicin formulations were developed to decrease the toxicity of the free drug (Lee 1998, Sadzuka 2000, Tseng 2002, Eliaz 2004, Charrois 2004).

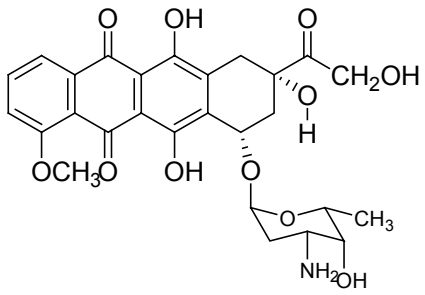

Figure 17 Doxorubicin

Doxil™ or Caelyx™ (soy PC:cholesterol:DSPE-PEG2000 at molar ratio 55:40:5) and Myocet™ (egg yolk PC:cholesterol at molar ratio 55:45) are two liposomal-doxorubicin formulations in use in cancer therapy (O'Brien 2004, Mrózek 2005).

Liposomal encapsulation could alter the biodistribution of doxorubicin with significant reductions in drug accumulation in cardiac tissues. Abraham et al. have investigated the physical and chemical characteristics of the encapsulated drug. In addition, in vitro and in vivo drug loading and release properties of the liposomal formulations have been characterized (Abraham 2002). Doxorubicin was encapsulated into either dimyristoylphosphatidylcholine (DMPC)/cholesterol or DSPC/cholesterol liposomes, where the entrapped salts were citrate, manganese sulfate ($MnSO_4$) or manganese chloride ($MnCl_2$).

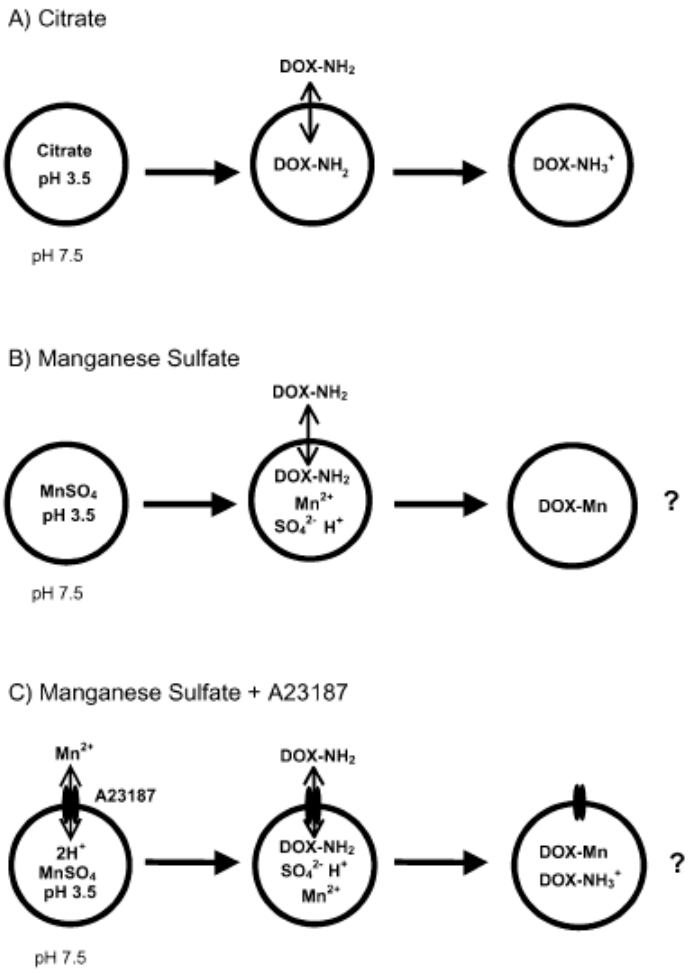

Figure 18 Methods of doxorubicin encapsulation into liposomes exhibiting the indicated gradients: (A) liposomes prepared in 300 mM citrate buffer, pH 3.5, and outside buffer exchanged to HEPES-buffered saline at pH 7.5, (B) liposomes prepared in 300 mM manganese sulfate, pH 3.5, and outside buffer exchanged to 300 mM sucrose/20 mM HEPES/15 mM EDTA at pH 7.5 and (C) which is identical to (B) except that the ionophore A23187 is added to the liposomes prior to doxorubicin addition (Abraham 2002).

The results supported the concept that drugs encapsulated in liposomes through use of ion gradients could form precipitates within the liposome. Cryo-TEM studies indicated that the doxorubicin precipitate consisted of fibrous-bundle aggregates in both citrate- and sulfate-containing liposomes. The formulations containing citrate exhibited both curved and circular electron dense structures that caused a slight distortion of the liposome shape. In contrast, the sulfate-containing formulations exhibited linear precipitates and a significant elongation of the liposome (Figure 19). The sulfate anion, smaller than the citrate anion, might form a tighter packing arrangement resulting in decreased flexibility. It was worth noting that these differences in liposome shape had little or no effect on the plasma liposomal lipid elimination profiles obtained following intravenous administration.

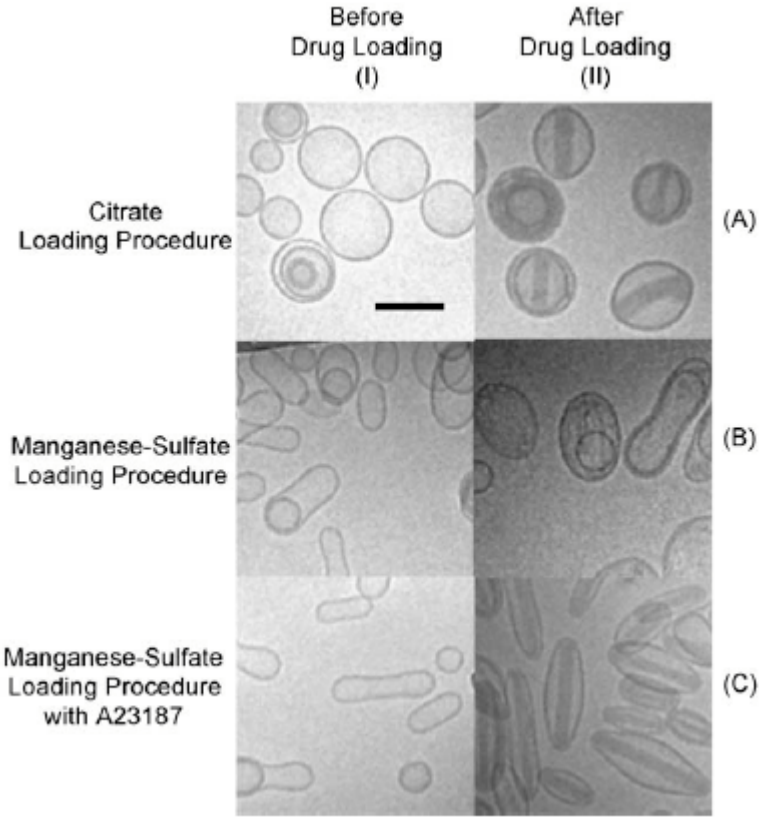

Figure 19 Cryo-TEM images of DMPC/cholesterol (55:45) liposomes either before or after drug loading achieving a final drug-to-lipid ratio of 0.2:1 (wt/wt) (Abraham 2002).

Doxorubicin-loaded liposomes prepared using the $MnSO_4$ and $MnCl_2$ procedures in the absence of the ionophore A23187 were strikingly different than doxorubicin-loaded liposomes using the citrate-based procedure. Following drug loading, both of these formulations had a purple color as compared to the citrate-loaded preparations that were orange in appearance. Cryo-TEM micrographs of the purple liposomal

formulations indicated the appearance of an electron dense precipitate without any distinguishable crystalline structures.

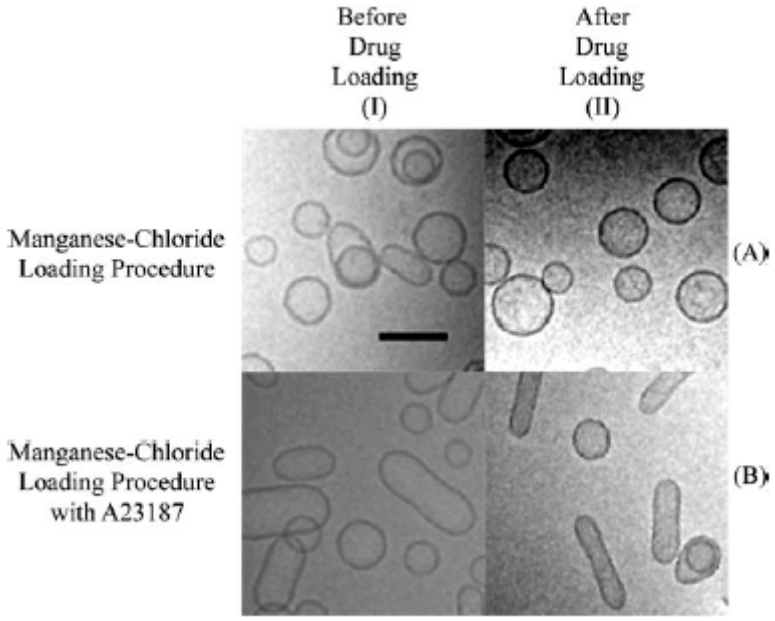

Figure 20 Cryo-TEM images of DMPC/cholesterol (55:45) liposomes either before or after drug loading achieving a final drug-to-lipid ratio of 0.2:1 (wt/wt) (Abraham 2002).

The data also indicated that for a drug like doxorubicin, the resulting formulations could retain entrapped drug even under conditions where was little or no residual pH gradient. An explanation for these results was that as doxorubicin had been encapsulated, the pH (inside) increased due to the consumption of protons as the neutral drug became protonated (charged) and thus in a membrane-impermeable state.

It has also been observed that drug release from DMPC/cholesterol liposomes was comparable regardless of whether doxorubicin was entrapped as a citrate based aggregate or a Mn^{2+} complex. However, in vivo drug release from DSPC/cholesterol liposomes indicated a measurable change in the rate of drug release following intravenous administration, where drug release was greater for those formulations that lack a pH gradient suggesting that drug release was dependent on lipid composition, internal pH, as well as the nature of the crystalline precipitate formed following encapsulation (Abraham 2002).

1.3.8. Targeted delivery of liposomes

Many investigators have done a lot of work on liposome targeting in order to achieve tissue or cell specific liposome uptake.

1.3.8.1. Development of epidermal growth factor-conjugated liposomes

Specific accumulation of liposomal substances in tumor cells was tried to be achieved by attachment of targeting agents to the liposomes. Epidermal growth factor (EGF) was used as a tumor seeking agent because of its overexpression in many tumor cells (Chaidarun 1994). Bohl Kullberg et al. (Bohl Kullberg 2002) investigated the possibility to attach EGF to DSPC/cholesterol/DSPE-PEG liposomes. EGF was coupled to maleimide-PEG-DSPE molecules. The EGF-conjugated micellar lipids were then incorporated into preformed liposomes, either empty or containing the DNA-binding compound, water soluble acridine (WSA), using the micelle transfer method. This incorporation needed a transfer temperature of 60°C. It has been observed that the high transfer temperature was accompanied by leakage of the liposomal contents. Also, lower level of incorporation was recorded for the preparation containing the highest amount of PEG-lipid (5 mol%).

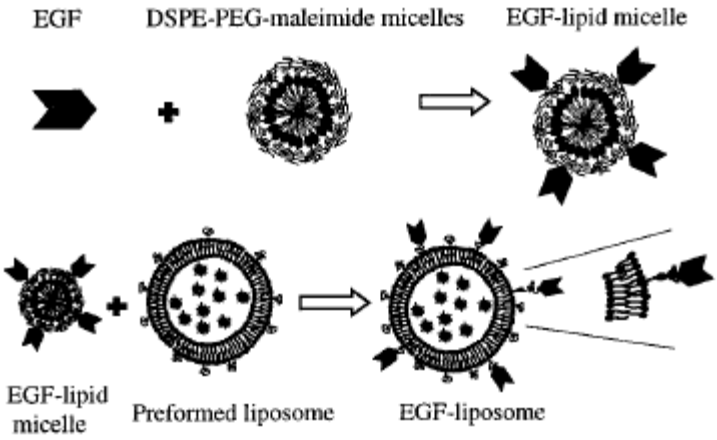

Figure 21 Schematic drawing of the micelle-transfer method. EGF is attached to DSPE-PEG-maleimide lipids in micelles via a thiol linkage. The EGF lipids, in the form of micelles, are mixed with preformed liposomes, and the EGF-PEG-DSPE molecules are thereby incorporated into the liposome membranes (Bohl Kullberg 2002).

A clear difference in the transfer was observed between empty and WSA-loaded liposomes. The amount of incorporated EGF-conjugated PEG-lipid was significantly lower for liposomes containing WSA than for unloaded liposomes with the same PEG-lipid content.

The receptor specificity was analyzed by incubating the EGF liposome conjugate with glioma cells with either blocked or unblocked receptors. The conjugate had EGF-receptor-specific cellular binding during the in vitro tests with those cells. However, the fraction of nonreceptor specific binding increased to about 30% in case of conjugates loaded with WSA which might be explained by modification of of the liposomal properties by WSA (Bohl Kullberg 2002).

1.3.8.2. Folate-targeted liposomes

The in vivo tissue distribution of folate-targeted liposomes (FTLs) injected intravenously in mice bearing folate receptor (FR)-overexpressing tumors has been compared to that of nontargeted liposomes (NTLs) of similar composition (Gabizon 2003). A small fraction of a folate-PEG-DSPE conjugate was incorporated in FTLs. Both FTLs and NTLs were pegylated with a PEG-DSPE conjugate to prolong circulation time. In comparison with NTLs, FTLs were cleared faster from circulation as a result of greater liver uptake. Despite the lower plasma levels, tumor levels of FTL-injected mice were not significantly different from those of NTL-injected mice.

A concomitant dose of free folic acid (FA) blocked the clearance of FTLs without modifying that of NTLs. Interestingly, the same codose of FA did not reduce tumor uptake of FTLs. The authors had two explanations for this: (a) the accumulation of FTLs in tumor was due to passive extravasation into malignant ascitic fluid based on the enhanced permeability and retention effect with no contribution of binding to cell FR, or (b) the higher (~1000-fold) affinity of liposome multivalent binding to multiple FR on the tumor cell surface prevented displacement of bound liposomes by free FA.

Although the results indicated that binding of FTLs to the tumor cell FR took place in vivo, it was unclear wheather significant binding of FTLs to tumor cell FR can also take place in solid tumors, where the movement of liposomes was expected to be much more limited (Gabizon 2003).

1.3.8.3. Liposomes targeted to CD44 receptors

As Eliaz and Szoka had incorporated multiple copies of the low molecular weight oligomer of hyaluronic acid (HA) into liposomes bilayer, they found that the modified liposomes could preferentially bind to and be taken up by, cells with a high density of CD44 receptors that bind to HA.

The results demonstrated that HA facilitated the recognition of liposomes by CD44-high-expressing B16F10 melanoma cells in culture and that, after cell surface binding

the liposomes were internalized into the targeted cells. HALs binding to B16F10 cells was inhibited by HA and monoclonal antibodies directed against the CD44 receptor. Thus, most of the HAL binding to B16F10 cells was attributed to interaction with the cell surface CD44 receptors. The control CV-1 cells which had a low CD44 density, similar to the CD44 density found on many normal cells in the body, showed little uptake indicating that HALs had high affinity to the B16F10 but not to CV-1 cells.
The chemotherapeutic results demonstrated that doxorubicin-containing HALs were more potent than free doxorubicin. Moreover, HALs decreased the cytotoxicity of doxorubicin to cells expressing low levels of the CD44 receptor. The authors suggested that the obtained in vitro resuts required additional preclinical testing in relevant animal tumor models (Eliaz 2001).

1.3.8.4. Antibody targeting of liposomes (immunoliposomes)

The growth factor receptor $p185^{HER2}$, encoded by HER2 protooncogene, represented an attractive target antigen for cancer immunotherapies (Park 1995). Anti-$p185^{HER2}$ immunoliposomes were developed as a tumor-targeting vehicle. Park and coworkers concluded that anti-$p185^{HER2}$ immunoliposomes might be promising therapeutic vehicles, in which cytotoxic agents such as doxorubicin could be targeted to $p185^{HER2}$-overexpressing tumors. It was demonstrated that anti-$p185^{HER2}$ immunoliposomes internalization took place via receptor-mediated endocytosis. Slower internalization rates were, however, observed in sterically stabilized liposomes, where PEG lipid at 2% of total phospholipid reduced the uptake and cytotoxicity of doxorubicin-loaded anti-$p185^{HER2}$ immunoliposomes in cultures of target cells.

1.3.8.5. Translocation of liposomes into cancer cells by cell-penetrating peptides

Tseng et al. demonstrated that two cell-penetrating peptides (CPPs), penetratin (PEN; DNA binding domain of the Drosophila melanogaster transcription factor antennapedia) and the HIV trans-activating transcriptional activator (TAT), could translocate liposomes into cells efficiently, but they could not illustrate the mechanism of penetration of each CPP.
Unilamellar liposomes composed of DSPC, cholesterol and N-[ω-methoxypoly(oxyethylene)-(R)-carbonyl]-DSPE (molar ratio 3:2:0.06) were prepared and peptidyl-PEG3400-DSPE was then transferred to the preformed liposomes.

Although CPPs, especially TAT, markedly improved the intracellular delivery of liposomal drugs, the in vitro cytotoxicity assays and animal tumor model studies could not demonstrate the superiority of CPP-coupled liposomes over plain liposomes. The results revealed that this approach was hampered by the very limited release of the free drug into the cytoplasm and nucleus. In addition, it was assumed that CPPs might increase nonspecific interactions with cells of normal tissues in vivo. The authors mentioned that an additional approach to enhance the intracellular release of the encapsulated drug was necessary (Tseng 2002).

1.3.9. Liposome cell interactions

Phospholipid transfer between small unilamellar liposomes formed from either DOPC or DOPC:DOPE (20:80 mol%) and Chinese hamster fibroblasts has been studied using isotopically asymmetric liposomes (Sandra 1979). Isotopically asymmetric liposomes were incubated with cells to assess whether lipids in the inner or outer leaflets, or both, of the liposomes bilayer participated in the lipid transfer process. Uptake of liposomes lipids was found to be directly proportional to the amount of radioactivity present in the outer leaflet of the liposomes, indicating that only the outer monolayer lipids became cell-associated during liposome-cell lipid transfer. It should be noted that if liposomes were taken up by cells as a result of an alternative mechanism such as fusion, endocytosis or a stable adsorption, uptake of their radioactive lipids should be proportional to the radioactivity present in both halves of the liposome bilayer.

The results also demonstrated that liposomes lipids were introduced preferentially into the outer leaflet of the cell plasma membrane by the lipid transfer process. The transfer of lipids between cells and liposomes represented a one-for-one exchange, a phospholipid specific exchange process that did not involve a net transfer of lipids to or from the cell. In a one-for-one exchange process, the number of lipid molecules at the cell surface should remain the same before and after their exchange. It was also noteworthy that the above mentioned transfer mechanism occurred without uptake of liposomes contents which in turn indicated that not all liposome-cell interactions should be accompanied by a release of liposomes contents (Sandra 1979).

1.3.10. Liposome content release

For a successful tumor therapy, it is important that a sufficient amount of drug becomes bioavailable so that the cancer cells can receive an appropriate dose of

drug (Allen 2004). In liposomes, the drug is inactive (not bioavailable) while associated with the carrier, and failure to release the drug from the carrier in a timely manner may result in a reduced therapeutic effect relative to the free drug (Meerum Terwogt 2002).

1.3.11. Distribution and uptake of liposomal doxorubicin

Davies et al. have found that liposomal doxorubicin (Caelyx) had an almost negligible effect on tumor growth. Therefore, they studied tumor growth and the microdistribution of liposomal doxorubicin with and without additional ionizing radiation in human osteosarcoma xenografts grown in mice. The authors observed that liposomal delivery of doxorubicin administered in combination with single-dose or fractionated radiotherapy delayed the growth of the tumor but they did not determine the exact mechanisms underlying the interactions. Direct inactivation of radioresistant hypoxic cells by doxorubicin probably was not a contributing factor to the delayed tumor growth because doxorubicin was not redistributed to hypoxic areas after radiation.

Successful delivery of doxorubicin to the tumor cells required that circulating liposomes extravasate and release doxorubicin that had to penetrate through the ECM. The study showed that a single fraction of radiation combined with Caelyx reduced the vascular transfer rate and the vascular volume. The observed reduction in vascular transfer rate suggested that radiation reduced the transfer rate of high molecular weight Caelyx. It should be mentioned that radiation was found not to disintegrate the liposomes.The results also demonstrated that doxorubicin released from the liposomes was located mainly in the tumor periphery before and after radiotherapy. After radiotherapy, doxorubicin was also localized around vessels in the central parts of the tumor. The uptake of doxorubicin in the central parts of the tumor increased two to four times after a single dose of radiation and one to three times after fractionated radiation (Davies 2004). The improved distribution of doxorubicin after radiotherapy might be due to doxorubicin-induced apoptosis which probably could alter the ECM structure (Zheng 2001).

1.3.12. Penetration of doxorubicin into solid tumors

The kinetics of doxorubicin uptake and efflux into tumor histocultures have been studied (Zheng 2001). The study indicated that the rate of doxorubicin penetration to the center of the tumor was dependent on initial extracellular drug concentration,

treatment time and tumor type. Doxorubicin penetration was restricted to the tumor periphery until the cell density was reduced as a result of doxorubicin-induced apoptosis. Drug penetration was faster at higher concentrations, and the effect of drug concentration on the penetration rate was more significant in tumors with high tumor-cell density than in tumors with low density.

1.3.13. Triggered release of liposomal contents

Although there were situations where slow release of drugs out of liposomes provided therapeutic benefit (Charrois 2004), the ability to control and produce a rapid release of a significant amount of drug directly in the tumor tissue or tumor vasculature would be extremely advantageous (Needham 2001). Lipid composition of the liposomal formulations determined the leakage rate of their content (Lim 1997). Liposomes with different release rates could be prepared by altering liposome fluidity through changing the fatty acyl chain length and/or degree of saturation of the PC component of the liposome.

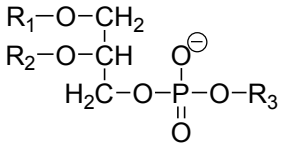

DMPC $R_1 = R_2 = C_{14:0}$

DPPC $R_1 = R_2 = C_{16:0}$

DSPC $R_1 = R_2 = C_{18:0}$

DOPE $R_1 = R_2 = C_{18:1}$

EPC $R_1 = C_{16:0}$ $R_2 = C_{18:1}$

Phosphatidylethanolamine (PE)

R_3 - $CH_2CH_2\overset{\oplus}{N}H_3$

Phosphatidylcholine (PC)

R_3 - $CH_2CH_2\overset{\oplus}{N}(CH_3)_3$

Polyethyleneglycol (PEG)

R_3 - $CH_2CH_2NH\text{-}O\text{-}[CH_2CH_2]_n\text{-}OH$

Figure 22 Structural formula of a phospholipid

1.3.13.1. Influence of liposomes composition on drug release characteristics

Lim et al. evaluated the antitumor activity of DSPC/cholesterol (55:45 mol%) and DMPC/cholesterol (55:45 mol%) liposomal mitoxantrone (Lim 1997). The examined liposomal formulations exhibited favorable drug retention characteristics. It was demonstrated that the in vivo rate of mitoxantrone release from DMPC/cholesterol liposomes was at least 68-fold greater than that from DSPC/cholesterol. Lim and his group attributed the difference in permeability characteristics for the two formulations to the differences in their gel-to-liquid crystalline phase transitions.

The pharmacodynamic characteristics of these formulations were characterized using murine tumor models where the primary site of tumor progression was in the liver. It was surprising that the differences in drug accumulation and leakage rates for DMPC/cholesterol and DSPC/cholesterol liposomes were not substantial when evaluated in vitro.

The authors had shown that mitoxantron delivery to the liver was enhanced when DSPC/cholesterol liposomes were used, in comparison with DMPC/cholesterol liposomes. Increased liposomal drug exposure in this tissue, however, did not improve the therapeutic activity. The DMPC/cholesterol liposomal formulation which exhibited reduced capacity to deliver the drug to the liver was significantly more effective. Thus, it is not sufficient to develop drug carriers that accumulate at the disease site in high levels; one must also engineer appropriate drug release rates (Lim 1997).

1.3.13.2. Drug release from temperature-sensitive liposomes

Research has been focused on temperature-sensitive materials (phase transitions) and local hyperthermia (the application of external power) to initiate a temperature-dependent change in the physical state of a liposome membrane in order to enhance its permeability (Kong 2000, Needham 2001).

The passive permeability of lipid bilayers to ions was shown to be significantly increased near their phase transitions (Ono 2002). The increased permeability of the liposomal membranes seen in the region of gel to liquid crystalline phase transition was most probably due to packing defects in phase boundaries between coexisting gel and liquid crystalline phases, since passage through the phase transition did not occur in all members of lipid population (domains of gel and liquid crystalline phase lipids must coexist during the transition). It has been found that a clinically relevant hyperthermic treatment should be in the range of 39-42°C. However, the achieved temperatures were non-homogeneous and none of the patients achieved high tumor temperatures (Anscher 1997). Consequently, the task was to reduce the transition temperature of the lipid bilayer so that it could enter the clinically attainable range for mild hyperthermia.

It has been demonstrated that amphipathic molecules like lysolipids could partition into the lipid bilayer interface up to tens of percents (Needham 2000). Moreover, upon dilution of the extra vesicular solution, the lysolipid was rapidly washed out. Based on this observation, Needham et al. hypothesized that the inclusion of an acyl

chain matched lysolipid such as monopalmitoylphosphatidylcholine (MPPC) in the DPPC gel phase might enhance the permeability at the gel-liquid crystalline phase transition as the lipid melted and the lysolipid was then free to partition back into a lysolipid-depleted aqueous phase and/or perturb the defect structure at these melted boundaries. Furthermore, since the MPPC had one acyl chain missing compared to the host lipid DPPC, this chain defect introduced a slightly increased fluidity to the bilayer accompanied by a reduction of the phase transition temperature from 41.4 to 40.5°C.

A significant problem for using hyperthermia clinically was the lower temperatures achieved in deeper sites compared to those in superficial sites (Conway 1983). Despite of the long use of hyperthermia in medicine, most of the trials were done in superficially accessible tumors, where the tissue could be heated effectively.

1.3.13.3. Thermosensitive polymer-modified liposomes

Kono and coworkers have designed cationic liposomes whose affinity to negatively charged membranes could be controlled by temperature (Kono 1999a). Cationic liposomes consisting of 3β-[N-(N',N'-dimethylaminoethane) carbamoyl]cholesterol and dioleoylphosphatidylethanolamine (DOPE) were modified with poly (N-acryloylpyrrolidine) having two dodecyl groups at the terminal (poly(APr)-$2C_{12}$), which is a thermosensitive polymer exhibiting a lower critical solution temperature (LCST) at ca. 52°C.

The authors investigated the temperature influence on charge density of the cationic liposomes by measuring zeta potential. Zeta potential of the unmodified cationic liposomes did not change between 20 and 60°C and was ca. 12 mV. The poly(APr)-$2C_{12}$-modified cationic liposomes had much lower zeta potential below 50°C. Thus, the highly hydrated polymer chains taking an extended conformation covered the liposome surface and accordingly shielded the positive charges below 50°C. By increasing the temperature above 50°C, the liposomes zeta potential increased suddenly indicating that the polymer chains transformed to dehydrated globules allowing the positively charged surface of the liposomes to be exposed.

Similarly, the polymer chains attached to the cationic liposomes suppressed their interaction with the anionic liposomes below LCST. But when the temperature had been raised above 50°C, aggregation and fusion of the polymer-modified cationic liposomes with the anionic liposomes were observed.

The interactions of the polymer-modified liposomes with the anionic liposomes were switched on at high temperature (50°C). Therefore, thermosensitive polymers which exhibit a lower LCST were required in order to prepare modified liposomes revealing the temperature-response around the physiological temperature.

Shortly after, Kono et al. modified egg yolk phosphatidylcholine liposomes with a copolymer of APr and N-isopropylacrylamide (NIPAM) having two dodecyl groups at the terminal (poly(APr-co-NIPAM)-2C_{12}) which exhibited an LCST at ca. 40°C (Kono 1999b). The effect of temperature on the interaction of the polymer modified liposomes with an African green monkey kidney cell line (CV1 cells) was investigated. It has been found that the amount of modified liposomes taken up by the cell was lower than that of the unmodified liposomes at 37°C. However, the amount of cell-associated liposome increased with raising the temperature. In comparison with the liposome uptake in the absence of serum, the uptake was significantly reduced in the presence of serum, probably due to adsorption of serum proteins on the liposome surface.

When calcein retention in the polymer-modified liposomes had been examined, it was reported that only a limited portion of the contents leaked out. There were no remarkable differences in their release behaviors at 37 and 42°C, indicating that the temperature-dependent hydrophobicity change of the polymer hardly affected the content release from the liposomes.

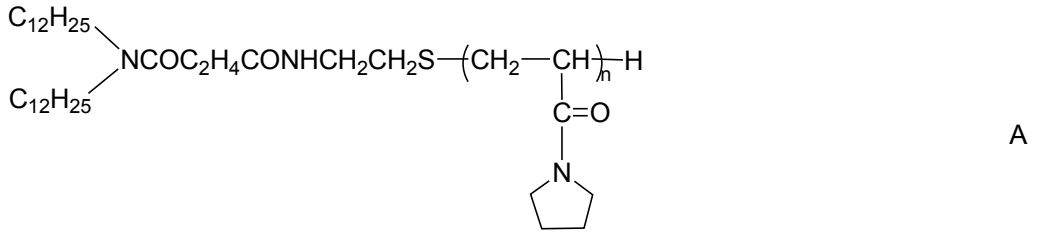

A

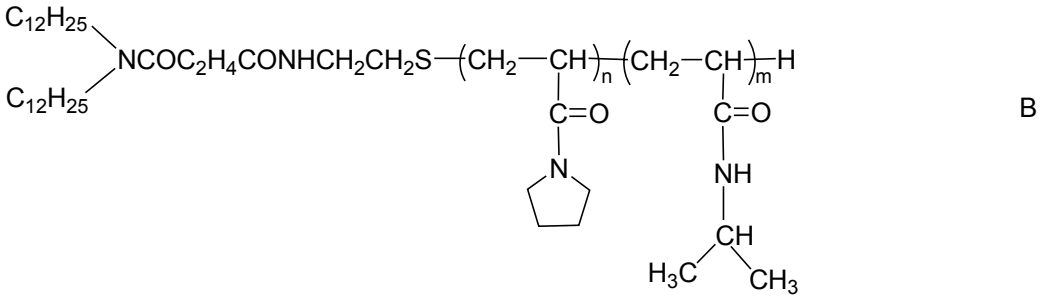

B

Figure 23 Structures of (A) poly(APr)-2C_{12} and (B) poly(APr-co-NIPAM)-2C_{12}.

1.3.13.4. The effect of pH on content release of non-pH-sensitive liposomes

Lee and coworkers examined the effect of pH on the rate of drug release from stable, non-pH-sensitive liposomes (Lee 1998). A pH-insensitive lipid composition, egg PC/cholesterol/folate-PEG-DSPE (60:40:0.1) was used. When liposomes entrapping doxorubicin were internalized by the cells via folate receptor-mediated endocytosis and then trafficked to acidic endosomes, doxorubicin release was enhanced. This is because the previous inward directed proton gradient required for doxorubicin remote loading disappeared. This change in proton gradient could drive the release of doxorubicin in an analogous but opposite direction to the initial remote loading mechanism.

Unfortunately, due to the additional presence of a pH gradient between the endosomes and cytosol, doxorubicin was partially retained in the extraliposomal endosomal compartments. The escape of some doxorubicin molecules into the cytosol and/or the nucleus might be due to the lower pH in the cytosols of some tumor cells.

1.3.13.5. pH-sensitive liposomes

pH-sensitive liposomes were developed to facilitate liposome fusion with endosomes at low endosomal pHs (at pH ~5 if endosomes are successfully accessed by specific targeting) (Conner 1984, Chu 1990, Hong 2002, Shi 2002, Guo 2003).

Studies of Connor et al. revealed that liposomes prepared from DOPE and palmitoylhomocysteine at molar ratio of 80:20 fused rapidly when the medium pH had been lowered from 7 to 5. The authors explained the pH effect by a change in the electrostatic interactions among the lipid headgroups. They also proposed that the low bilayer solubility of the protonated palmitoylhomocysteine might result in domains of palmitoylhomocysteine at acidic pH and consequently promoting lateral phase separation of the bilayer lipids, a major cause of fusion. Moreover, it was suggested that other long-chain amphiphiles containing carboxylic groups, such as fatty acids, can also be used for acid-induced liposome fusion (Conner 1984).

Chu and coworkers showed that pH-sensitive liposomes composed of DOPE: cholesterylhemisuccinate (60:40) could deliver encapsulated fluorescent molecules into the cytoplasm. However, the efficiency of cytoplasmic delivery accounted for less than 10% of the liposome contents that became cell associated (Chu 1990).

Hong et al. tried to solve the problems of the lack of stability in blood and the short blood circulation time of pH-sensitive liposomes by inclusion of DSPE-PEG in the

liposomal bilayers (Hong 2002). Incorporation of DSPE-PEG enhanced the serum stability of both DOPE/ oleic acid (70:30) and DOPE/dipalmitoylsuccinylglycerol (70:30) liposomes, but also shifted the pH-response curve to more acidic regions and reduced the maximum leakage percentage. DSPE-PEG had, however, lower effect on DOPE/dipalmitoylsuccinylglycerol liposomes than on DOPE/ oleic acid liposomes. In other words, DOPE/dipalmitoylsuccinylglycerol liposomes incorporating DSPE-PEG were more pH sensitive and serum stable.

Tendency of PE to enhance the acid induced membrane fusion was found to be due to conversion of PE bilayer into the hexagonal phase (Guo 2003).

However, while pH-sensitive liposomes might be effective in cytosolic drug delivery in vitro, they were less successful in vivo, probably due to loss of their fusogenicity when exposed to serum (Lee 1998).

1.3.13.6. Liposomal drug release by phospholipase A_2 (PLA_2)

Davidsen et al. designed an experimental biophysical model system for improved drug release based on elevated levels of PLA_2 at the diseased target tissue (Davidsen 2003). The principle was built in a dual virtual trigger mechanism of simultaneous (i) enhanced drug release selectively at the target tissue and (ii) enhanced transport of the drug into the diseased cells. The model system consisted of a polymer-coated liposome carrier and a model target membrane. The carrier was a unilamellar DPPC liposome incorporated with DPPE-PEG2000, whereas the target membrane was another liposome made of 1,2-di-O-stearoylphosphocholine (1,2-di-O-SPC), a phospholipid where the acyl linkages of the stearoyl chains are ether bonds. In contrast to DPPC, 1,2-di-O-SPC is inert towards PLA_2-catalyzed hydrolysis thereby mimicking the stability of a target cell membrane toward degradation by its own enzymes.

The experimental assay involved entrapment of a water-soluble fluorescent calcein model drug, in a self-quenching concentration, in the nonhydrolyzable target liposome. The enhanced level of PLA_2 at the target membrane was simulated by adding PLA_2 to initiate the hydrolytic reaction in a suspention of the carrier and target liposomes. The permeation of calcein across the 1,2-di-O-SPC target membrane was monitored by the increase in fluorescence.

A similar experiment was performed with conventional bare DPPC liposomes to determine the effect of the presence of PEG-lipid. Furthermore, experiments without enzymes were carried out where 1-palmitoyl-2-hydroxy-sn-glycero-3-phosphocholine

(lysoPPC) and palmitic acid (PA) were added simultaneously or separately to the target liposomes to discriminate the permeability-enhancing effect of lysoPPC from that of PA. The obtained results indicated that polymer-grafted liposomes were susceptible to PLA_2-catalyzed degradation. Moreover, the hydrolysis products, lysoPPC and PA, were found to enhance the permeability of the target membrane.

1.3.13.7. Light-induced calcium ions (Ca^{2+}) release from diplasmenylcholine liposomes

Wymer et al. presented a system consisted of a mixture of two different population of liposomes, one composed of synthetic diplasmenylcholine (1,2-dihexadec-1'-enyl-sn-glycero-3-phosphocholine (DPP1sCho)) containing Ca^{2+} as a signaling agent and the second composed of DPPC with Encapsulated calcein as the reporter molecule. The sensitizing agent, bacteriochlorophyll (BChl), was incorporated into the liposomal bilayer of DPP1sCho. Dihydrocholesterol (DHC) and DPPE-PEG5000 were also included in the DPP1sCho liposome formulation. The authors proposed that BChl-sensitized photooxidation produced singlet oxygen which mediated cleavage of DPP1sCho vinyl ether bonds, producing two single-chain surfactants whose accumulation in the liposomal membranes led to increased membrane permeability.

It was observed that Ca^{2+}-containing BChl:DPP1sCho:DHC:DPPE-5000 (0.5:85:10:5) could be phototriggered using 800 nm excitation resulting in Ca^{2+} release. Photorelease of Ca^{2+} could activate extravesicular calcium-dependent PLA_2 which in turn catalyzed DPPC hydrolysis, leading to calcein release.

It should be mentioned that activation of bee venom PLA_2, used in the experiments required high Ca^{2+} concentrations (Wymer 1998).

1.3.13.8. Mechanical disruption of liposomes (ultrasound-triggered release)

Acoustically active liposomes have been found to have a potential to carry pharmaceutics and their acoustic activity could enable them to respond to ultrasound stimulation by releasing their contents (Huang 2004). Because they contained air, these liposomes could release their contents upon ultrasound stimulation. As a test molecule, calcein was added in the hydration step. The procedure of freeze-thawing in the presence of mannitol was responsible for solute encapsulation, as well as entrapment of air which was necessary for the liposomal acoustic activity.

An encapsulation efficiency of about 15% was obtained. Three possible kinds of particles could be obtained: (a) those containing just calcein, (b) those containing just

air and (c) those containing both air and calcein. Based on the observation that most echogenic liposomes floated and a rapid pressure drop caused a release of a considerable proportion of their calcein content, the authors concluded that the bulk of the liposomes belonged to the third category, that is, air and calcein entrapped in the same particle.

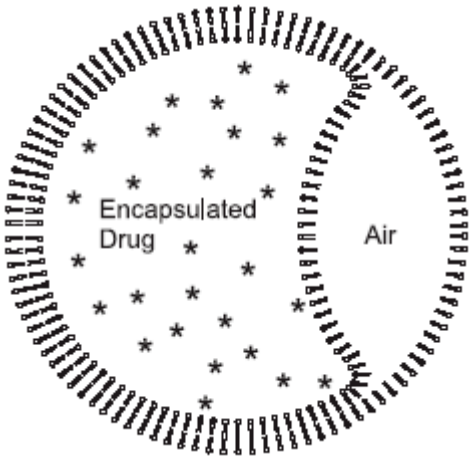

Figure 24 Suggested structure of an acoustically active liposome. It is expected that considerable heterogeneity exists in the preparation such that the proportion of volume occupied by air and aqueous compartments would vary considerably. Another configuration is also possible, a lipid monolayer-covered air bubble within the aqueous compartment of an conventional liposome (Huang 2004).

The authors presumed that upon exposure of acoustically active liposomes to ultrasound, the air pocket expanded, stressing the monolayers bounding it as well as those in the adjacent bilayer (surrounding bilayer in case of an isolated air bubble within the liposome). Because the stress exceeded the elastic limit of the weakest surface, either the bilayer or the monolayers could rend leading to loss of some or all of liposomal contents depending on how long the resealing took.

It was observed that slow pressure reduction was relatively ineffective which might be due to a gradual loss of air by diffusion into the external aqueous phase. 30% ultrasound-triggered release was achieved by applying 1 MHz ultrasound and power of 2 W/cm^2 for 10 s (Huang 2004).

1.3.14. Liposomes as drug delivery vehicles for boron agents

High accumulation and selective delivery of boron into tumor were confirmed to be important factors in BNCT (Barth 1990a 1990b). For favorable therapeutic effect, the ^{10}B concentration should be 20-30 μg ^{10}B per g tumor tissue (20-30 ppm), corresponding to approximately 10^9 ^{10}B atoms per tumor cell (Barth 1992). Although

targeting of ^{10}B to tumors has been extensively investigated (Soloway 1964, Schinazi 1978, Fairchild 1990), most of the targeting approaches have drawbacks.

Most receptors and antigens were found to be present in levels such as 10^4 -10^6 per cell, which in turn means that only complex macromolecular compounds carrying large amount of boron were candidates for receptor- and antigen-mediated delivery (Soloway 1964). Accordingly, receptor or antigen mediated uptake were difficult to be applied (Alam 1989). Also, significant normal tissue uptake of porphyrin derivatives containing boron limited their use in BNCT (Miura 1989, Kahl 1989).

The possibility of developing drug delivery modalities consisting of liposomes as vehicles for boron-containing compounds has been studied. Water-soluble boron agents could be encapsulated in the liposomal aqueous compartment (Shelly 1992, Feakes 1994, Johnsson 1999), whereas lipophilic boron-containing moieties could be incorporatd within the bilayer membrane (Feakes 1995).

It was observed that increasing the concentration of the aqueous borane salt solution in the liposomes had adverse effects on the stability of the liposomes. The encapsulation approach is consequently retarded by the limited amounts of hydrophilic boron compounds which could be encapsulated inside the liposomes. However, incorporation of lipophilic boron compounds in the liposome bilayer was able to increase the boron content of the liposomes without affecting their stability (Feakes 1995).

A nido-carborane lipid with a one-tailed moiety was synthesized (compound **1**, Figure 25) and liposomes were prepared by incorporating it into bilayer consisting of DSPC and cholesterol (Feakes 1995). Structurally, this boron-containing species was characterized by a hydrophilic nido-carborane anion headgroup and a long saturated alkyl tail. The experiments conducted with these liposomes demonstrated that a lipophilic boron-containing compound could be embedded in the bilayer membrane of unilamellar liposomes and delivered selectively to the tumor. Additionally, the liposomes exhibited significantly lower liver and spleen boron concentrations, as compared with previous studies with aqueous sodium salts of borane anions encapsulated in a neutral membrane composed of an equimolar mixture of DSPC and cholesterol (Shelly 1992, Feakes 1994). Moreover, dose enhancement for a given volume of the liposomes could be achieved by incorporating both the hydrophilic and lipophilic boron-containing compounds within the same liposome formulation (Feakes 1995).

Thereafter, a nidocarborane lipid with a double-tailed moiety (compound **2**, Figure 25) was synthesized and could be used in preparation of liposomes without and with helper lipids (Nakamura 2004). The authors evidenced that stable liposomes with high boron content were obtained.

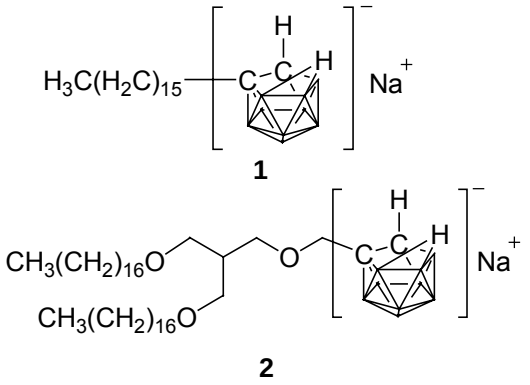

Figure 25 Structures of the lipophilic boron compounds **1** and **2**.

1.4. Experimental techniques

1.4.1. Differential scanning calorimetry (DSC)

The DSC instrument measures the differential power required to maintain the temperature, in up-scan or down-scan mode of a sample (in a suitable solvent) at the same value as the solvent in a reference cell as the overall temperature of the system is altered, at a fixed scan rate. In another words it measures the heat change that occurs during controlled increase (or decrease) in temperature . Power is converted to apparent molar excess heat capacity (kJ $mol^{-1}K^{-1}$).

An adiabatic shield kept at the same temperature as the cells prevents any heat exchange of the cells with the environment so that the heat uptake of the sample corresponds to the known electric power of the heater.

At a certain point, the sample cell needs to be heated more than the reference cell as a result of passing through a transition from one phase to another. At phase transition temperature, extra heat is required in order to maintain the rise in temperature of the sample pan equal to that of the reference. The thermopile between the reference and sample cells senses the off-balance temperature (ΔT) and produces a corresponding voltage. The amplified voltage is used to derive the auxiliary heater on the sample cell, which then acts to keep the off balance signal between the reference and sample cell close to zero. A signal proportional to the differential electrical power supplied to both cells can then be recorded (Y axis) as a function of temperature (X axis) (Leharne 1998).

1.4.2. Isothermal titration calorimetry (ITC)

The partition coefficient for the binding of a ligand to liposomes can be determined by ITC. ITC is based on a series of injections of a liquid sample from a syringe which is under computer control into the calorimeter cell under isothermal conditions.

When ligand (L) is injected into the sample cell containing a solution of macromolecule (M), the two materials interact and heat is released or absorbed in direct proportion to the amount of binding.

The feedback control circuits, linked to heaters around the sample solution, maintain the sample cell at the same temperature as the reference cell (containing the solvent). The increase or decrease in temperature of the solution in the sample cell following injection of an aliquot is compensated by the feedback system to regain the state.

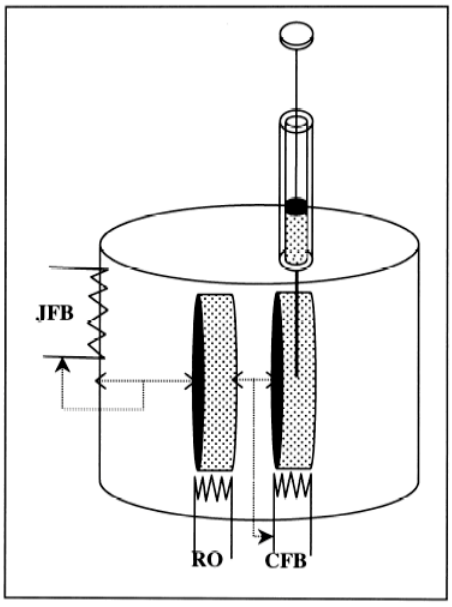

Figure 26 Schematic diagram of a titration calorimeter. The reference cell is heated continuously with a very low power (RO) whereas the mixing cell is connected to a second heater (CFB). Reference and mixing cell are shielded from the environment by an adiabatic jacket which is heated by a third heating system (JFB) (Heerklotz 2000).

The displayed signal is a series of pulses showing rate of heating as a function of time. The area of each injection peak is equal to the total heat released for that injection. When this integrated heat is plotted against the molar ratio of ligand added to macromolecule in the cell, a complete binding isotherm for the interaction is obtained. The time interval between the injections must be sufficiently long for the

new equilibrium state to be reached. This condition is confirmed by a baseline between the pulses.

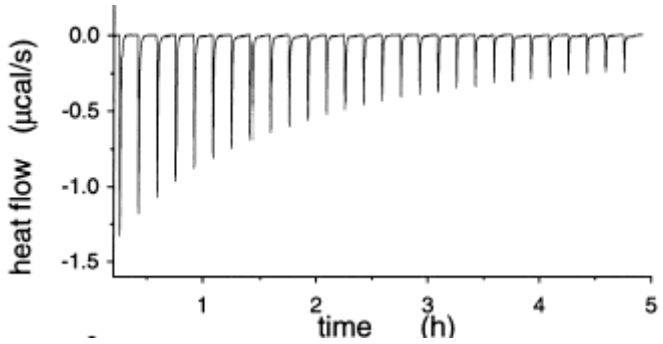

Figure 27 Raw calorimetric data from ITC. Each peak shows the heat produced by serial injections (Heerklotz 2000).

At the beginning of the titration there is an excess of binding sites. As more of the solution from the syringe is added the available binding sites in the cell become saturated until no further net binding occurs. The exothermic or endothermic heat change will be large initially and will be reduced until no further binding is possible (the only heat observed at this point is that resulting from the dilution of the syringe contents into the solution in the calorimeter cell) (Blandamer 1998, Tame 1998).

1.4.3. Fluorescence resonance energy transfer (FRET)

FRET is a distance-dependent interaction between the electronicly excited states of two dye molecules. Thus, the emission energy of a donor fluorochrome acts as the excitation energy for an acceptor fluorochrome. Accordingly, FRET is an excellent tool for investigating a variety of biological phenomena that produce changes in molecular proximity.

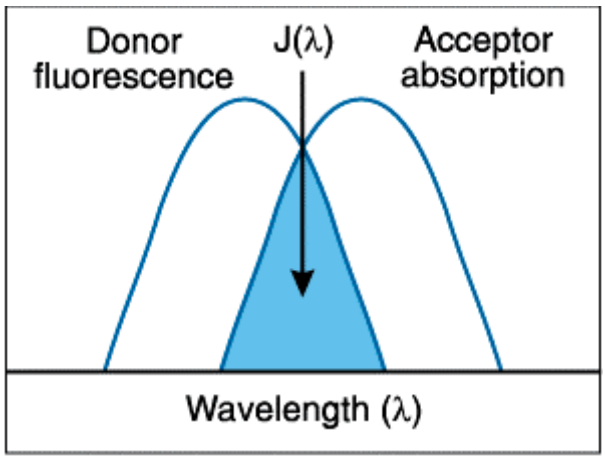

Figure 28 Schematic diagram illustrating the spectral overlap of the donor emission and the acceptor absorption (meds.queensu.ca/qcri/flow/2photon.html).

If FRET takes place, one should observe a decrease of donor intensity accompanied with an increase of acceptor intensity, due to the fact that part of the donor excited state energy has been transferred and is not available to be used for donor fluorescence emission (Szöllõsi 2002, Nunes-Correia 2002).

1.4.4. Cryo-transmission electron microscopy (Cryo-TEM)

Cryo-TEM was found to be an important tool for the investigation of structures formed by amphiphilic molecules in aqueous solutions. In the cryo-TEM method the solution is applied to a microscopy grid in such a way that a very thin aqueous film is formed. The thin film is then plunged into liquid ethane just above its freezing point where the film very rapidly vitrifies without crystallization. After vitrification, the grid with the vitrified film is transferred to the microscope, and examined at liquid nitrogen temperature. The method enables the structures captured in the vitrified film to be observed without dehydration and consequently no important reorganization takes place. The difference in electron density between the atoms of the amphiphile and the surrounding water is responsible for the contrast. Because ~4 nm is the smallest dimension that can be resolved, the rounded shape and the inner aqueous compartment of a liposome can be seen, whereas micelles are seen as dots. The thickness of the film, as well as the upper size of an object is limited to about 500 nm; otherwise the scattering of electrons by water gets too large and the cooling rate during vitrification too slow (Almgren 2000).

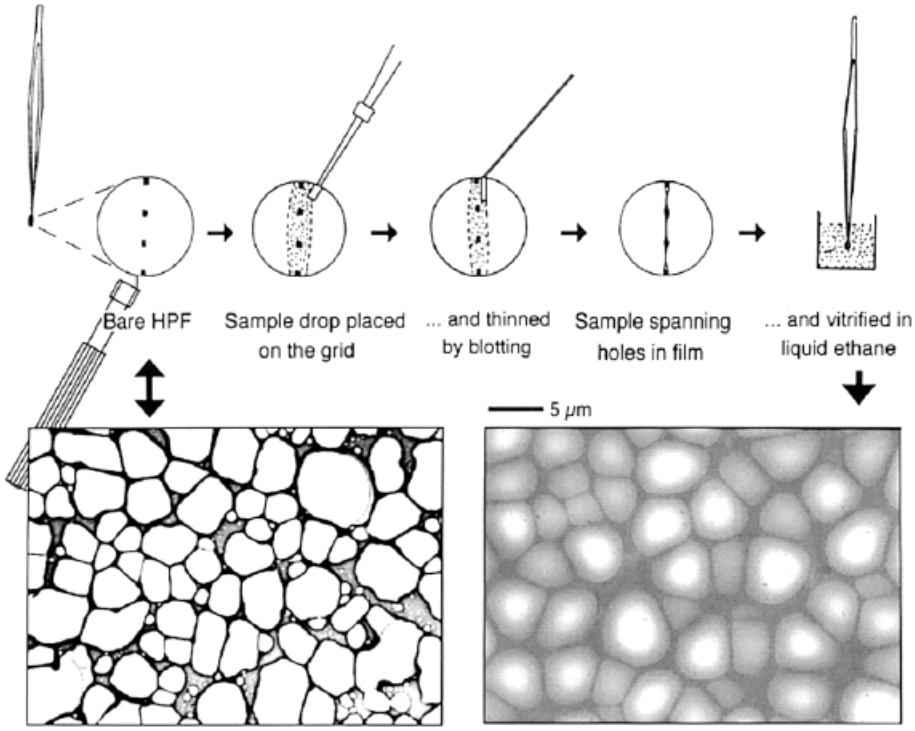

Figure 29 A holey polymer film, empty and after sample application, blotting and vitrification (Almgren 2000).

A climate chamber is used to prevent evaporation during the film preparation. Egelhaaf et al. developed controlled environment vitrification system for cryo-TEM (Egelhaaf 2000). A chamber reduces the time between blotting and vitrification, during which the sample is susceptible to changes.

The chamber is formed from two concentric Plexiglas tubes (a) and (b). Through their interspace, water of an appropriate temperature is circulated allowing thermal isolation of the chamber from its surrounding. Humidity is controlled by a gentle flow of gas which has the desired saturation and temperature.

The samples can be equilibrated inside the chamber using a special holder (c) and then transferred to the support grid. The specimen support grid with the holey carbon film is held by tweezers (d), which can be propelled downwards by a pneumatic cylinder. The plunge velocity (3 m s^{-1}) together with the plunge depth (30 mm) and the high cooling rate (of the order of 10^6 K s^{-1}), ensures that the sample reaches the cryogen temperature before it stops.

Crystallization of the vitrified sample or its contamination with water crystals due to humidity is avoided. Thus, a constant dry atmosphere inside the polystyrene box (h) containing the liquid cryogen is maintained by a continuous flow of cold and dry nitrogen generated by the evaporation of liquid nitrogen. This is obtained by a gentle

heating with a resistor (i) placed in the liquid nitrogen. The liquid nitrogen level is indicated by a wooden stick (k). The cryogen (ethane) is kept in a small vessel (m), which can be moved vertically and fixed at two heights. During plunging the vessel is in the upper position. After plunging it is slowly lowered, which removes the vitrified specimen from the cryogen while allowing the cryogen to drain off. The whole polystyrene box is then shifted, which positions the grid over a second vessel (n). This vessel is filled with liquid nitrogen and contains a transfer box. Finally, the sample is transferred to the microscope.

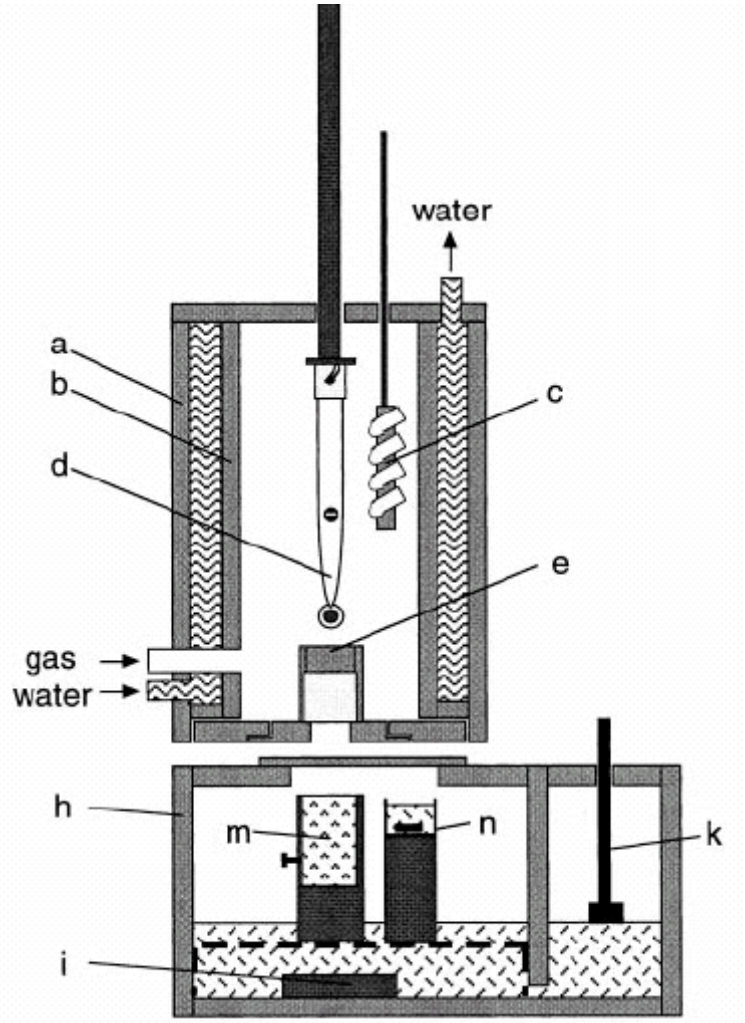

Figure 30 Schematic diagram of controlled environmental vitrification system and cryogen reservoir (Egelhaaf 2000).

1.4.5. Assessment of cell cytotoxicity

Tetrazolium salts are used extensively in cytotoxicity assays (Berridge 1996). In the assay, tetrazolium salts are metabolically reduced to highly colored end products called formazans. The tetrazolium salt WST-1 (4-[3-(4-Iodophenyl)-2-(4-nitrophenyl)-

2H-5-tetrazolio]-1,3-benzene disulfonate) is efficiently reduced by mitochondrial dehydrogenases in viable cells to soluble formazan. An increase in the number of metabolically active cells results in an increase in the overall activity of mitochondrial dehydrogenases, leading to an increase in the amount of formazan dye formed. The produced formazan dye is quantified by a scanning multiwell spectrophotometer (ELISA reader).

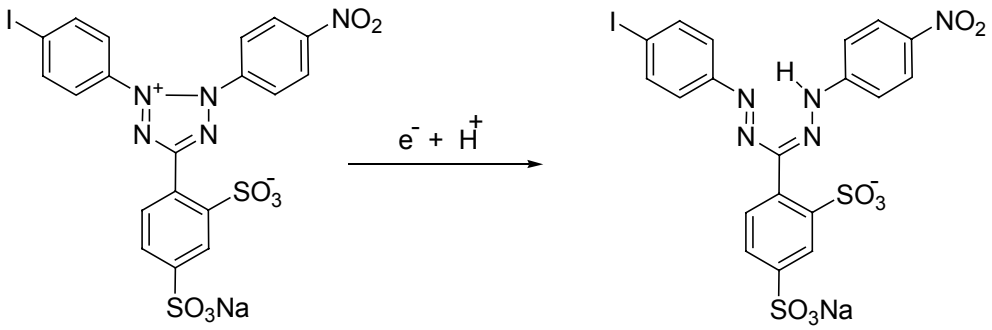

A B

Figure 31 Cleavage of the tetrazolium salt WST-1 (A) to formazan (B).

2. Aim of the work

Previous studies in our working group have evidenced a strong and persistent binding of BSH to tumor tissue (Otersen 1997). The investigations of Lutz et al. showed an interaction of BSH with the choline headgroups of PC (Lutz 2000). Thereafter, Neumann et al. found that BSH was strongly associated with the extracellular structures, the cell membrane and the electron dense regions within the nucleus of glioblastoma multiform tissue sections of patients having received BSH prior to surgery (Neumann 2002). For this reason, we decided to further investigate this phenomenon by studing the interaction of BSH with model membranes.

2.1. Determination of physical changes induced in different liposomal formulations by BSH

Liposomes of different compositions were prepared and used as a model for cell membrane. The interaction of BSH with liposomes consisting of DODAB alone or with DOPC or DOPE were investigated by determining the zeta potential and the particle size of these liposomes as a function of BSH concentration. We assumed a firm binding of BSH with the headgroups of the liposomes. We wanted to further investigate this phenomenon. Accordingly, we determined the changes in thermodynamic parameters induced in liposomes composed of DMPC or DPPC by BSH using the DSC. The partition coefficient and the enthalpies for the binding of BSH to that liposomes were determined by ITC. The stability of the liposomes in absence and presence of BSH was checked by performing leakage experiments. Their morphology was examined by cryo-transmission electron microscopy (cryo-TEM). We found that the BSH-induced changes in the liposomes led to a release of their contents as confirmed by the leakage experiments.

2.2. Triggered release of liposome contents by BSH

We proved that BSH can be used as a tool to trigger the release of substances encapsulated in liposomes. Our next goal was to optimize the conditions of the leakage experiments since the rates and release levels were confirmed to be dependent on the liposome composition as well as the BSH concentrations. We prepared various liposomal formulations in order to establish the lipid composition susceptible to BSH. Liposomes composed of mixture of DPPC mixed with 2 mol% DSPE-PEG2000 were prepared and the ability of BSH to perturb their membranes

was determined. Also, we tried to find out a mechanism by which the mode of action of BSH can be explained.

2.3. Synthesis and liposomal preparation of two dodecaborate cluster lipids for boron neutron capture therapy

Because of the relatively large intracellular accumulations of boron (approximately 20-30 μg of boron-10 per gram of tumor) required for successful BNCT, a selective delivery of boron-10 to tumor tissues was necessary. For this reason, we decided to incorporate boron-containing lipids into liposomes using them for transporting boron to the tumor site. A new class of lipids, containing the *closo*-dodecaborate cluster; S-(N,N-(2-dimyristoyloxyethyl)-acetamido)-thioundecahydro-closo-dodecaborate (2-) and S-(N,N-(2-dipalmitoyloxyethyl)-acetamido)-thioundecahydro-closo-dodecaborate (2-), was synthesized and incorporated into liposomal formulations to increase the therapeutic efficiency of BNCT.

3. Results

3.1. Interaction of BSH with cationic liposomes (Appendix I)

BSH changed the positive zeta potential values of cationic liposomes consisting of DODAB to neutral and then to negative values. We explain this by a firm binding of BSH to the positively charged head groups of the liposomes.

Maximum particle size and minimum zeta potential values were recorded when BSH was added in a concentration approximately half of that of the lipid. The particle size was smaller at both higher and lower concentrations of BSH.

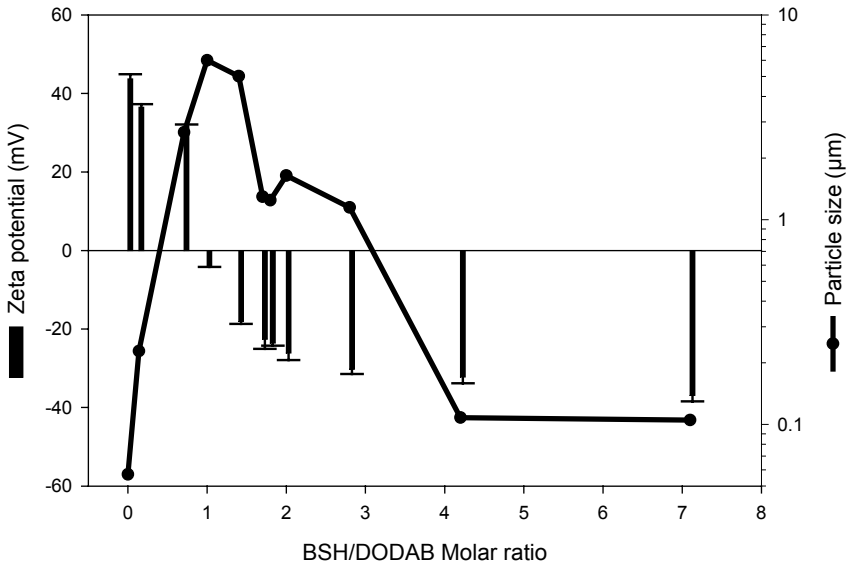

Figure 32 Zeta potential and particle size of DODAB liposomes as a function of the molar ratio between BSH and the lipid.

Similarly, when BSH was added to cationic liposomes prepared from DODAB/DOPC and DODAB/DOPE, the zeta potential passed from positive to negative values. Maximum particle sizes were recorded at zeta potential value of ~0 mV.

3.2. Interaction of BSH with neutral liposomes prepared from DMPC (Appendix III)

3.2.1. Cryo-TEM

Cryo-TEM showed severe changes in the shape of DMPC liposomes under the effect of BSH.

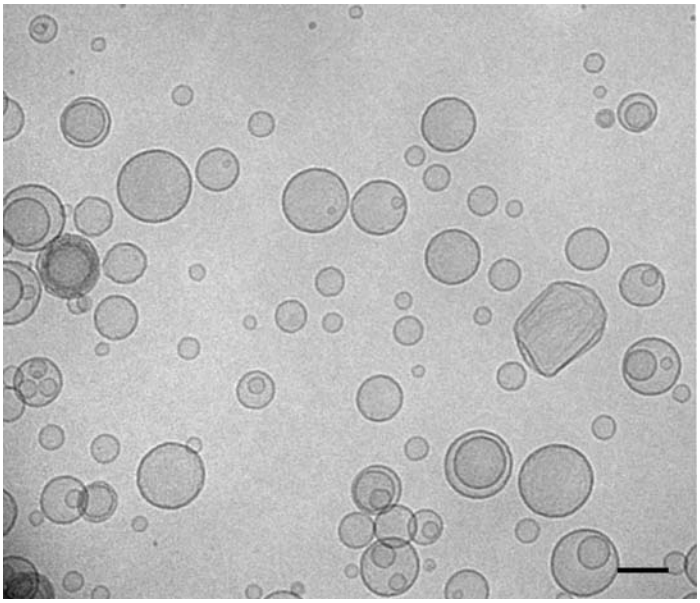

Figure 33 Cryo-TEM of 10 mM DMPC liposomes. Scale bar 100 nm.

DMPC liposomes were incubated with either 10 or 100 mM BSH overnight at different temperatures (4, 25, 37°C). Aggregation and thickening of the walls of the liposomes were generally observed, but were more pronounced at 25 and 37°C.

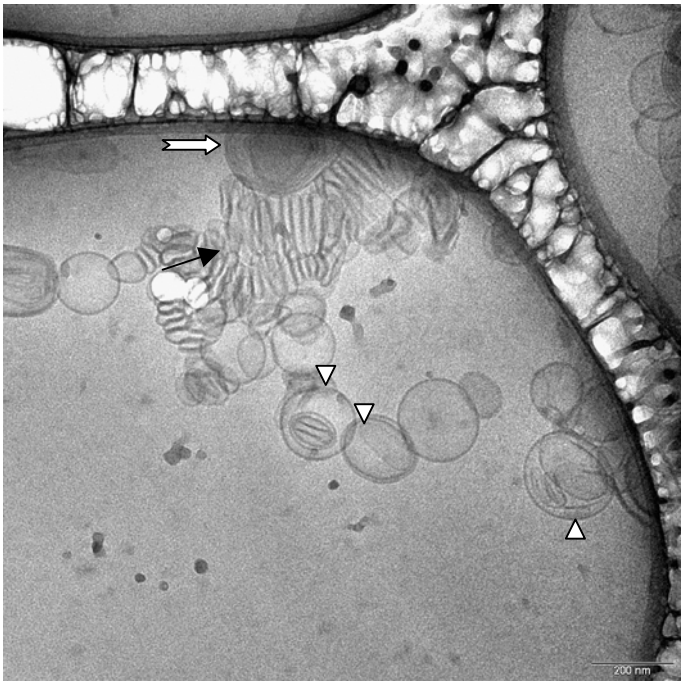

Figure 34 DMPC liposomes (10 mM lipid) incubated with 10 mM BSH overnight at 4°C. Scale bar 200 nm. The white arrow indicates compact multilamellar structure. The black arrow aggregate of unilamellar liposomes which are flattened in the contact region. The arrowheads indicate lipid bilayers built around another liposomal structures.

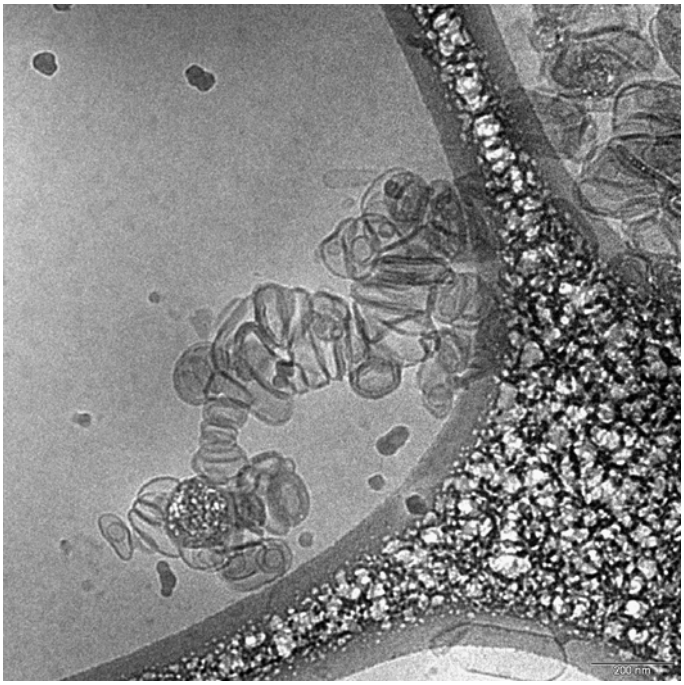

Figure 35 DMPC liposomes (10 mM lipid) incubated with 100 mM BSH overnight at 4°C.

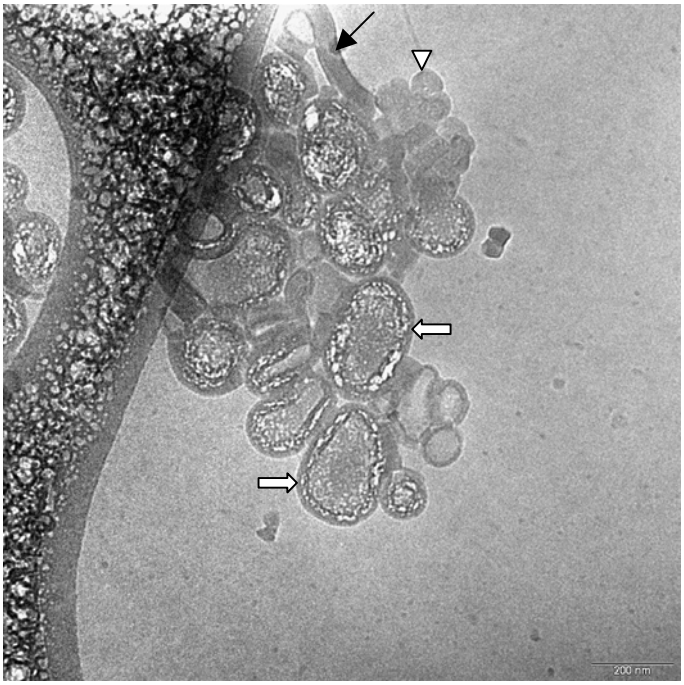

Figure 36 DMPC liposomes (10 mM lipid) incubated with 10 mM BSH overnight at 25°C. The black arrow indicates stack of tightly associated lipid bilayers which are not closed. The arrowhead indicates aggregated multilamellar liposomes. The white arrows mark multilamellar complexes containing lipid structures (most probably hexagonal phases). A rather radiation damage can be noticed (white spots).

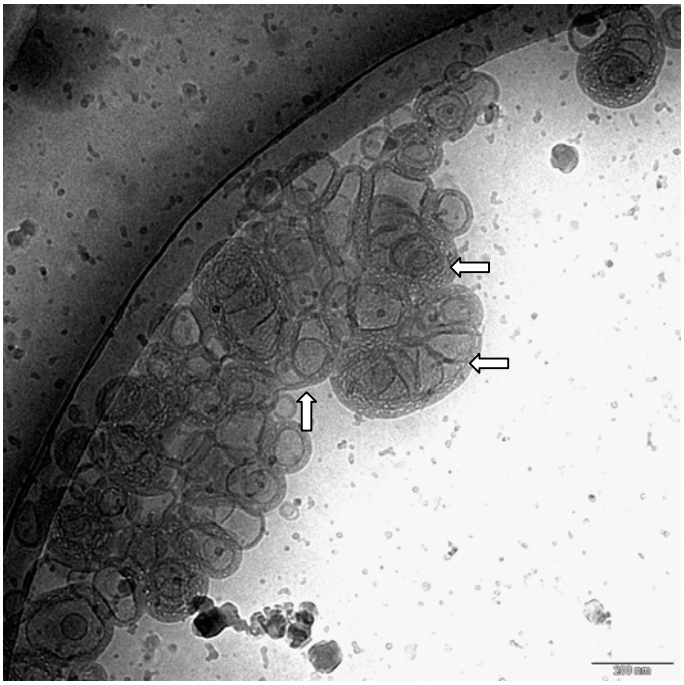

Figure 37 DMPC liposomes (10 mM lipid) incubated with 100 mM BSH overnight at 25°C. The arrows mark multilamellar structures enclosing either deformed or multilamellar liposomes.

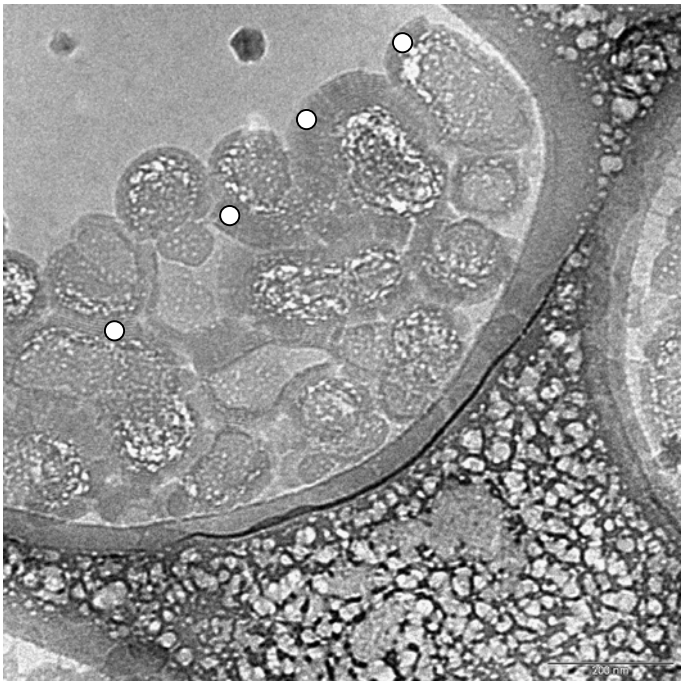

Figure 38 DMPC liposomes (10 mM lipid) incubated with 10 mM BSH overnight at 37°C. The circles indicate incomplete outer bilayers.

For liposomes incubated with 100 mM BSH at 37°C, open structures could be seen in the images.

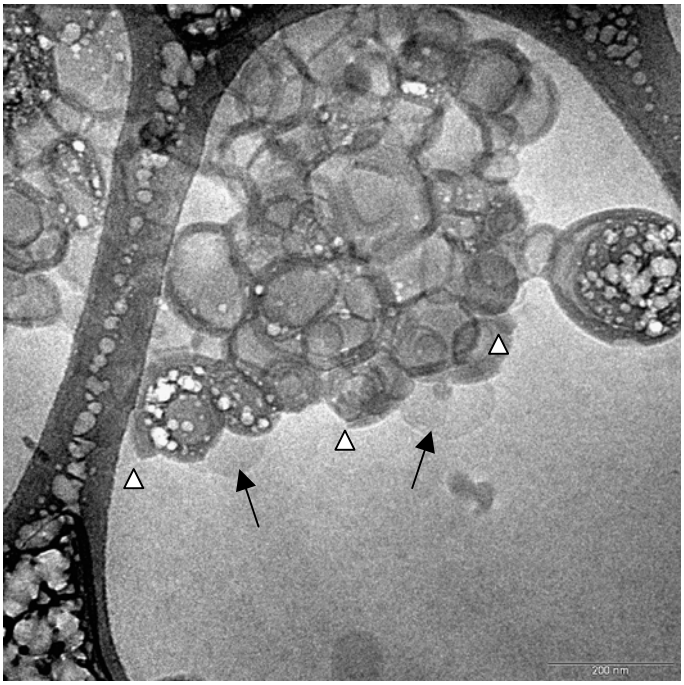

Figure 39 DMPC liposomes (10 mM lipid) incubated with 100 mM BSH overnight at 37°C. The arrowheads mark unclosed bilayer, whereas the arrows indicate open bilayer sheets.

3.2.2. Effect of choline

The effect of choline on the interaction between BSH and DMPC liposomes was checked by carrying out cryo-TEM and zeta potential experiments with a mixture of choline and BSH instead of BSH alone. It was observed that the presence of choline resulted in a reduction in morphological changes induced in the liposomes. In addition, zeta potential measurements indicated that a mixture of BSH and choline had less influence on zeta potential compared to the effect exerted by BSH alone.

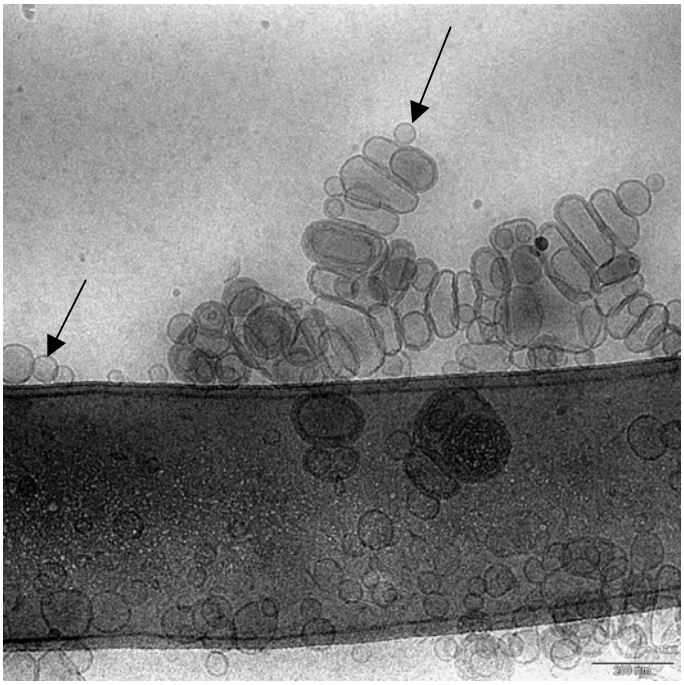

Figure 40 DMPC liposomes incubated with a mixture of 10 mM BSH and 400 mM choline overnight at room temperature. The arrows indicate the presence of original liposomes.

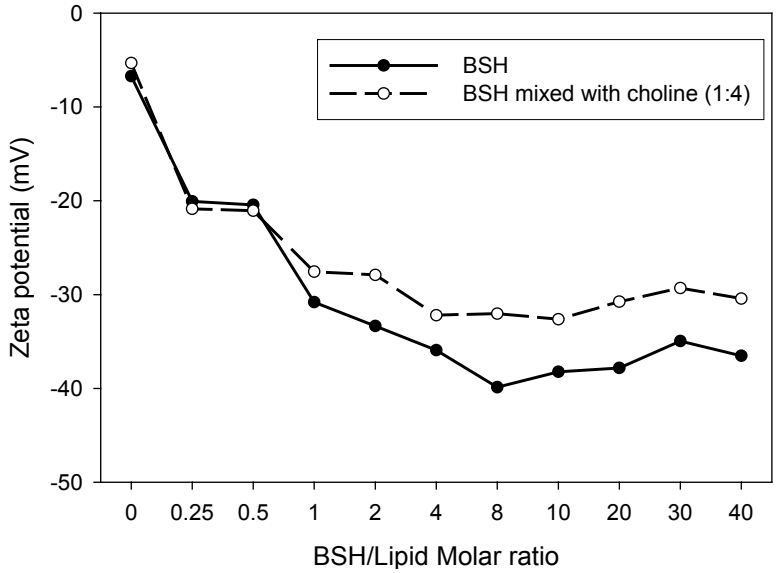

Figure 41 Zeta potential as a function of the concentration of either BSH or of a mixture of BSH and choline.

3.2.3. DSC

DSC upscans demonstrated that DMPC liposomes had a main transition peak at 24.3°C as well as a pretransition peak at 14.95°C. Very low concentrations of BSH led to disappearance of the pretransition peak.

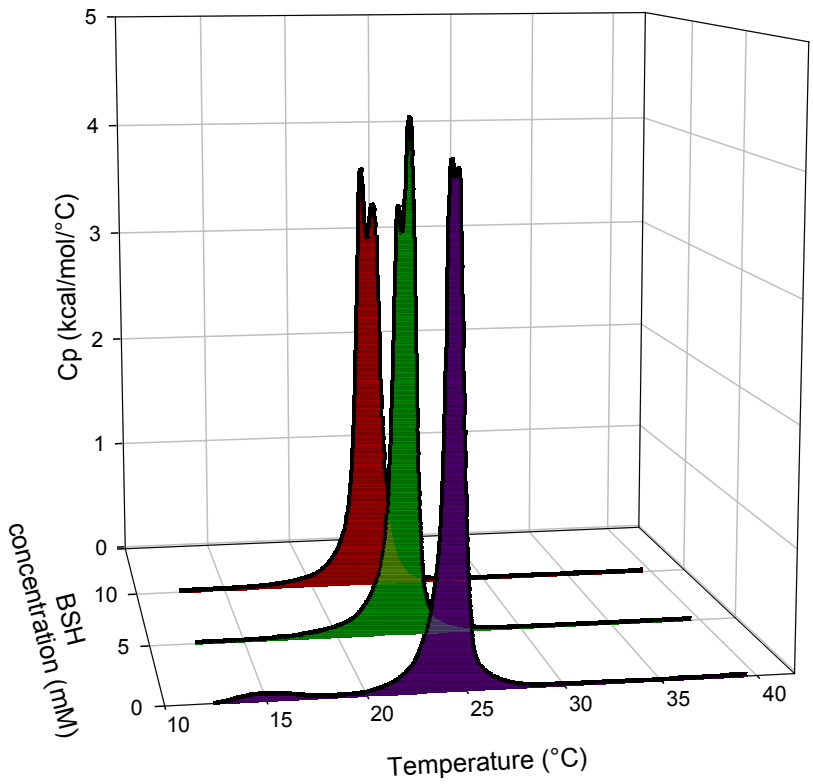

Figure 42 DSC scans of 10 mM DMPC liposomes without and with small concentrations of BSH.

It was also recorded that increasing BSH concentrations lowered the main transition temperature of DMPC liposomes. The main transition temperature increased, however, again at concentrations higher than 100 mM BSH. A broad and small peak appeared at 25.59°C when the liposomes were incubated with 50 mM BSH. Interestingly, increasing BSH concentrations resulted in a shift of this peak to higher temperatures.

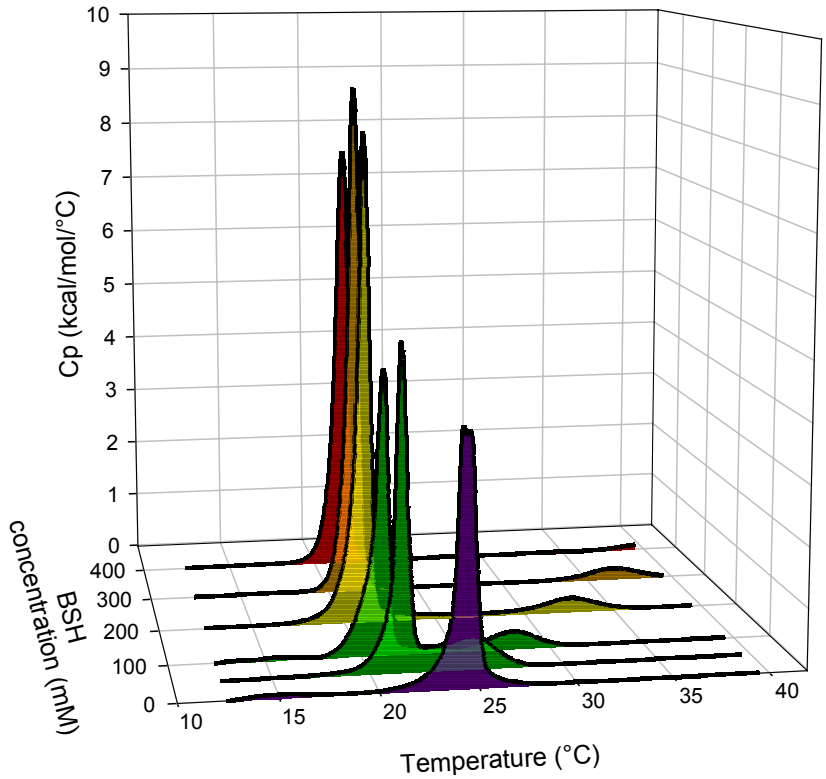

Figure 43 DSC scans of 10 mM DMPC liposomes with varying concentrations of BSH.

Moreover, concentrations more than 100 mM BSH led to a significant increase in the total enthalpy change.

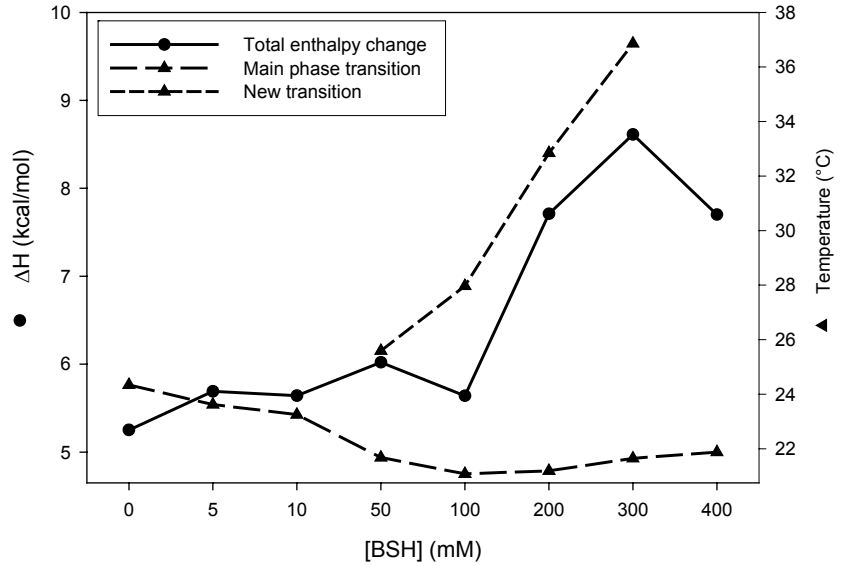

Figure 44 Phase transition temperatures and total enthalpy change of DMPC liposomes as a function of BSH concentrations. 10 mM DMPC liposomes are incubated with different concentrations of BSH for 2h at 4°C before the start of the scan.

The calorimetric titration data demonstrated that binding of BSH to DMPC liposomes is a weak one, with an association constant similar to an enzyme-substrate binding. The upward curvature of the apparant association isotherm means that further BSH molecules are bound more avidly or that a large number of binding sites become available. In other words, the association constant increases with the increasing amounts of BSH bound.

Titration with higher BSH concentrations did not work. High BSH concentrations have high dilution heat which interferes with the heat released by the binding of BSH to the liposomes. We worked, however, with BSH concentration range having insignificant heat of dilution. Consequently, the heat release is probably not influenced by other phenomena.

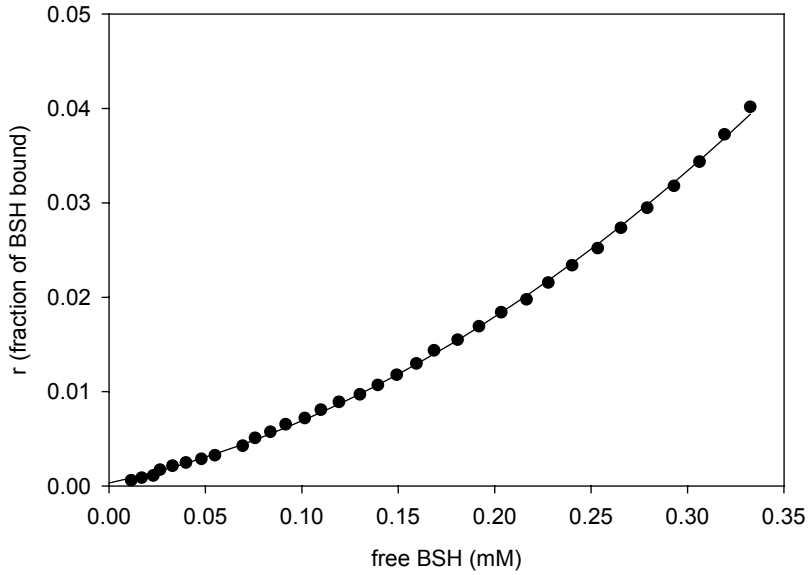

Figure 45 Apparant association isotherm (binding ratio versus free BSH concentration).

3.2.4. Leakage

The BSH-induced changes in the liposomal morphology suggest that there must have been release of content. Accordingly, we followed the liposome content release by dequenching of carboxyfluorescein encapsulated in liposomes at self-quenching concentration. The results obtained from leakage experiments evidenced the ability of BSH to induce leakage of contents of DMPC liposomes, an effect associated with BSH and which could not be achieved by other divalent anions.

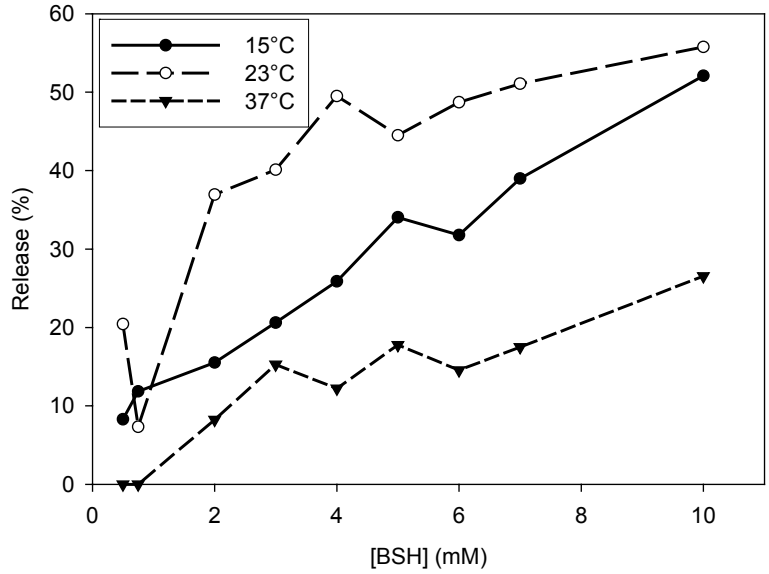

Figure 46 Extent of leakage of CF from DMPC liposomes, expressed in release percentages after 3 minutes incubation, as a function of BSH concentration, at 15, 23 and 37°C.

3.2.5. Lipid mixing

Lipid mixing of the liposomal membranes was determined as a function of BSH concentrations and found to be very limited.

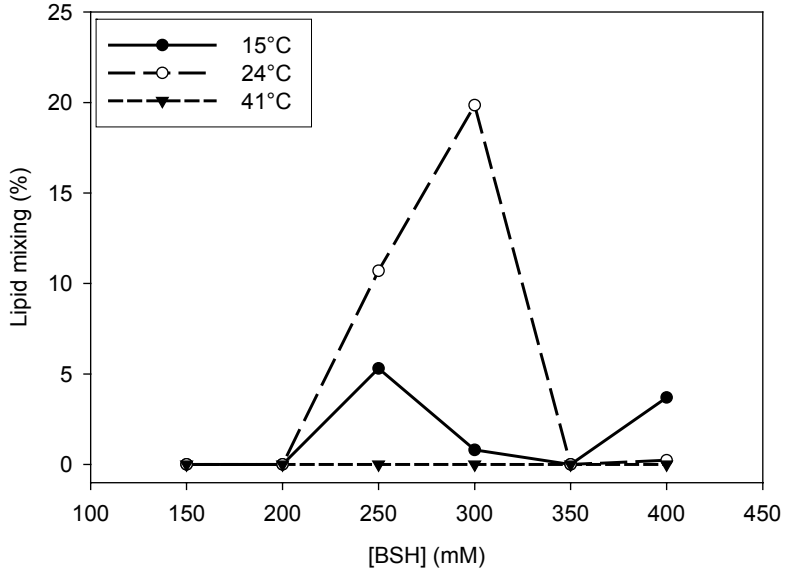

Figure 47 Percentage of lipid mixing versus BSH concentration.

3.3. Interaction of BSH with neutral liposomes composed of DPPC (Appendix II)

Cryo-TEM images indicated that incubation of DPPC liposomes with BSH at 37°C led to their aggregation. When the liposomes were incubated with BSH at 45°C, the aggregation and deformation of their shapes were dramatic.

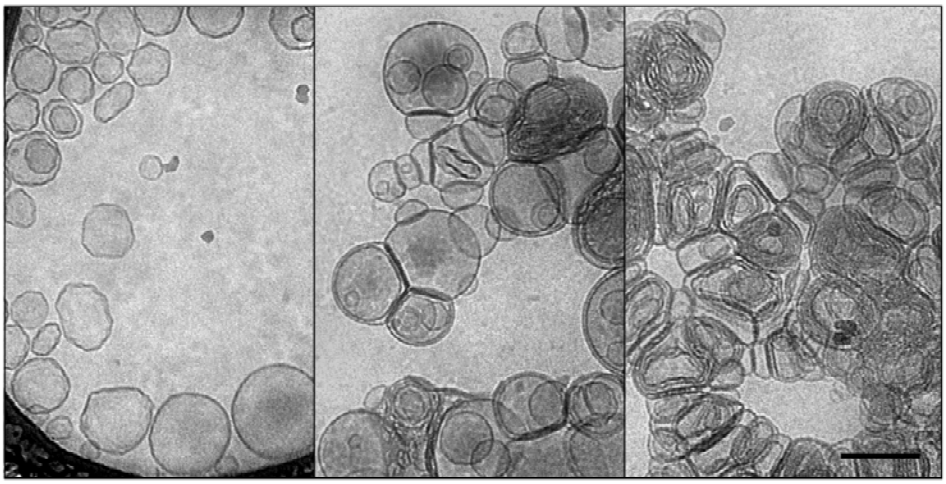

Figure 48 Cryo-TEM pictures of 10 mM DPPC liposomes (left) incubated with 10 mM BSH at 37°C (center) and 45°C (right).

BSH was confirmed to trigger release of DPPC liposomes content in a dose-dependent manner.

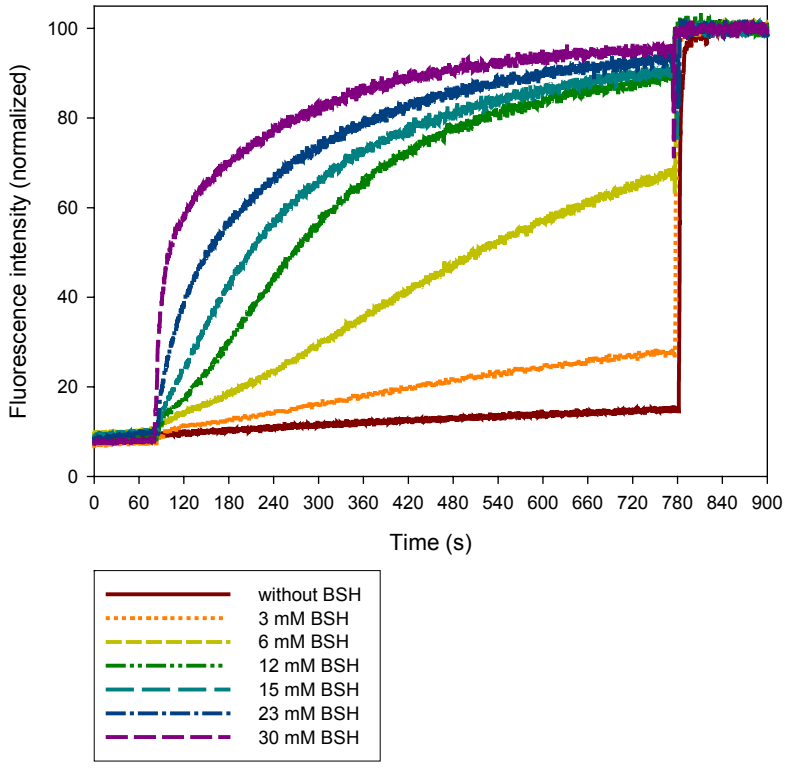

Figure 49 Release of CF (measured as increase of fluorescence) from DPPC liposomes.

The DSC scans demonstrated that BSH lowered both the main and pretransition temperatures of DPPC liposomes.

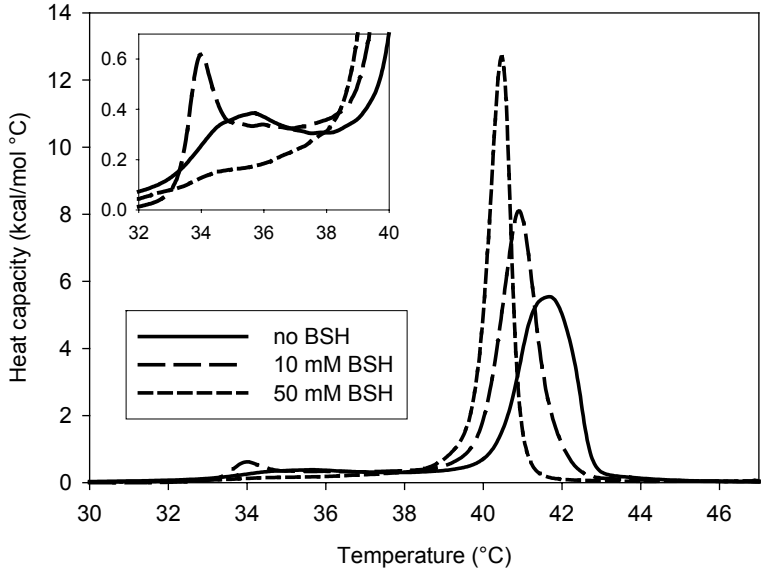

Figure 50 DSC scans of 5 mM DPPC in absence and presence of 10 and 50 mM BSH. Inset: Enlargement of the pretransition area.

3.4. Interaction of BSH with DPPC:DSPE-PEG (98:2 mol%) liposomes (Appendix II)

When we investigated the effect of BSH on the extent of content release of liposomes composed of DPPC:DSPE-PEG2000 at 98:2 molar ratio, we found that BSH was able to induce their leakage. Additionally, we noticed that low BSH concentrations resulted in sigmoidal release curves. The initial velocity and extent of release were dependent on BSH concentration.

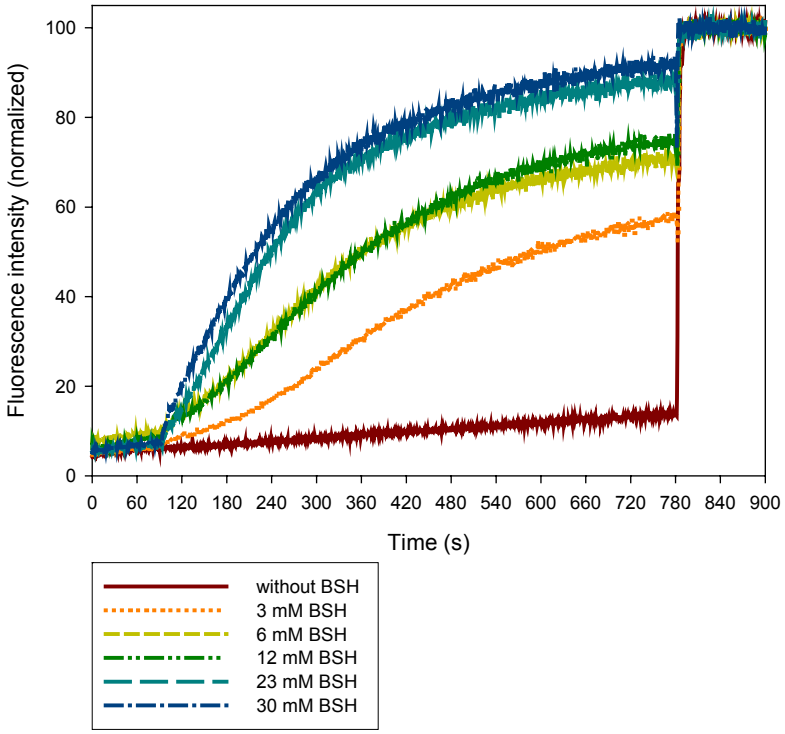

Figure 51 CF release from DPPC:DSPE-PEG (98:2 mol%) liposomes.

Another important observation was that BSH did not induce changes in morphology of DPPC-PEG liposomes, although their contents were released rapidly, indicating that BSH can exert its effects on the isolated liposomes.

A combination of BSH and doxorubicin-containing DPPC-PEG liposomes resulted in higher cytotoxicity levels compared to those obtained when the cells were exposed to BSH or to doxorubicin-containing DPPC-PEG liposomes alone.

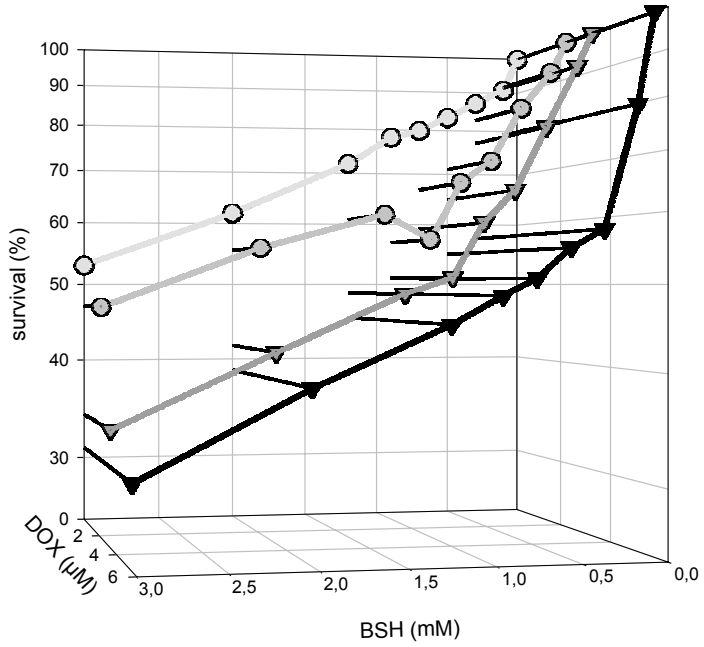

Figure 52 Cell survival of V79 Chinese hamster cells exposed to BSH and/or increasing amounts of doxorubicin-containing liposomes prepared from DPPC with 2 mol% DSPE-PEG.

3.5. Synthesis and liposomal preparation of two dodecaborate cluster lipids for BNCT (Appendix IV)

Two dodecaborate cluster lipids with a double-tailed moiety were synthesized (S-(N,N-(2-dimyristoyloxyethyl)-acetamido)-thioundecahydro-closo-dodecaborate (2-) (B-6-14) and S-(N,N-(2-dipalmitoyloxyethyl)-acetamido)-thioundecahydro-closo-dodecaborate (2-) (B-6-16)).

The DSC measurements indicated that B-6-14 and B-6-16 had main phase transition temperatures of 18.8 and 37.9°C, respectively. B-6-14 could form liposomal vesicles above its transition temperature, whereas upon cooling below the transition temperature, stiff bilayers were formed.

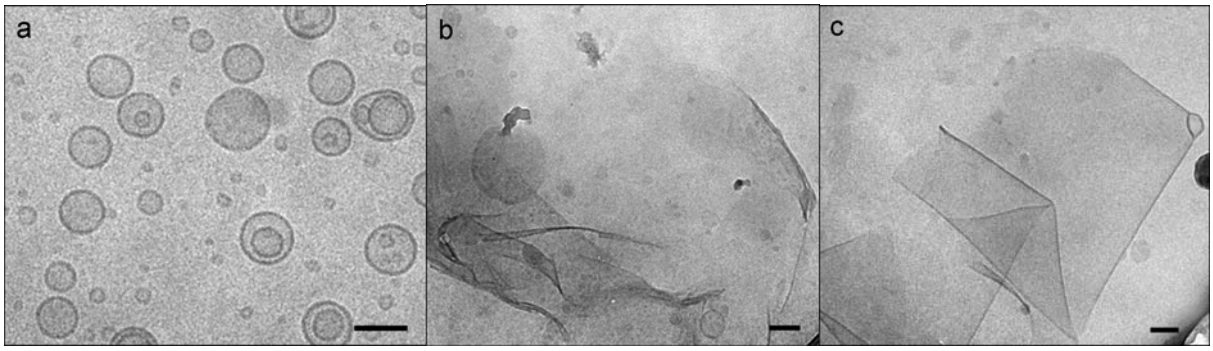

Figure 53 Cryo-TEM pictures of a preparation of B-6-14 prepared by extrusion at 50°C and vitrification from 30°C(a), prepared by extrusion at 50°C, storage at 4°C for one week and vitrification from 25°C (b) and B-6-16 prepared as sample b (c). Scale bare 100 nm.

The cryo-TEM images demonstrated that boron cluster lipids were able to form liposomes in the presence of distearoylphosphatidylcholine and cholesterol as helper lipids. The two liposomal formulations were found to be highly negatively charged.

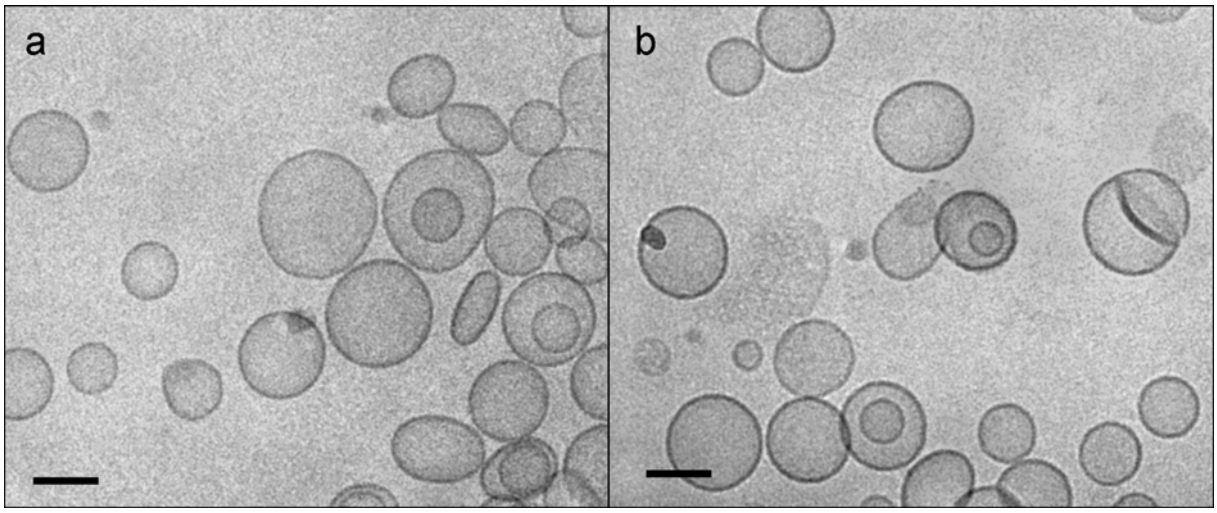

Figure 54 Cryo-TEM pictures of liposomes prepared from an equimolar mixture of DSPC, cholesterol and B-6-14 (a) or B-6-16 (b). Scale bar 100 nm.

4. Discussion

4.1. Interaction of BSH with cationic liposomes (Appendix I)

The interaction between BSH and cationic liposomes synthesized from DODAB was investigated by determining the zeta potential, which provides a measure of the liposome net charge, and the size of the particles as a function of the molar ratio between BSH and the lipid.

Neutralization of the surface charge of DODAB liposomes by BSH was observed indicating a firm binding of BSH with the head groups of the liposomes.

Large aggregates were observed at neutral zeta potential values. We concluded that the positively or negatively charged particles repelled each other and remained separate, whereas the neutral complexes tended to stick together.

Cationic liposomes composed of binary mixtures of lipids that contained either DOPC or DOPE as the neutral lipid and DODAB as the cationic lipid were prepared. The BSH concentration required to neutralize their surface charges and to produce maximum particle sizes was generally higher than that required for the same amount of pure DODAB liposomes. We suggest that the BSH binding to pure DODAB liposomes is stronger than that to DODAB/DOPC or DODAB/DOPE liposomes.

4.2. Interaction of BSH with neutral liposomes prepared from DMPC (Appendix III)

Neutral liposomes composed of DMPC were prepared and subjected to the action of BSH.

Cryo-TEM pictures for DMPC liposomes incubated overnight with BSH at different temperatures indicated extensive changes in the liposomal morphology, especially at higher temperatures (37°C). We explain formation of these structures by a mechanism involved rupture of some of the aggregating liposomes and wrapping of their membranes around another intact liposomes.

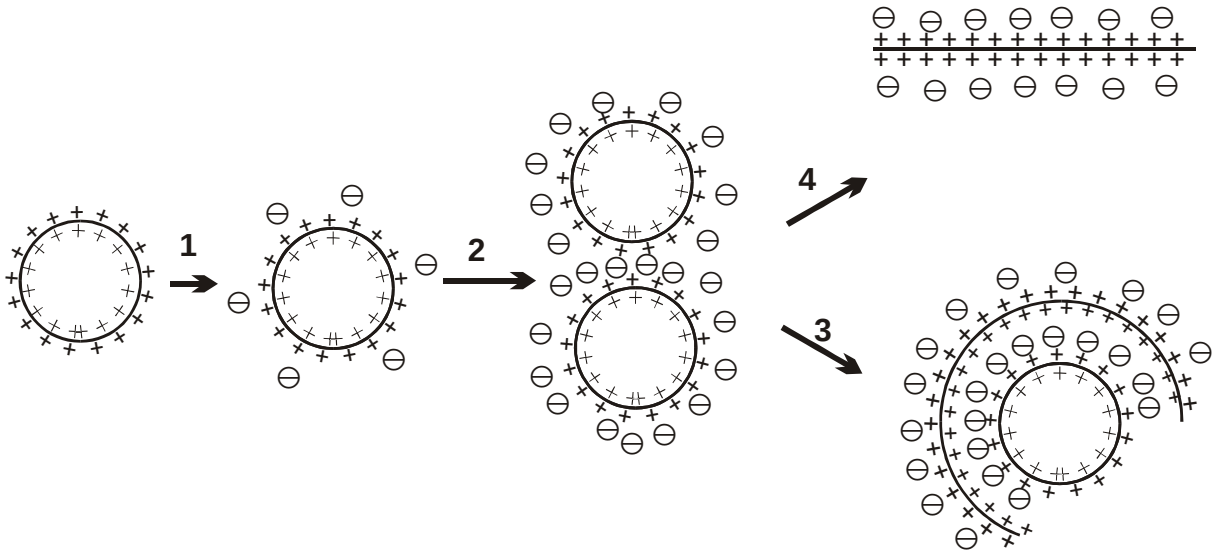

Figure 55 Schematic diagram illustrating the hypothesized mechanism of action of BSH. Choline groups of the liposomes are symbolized by positive signs, whereas BSH molecules are symbolized as negative circles.

The proposed mechanism entails the formation of liposomal aggregates under the effect of BSH due to an electrostatic interaction between BSH molecules and choline groups of the liposomes (Step 2).

A strong adherence between the liposomes leads to a rupture of some of them (Step 3). The resulting open bilayers either build around a central vesicle or cover only parts of the inner liposomes producing concentric bilayers of multilamellar liposomes or open bilayer segments. We assume that BSH molecules act as adhesion points between the bilayers stabilizing the formed multilamellar complexes.

Opening of the liposomes into bilayer sheets occurs at high temperature and high BSH concentration.

The influence of choline presence on the effectiveness of BSH was investigated and found to inhibit the BSH action to an extent. This observation is an evidence that the quaternary ammonium salt in the liposomes headgroups is required for an interaction with BSH.

Using DSC, we recorded the phase transition behavior of DMPC liposomes in absence and presence of different concentrations of BSH. We observed that low concentrations of BSH led to a disappearance of the pretransition peak. We could not clarify if this phenomenon is due to the influence of BSH on the headgroup behavior or on the acyl chain packing. A shift in the main transition of DMPC liposomes to lower temperatures in the presence of BSH indicated an increase in the alkyl chain

mobility which in turn means bilayer perturbation (Różycka-Roszak 2004). The main transition temperature started, however, to increase again when the liposomes were incubated with concentrations higher than 100 mM BSH. Additionally, the enthalpy change increased significantly with BSH concentration over 100 mM. An ordering effect induced by high BSH concentrations probably gives rise to this behavior (Ali 2000). Hysteresis was observed between the heating and cooling scans and interpreted by formation of dehydrated structures (Hobai 1998, Epand 2000), most probably bilayers sandwiching the BSH molecules between them.

For liposomes incubated with 50 mM BSH, a small third peak was recorded at 25.59°C. The peak's position was found to be dependent on BSH concentrations, where increasing BSH concentrations resulted in a shift of this peak to higher temperatures. We attribute this peak to stable structures which may also possess dehydrated headgroups. Similar results were obtained when the interaction of DNA with PC liposomes has been investigated using DSC (Süleymanoglu 2004). Süleymanoglu explained a shift in lipid-DNA nanocondensate transition toward higher temperatures by an increase in thermal stability of DNA-mediated ternary complex. Additionally, Giehl et al. interpreted a shoulder at higher temperatures in their DSC scans by a partial dehydration of the headgroup region (Giehl 1999).

The upward curvature of the apparent association isotherm have two explanations: (1) BSH molecules bound cooperatively to DMPC liposomes, (2) at higher binding ratios, a larger number of binding sites became available due to formation of new structures.

We recorded leakage of contents of DMPC liposomes under the effect of BSH and explained it by deformation and/or rupture of the extensively aggregated liposomes. The extent of release was found to be maximum near the phase transition of DMPC (23°C), whereas it was significantly lower at higher and lower temperatures.

We started to test the ability of BSH to trigger release of contents of different liposomal formulations with the main phase transition just above the physiological temperature.

4.3. Interaction of BSH with neutral liposomes prepared from DPPC (Appendix II)

We proved that DPPC liposomes release their contents upon addition of BSH. BSH showed a concentration-dependent effect on the extent and initial rate of leakage. Sigmoidal release was recorded only at low BSH concentrations.

Cryo-TEM images showed aggregation and deformation of 10 mM liposomes incubated overnight with 10 mM BSH. The changes in liposomal shape were drastic for liposomes incubated with BSH at 45°C compared to those obtained when the experiment was carried out at 37°C. The lesser extent of aggregation or deformation at lower temperatures was expected since lowering the temperature causes an increased rigidity of the bilayer membrane.

4.4. Interaction of BSH with DPPC:DSPE-PEG (98:2 mol%) liposomes (Appendix II)

Sterically stabilized liposomes are used clinically due to their ability to circulate for prolonged periods with stable retention of their contents (Gabizon 1988, Blume 1990). However, because of the stable lipid composition of sterically stabilized liposomes, they have low clinical activity (Meerum Terwogt 2002). This is because only a small fraction of the drug can release from the liposomes (Eliaz 2004).

We studied the interaction of BSH with liposomes prepared from DPPC and PEG lipid at a molar ratio 98:2. By mixing DPPC and DSPE-PEG at a 98:2 molar ratio, liposomes nearly impermeable to carboxyfluorescein were obtained.

Surprising was the finding that BSH triggered release of pegylated liposomes contents without inducing their aggregation. We concluded that the BSH-induced leakage of the liposomes is not only due to their aggregation, but also due to perturbation of the bilayers of separate liposomes.

It is also noteworthy that the incorporation of PEG lipid to DPPC liposomes led to higher leakage percentages over a period of ~11 min, as well as more pronounced sigmoidal release curves especially at very low BSH concentrations.

Our in vitro studies demonstrated that doxorubicin-containing liposomes had low toxicity, in agreement with the studies which showed that entrapped doxorubicin in liposomes had lower toxicity compared to that of the free drug (Lee 1998, Sadzuka 2000, Tseng 2002, Eliaz 2004, Charrois 2004). Meanwhile, in presence of different concentrations of BSH, higher cytotoxicity levels were recorded, indicating that certain amount of doxorubicin were liberated from the liposomes into cell medium.

5. Conclusions and outlook

A strong interaction of BSH with model lipid membranes has been confirmed and explained by binding of BSH to the positively charged headgroups of the liposomes.

The interaction between BSH and liposomes of different compositions has been found to induce dramatic changes in the liposomes leading to triggered release of their contents.

The extent of release is maximal near the phase transition temperature of the liposomes.

DMPC liposomes are not very useful because of the low phase transition.

In addition to use of liposomes as model systems due to their mimicry of biological membranes (Bangham 1965, Sessa 1968, Bangham 2005), they are also in use as drug delivery vehicles since they can carry various pharmaceutical substances (Crommelin 2002, Allen 2004).

Successful liposomal formulations should be able to hold the drug tightly during their circulation through the blood and accordingly the body. But once in tumor tissue, the drug must be released rapidly from the liposomes. However, it has been found that the accumulated liposomes at the tumor sites release their contents slowly leading to a decrease in their liposomal efficiency. Intensive studies have been made to trigger the release of liposomal contents, but most of them have drawbacks.

Liposomal formulations able to release their contents as a response to BSH may provide a highly advantageous approach in the drug delivery field.

BSH may enable rapid release of contents from tissue-accumulated or cellular-internalized liposomes. BSH-induced content release of those liposomes will probably be a desirable approach especially for the treatment of distant metastases where the tumor is either inaccessible or with unknown location.

6. Summary

6.1. Interaction of BSH with various liposomal formulations

BSH is one of the two boron compounds in use in BNCT. Triggered release of liposome contents by BSH has been achieved. We used liposomes of different compositions as a model for studying the interaction of BSH with cell membranes. The interaction of BSH with cationic liposomes of different compositions was investigated. Zeta potential and size measurements of the liposomes in absence and presence of BSH indicated a firm binding of BSH with the headgroups of these liposomes.

Beside exploiting the liposomes as model for cell membranes, there is also great interest in liposomes as drug carriers. To have a pronounced therapeutic effect, the release of the drug from the liposomes should be as complete as possible. Because of this, developing tools for triggering release of agents encapsulated inside the aqueous compartment of the liposomes is an important factor in the liposome drug delivery systems.

We studied the interaction of BSH with neutral liposomes prepared either from DMPC or DPPC lipids and proved that they released their contents under the influence of BSH within minutes.

Furthermore, we tested the effect of BSH on the extent of content release of pegylated liposomes because they are the most favorable drug carriers in delivery systems. We found that incorporation of 2 mol% DSPE-PEG2000 did not affect the extent of leakage but only affected the initial velocity of carboxyfluorescein release.

Altogether, the results showed a strong interaction between BSH and liposomes of different compositions. Release of the liposomal contents was achieved by this interaction. We explaine the BSH action by binding of BSH to the headgroups of the liposomes. In addition, we assume that the effect exerted by BSH is dependent on the nature of lipids in the liposomes.

6.2. Synthesis and liposomal preparation of two dodecaborate cluster lipids for BNCT

A new class of lipids, containing the closo-dodecaborate cluster, was synthesized. B-6-14 and B-6-16 have a double-tailed lipophilic part and a headgroup carrying a double negative charge. Each of them was incorporated into liposomes composed of

equimolar amounts of DSPC and cholesterol for the purpose of delivery of boron-containing compounds to tumor tissues.

7. Zusammenfassung

7.1. Wechselwirkung von BSH mit verschiedenen Liposomen

BSH ($Na_2B_{12}H_{11}SH$) ist eine borreiche Verbindung, die in der Bor-neutroneneinfangstherapie (BNCT) benutzt wird. Ausschüttung des Inhalts der Liposomen ist durch BSH ausführbar. Wir haben mit den Liposomen als Modell gearbeitet, um die BSH-Interaktionen mit Zellmembranen zu untersuchen. BSH veränderte das positive Zeta-Potential kationischer Liposomen bestehend aus Dimethyldioctadecylammoniumbromid (DODAB) zu neutralen und anschließend zu negativen Werten. Wir erklärten dieses Phänomen mit einer starken Bindung von BSH an die positiven Kopfgruppen der Liposomen.

Diese Resultate waren auch reproduzierbar, wenn BSH zu kationischen Liposomen bestehend aus DODAB/Diolylphosphatidylcholin (DOPC) oder DODAB/Diolyphosphatidylethanolamin (DOPE) hinzugeben wurde.

Liposomen sind einerseits ein Modell für Zellmembranen und auf der anderen Seite können sie als Trägersysteme für Arzneistoffe dienen. Für einen therapeutischen Effekt benötigt man eine komplette Freisetzung des Arzneistoffes aus den Liposomen. Deshalb ist es wichtig, Methoden zur gezielten Freisetzung der eingekapselten Reagenzien aus Liposomen zu entwickeln.

Wir erforschten die Interaktion von BSH mit Dipalmitoylphosphatidylcholin (DPPC)- und Dimyristoylphosphatidylcholin (DMPC)-Liposomen und fanden eine Freisetzung des Liposomeninhalts unter dem Einfluß von BSH innerhalb von Minuten.

Weiterhin testeten wir den Effekt von BSH auf pegylierte Liposomen, da sie die meist favorisierten Arzneistoff-Transporter sind. Wir fanden, dass die Beimischung von 2 % DSPE-PEG keinen Effekt auf die Leckage ausübt, allerdings wurde die Anfangsgeschwindigkeit der Carboxyfluorescein-Freisetzung hierdurch beeinflußt.

Eine andere wichtige Beobachtung war, dass BSH keine Änderungen in der Morphologie der DPPC-PEG-Liposomen sowie keine Aggregation induzierte, dementsprechend hatte BSH auch einen Effekt auf isolierte Liposomen.

Aus einer Kombination von BSH und Doxorubicin-haltigen Liposomen ergab sich eine höhere Zytotoxizität im Vergleich zur separaten Inkubation mit BSH oder Doxorubicin-haltigen Liposomen.

Fazit: Die Ergebnisse belegen eine starke Wechselwirkung zwischen BSH und Liposomen unterschiedlichster Zusammensetzung. Diese Wechselwirkung führt zur

Freisetzung des liposomalen Inhalts. Wir erklären diesen BSH-Effekt mit der Bindung von BSH an die Lipidkopfgruppen der Liposomen. Zudem ist die BSH-Interaktion höchstwahrscheinlich abhängig von der Art der Lipide in den Liposomen.

7.2. Synthese und Liposomenpräparation von zwei Dodecaboratcluster-Lipiden für die BNCT

Zwei Dodecaboratcluster-Lipide mit dem Borcluster als Kopfgruppe und zwei Alkylketten (S-(N,N-(2-dimyristoyloxyethyl)-acetamido)-thioundecahydro-closo-dodecaborat (2-) (B-6-14) and S-(N,N-(2-dipalmitoyloxyethyl)-acetamido)-thioundecahydro-closo-dodecaborat (2-) (B-6-16)) wurden synthetisiert.

Beide borhaltigen Lipide wurden separat in Liposomen eingebettet, die aus gleichen Anteilen von Disteaorylphosphatidylcholin und Cholesterin bestanden. Das Ziel hierbei war eine hohe Borkonzentration innerhalb der Liposomen.

8. References

Abraham, S. A.; Edwards, K.; Karlsson, G.; MacIntosh, S.; Mayer, L. D.; McKenzie, C., and Bally, M. B. Formation of transition metal-doxorubicin complexes inside liposomes. Biochim Biophys Acta. 2002 Sep 20; 1565(1):41-54.

Alam, F.; Barth, R. F., and Soloway, A. H. Boron containing immunoconjugates for neutron capture therapy of cancer and for immunocytochemistry. Antibody, Immunoconjugates and Radiopharmaceuticals. 1989; 2:145-163.

Ali, S.; Minchey, S.; Janoff, A., and Mayhew, E. A differential scanning calorimetry study of phosphocholines mixed with paclitaxel and its bromoacylated taxanes. Biophys J. 2000 Jan; 78(1):246-256.

Allen, T. M. and Cullis, P. R. Drug delivery systems: entering the mainstream. Science. 2004 Mar 19; 303(5665):1818-1822.

Allen, T. M. Liposomal drug formulations. Rationale for development and what we can expect for the future. Drugs. 1998 Nov; 56(5):747-756.

Almgren, M.; Edwards, K., and Karlsson, G. Cryo transmission electron microscopy of liposomes and related structures. Colloids and Surfaces A. 2000; 174:3-21.

Amano, K. Boron-10-mercaptoundecahydrododecaborate distribution in human brain tumors as studied by neutron-induced alpha-autoradiography. Hatanaka, H. Boron-neutron capture therapy for tumors. Niigata: Nishimura; 1986; pp. 107-115.

Anscher, M. S.; Samulski, T. V.; Dodge, R.; Prosnitz, L. R., and Dewhirst, M. W. Combined external beam irradiation and external regional hyperthermia for locally advanced adenocarcinoma of the prostate. Int J Radiat Oncol Biol Phys. 1997 Mar 15; 37(5):1059-1065.

Bangham, A. D. Liposomes and the physico-chemical basis of unconsciousness. FASEB J. 2005 Nov; 19(13):1766-1768.

Bangham, A. D.; Standish, M. M., and Watkins, J. C. Diffusion of univalent ions across the lamellae of swollen phospholipids. J Mol Biol. 1965 Aug; 13(1):238-52.

Barlow, J. J.; Piver, M. S.; Chuang, J. T.; Cortes, E. P.; Onuma, T., and Holland, J. F.

Adriamycin and bleomycin, alone and in combination, in gynecologic cancers. Cancer. 1973 Oct; 32(4):735-743.

Barth, R. F.; Soloway, A. H., and Fairchild, R. G. Boron neutron capture therapy for cancer. Sci Am. 1990a Oct; 263(4):100-3, 106-107.

Barth, R. F.; Soloway, A. H., and Fairchild, R. G. Boron neutron capture therapy of cancer. Cancer Res. 1990b Feb 15; 50(4):1061-1070.

Barth, R. F.; Soloway, A. H.; Fairchild, R. G., and Brugger, R. M. Boron neutron capture therapy for cancer. Realities and prospects. Cancer. 1992 Dec 15; 70(12):2995-3007.

Bartucci, R.; Pantusa, M.; Marsh, D., and Sportelli, L. Interaction of human serum albumin with membranes containing polymer-grafted lipids: spin-label ESR studies in the mushroom and brush regimes. Biochim Biophys Acta. 2002 Aug 19; 1564(1):237-242.

Bergstrand, N.; Bohl, E.; Carlsson, J.; Edwards, K.; Ghaneolhosseini, H.; Gedda, L.; Johnsson, M.; Silvander, M., and Sjöberg, S. Stabilised liposomes with double targeting for use in BNCT. Cambridge, UK: Royal Society of Chemistry; 2000; pp. 131-134.

Berridge, M. V.; Tan, A. S.; McCoy, K. D., and wang, R. The biochemical and cellular basis of cell proliferation assays that use tetrazolium salts. Biochemica. 1996; 4:14-19.

Blandamer, M. J. Thermodynamic background to isothermal titration calorimetry. J.E. Ladbury and B.Z. Chowdhry. Biocalorimetry - Applications of Calorimetry in the Biological Sciences. John Wiley & Sons Ltd.; 1998; pp. 5-25.

Blume, G. and Cevc, G. Liposomes for the sustained drug release in vivo. Biochim Biophys Acta. 1990 Nov 2; 1029(1):91-97.

Bohl Kullberg, E.; Bergstrand, N.; Carlsson, J.; Edwards, K.; Johnsson, M.; Sjoberg, S., and Gedda, L. Development of EGF-conjugated liposomes for targeted delivery of boronated DNA-binding agents. Bioconjug Chem. 2002 Jul-2002 Aug 31; 13(4):737-743.

Ceberg, C. P.; Persson, A.; Brun, A.; Huiskamp, R.; Fyhr, A. S.; Persson, B. R., and Salford, L. G. Performance of sulfhydryl boron hydride in patients with grade III and IV astrocytoma: a basis for boron neutron capture therapy. J Neurosurg. 1995 Jul; 83(1):79-85.

Chaidarun, S. S.; Eggo, M. C.; Sheppard, M. C., and Stewart, P. M. Expression of epidermal growth factor (EGF), its receptor, and related oncoprotein (erbB-2) in human pituitary tumors and response to EGF in vitro. Endocrinology. 1994 Nov; 135(5):2012-2021.

Charrois, G. J. and Allen, T. M. Drug release rate influences the pharmacokinetics, biodistribution, therapeutic activity, and toxicity of pegylated liposomal doxorubicin formulations in murine breast cancer. Biochim Biophys Acta. 2004 May 27; 1663(1-2):167-177.

Chu, C. J.; Dijkstra, J.; Lai, M. Z.; Hong, K., and Szoka, F. C. Efficiency of cytoplasmic delivery by pH-sensitive liposomes to cells in culture. Pharm Res. 1990 Aug; 7(8):824-834.

Connor, J.; Yatvin, M. B., and Huang, L. pH-sensitive liposomes: acid-induced liposome fusion. Proc Natl Acad Sci U S A. 1984 Mar; 81(6):1715-1718.

Conway, J. Assessment of a small microwave (2450 MHz) diathermy applicator as suitable for hyperthermia. Phys Med Biol. 1983 Mar; 28(3):249-256.

Crommelin, D. J. A.; Bos, G. W., and Storm, G. Liposomes: successful carrier systems for targeted delivery of drugs. The Drug Delivery Companies Report. Autumn/Winter 2002.

Davidsen, J.; Jorgensen, K.; Andresen, T. L., and Mouritsen, O. G. Secreted phospholipase A_2 as a new enzymatic trigger mechanism for localised liposomal drug release and absorption in diseased tissue. Biochim Biophys Acta. 2003 Jan 10; 1609(1):95-101.

Davies, C. de L.; Lundstrom, L. M.; Frengen, J.; Eikenes, L.; Bruland, O. S.; Kaalhus, O.; Hjelstuen, M. H., and Brekken, C. Radiation improves the distribution and uptake of liposomal doxorubicin (caelyx) in human osteosarcoma xenografts. Cancer Res. 2004 Jan 15; 64(2):547-553.

Dreher, M. R.; Liu, W.; Michelich, C. R.; Dewhirst, M. W.; Yuan, F., and Chilkoti, A. Tumor vascular permeability, accumulation, and penetration of macromolecular drug carriers. J Natl Cancer Inst. 2006 Mar 1; 98(5):335-344.

Du, H.; Chandaroy, P., and Hui, S. W. Grafted poly-(ethylene glycol) on lipid surfaces inhibits protein adsorption and cell adhesion. Biochim Biophys Acta. 1997 Jun 12; 1326(2):236-248.

Duzgunes, N.; Wilschut, J.; Fraley, R., and Papahadjopoulos, D. Studies on the mechanism of membrane fusion. Role of head-group composition in calcium- and magnesium-induced fusion of mixed phospholipid vesicles. Biochim Biophys Acta. 1981 Mar 20; 642(1):182-195.

Edwards, K.; Johnsson, M.; Karlsson, G., and Silvander, M. Effect of polyethyleneglycol-phospholipids on aggregate structure in preparations of small unilamellar liposomes. Biophys J. 1997 Jul; 73(1):258-266.

Egelhaaf, S. U.; Schurtenberger, P., and Muller, M. New controlled environment vitrification system for cryo-transmission electron microscopy: design and application to surfactant solutions. J Microsc. 2000 Nov; 200(Pt 2):128-139.

Eliaz, R. E. ; Nir, S.; Marty, C., and Szoka, F. C. Jr. Determination and modeling of kinetics of cancer cell killing by doxorubicin and doxorubicin encapsulated in targeted liposomes. Cancer Res. 2004 Jan 15; 64(2):711-718.

Eliaz, R. E. and Szoka, F. C. Jr. Liposome-encapsulated doxorubicin targeted to CD44: a strategy to kill CD44-overexpressing tumor cells. Cancer Res. 2001 Mar 15; 61(6):2592-2601.

Epand, R. M.; Bach, D.; Borochov, N., and Wachtel, E. Cholesterol crystalline polymorphism and the solubility of cholesterol in phosphatidylserine. Biophys J. 2000 Feb; 78(2):866-873.

Fairchild, R. G. and Bond, V. P. Current status of 10B-neutron capture therapy: enhancement of tumor dose via beam filtration and dose rate, and the effects of these parameters on minimum boron content: a theoretical evaluation. Int J Radiat Oncol Biol Phys. 1985 Apr; 11(4):831-840.

Fairchild, R. G.; Kahl, S. B.; Laster, B. H.; Kalef-Ezra, J., and Popenoe, E. A. In vitro determination of uptake, retention, distribution, biological efficacy, and toxicity of boronated compounds for neutron capture therapy: a comparison of porphyrins with sulfhydryl boron hydrides. Cancer Res. 1990 Aug 15; 50(16):4860-4865.

Feakes, D. A. ; Shelly, K., and Hawthorne, M. F. Selective boron delivery to murine tumors by lipophilic species incorporated in the membranes of unilamellar liposomes. Proc Natl Acad Sci U S A. 1995 Feb 28; 92(5):1367-1370.

Feakes, D. A. ; Shelly, K.; Knobler, C. B., and Hawthorne, M. F. Na3[B20H17NH3]: synthesis and liposomal delivery to murine tumors. Proc Natl Acad Sci U S A. 1994 Apr 12; 91(8):3029-3033.

Finkel, G. C.; Poletti, C. E.; Fairchild, R. G.; Slatkin, D. N., and Sweet, W. H. Distribution of 10B after infusion of Na210B12H11SH into a patient with malignant astrocytoma: implications for boron neutron capture therapy. Neurosurgery. 1989 Jan; 24(1):6-11.

Fulham, M. J.; Bizzi, A.; Dietz, M. J.; Shih, H. H.; Raman, R.; Sobering, G. S.; Frank, J. A.; Dwyer, A. J.; Alger, J. R., and Di Chiro, G. Mapping of brain tumor metabolites with proton MR spectroscopic imaging: clinical relevance. Radiology. 1992 Dec; 185(3):675-686.

Gabel, D.; Foster, S., and Fairchild, R. G. The Monte Carlo simulation of the biological effect of the 10B(n, alpha)7Li reaction in cells and tissue and its implication for boron neutron capture therapy. Radiat Res. 1987 Jul; 111(1):14-25.

Gabel, D.; Preusse, D.; Haritz, D.; Grochulla, F.; Haselsberger, K.; Fankhauser, H.; Ceberg, C.; Peters, H. D., and Klotz, U. Pharmacokinetics of Na2B12H11SH (BSH) in patients with malignant brain tumours as prerequisite for a phase I clinical trial of boron neutron capture. Acta Neurochir (Wien). 1997; 139(7):606-11; discussion 611-612.

Gabizon, A. and Papahadjopoulos, D. Liposome formulations with prolonged circulation time in blood and enhanced uptake by tumors. Proc Natl Acad Sci U S A. 1988 Sep; 85(18):6949-6953.

Gabizon, A.; Horowitz, A. T.; Goren, D.; Tzemach, D.; Shmeeda, H., and Zalipsky, S.

In vivo fate of folate-targeted polyethylene-glycol liposomes in tumor-bearing mice. Clin Cancer Res. 2003 Dec 15; 9(17):6551-6559.

Giehl, A.; Lemm, T.; Bartelsen, O.; Sandhoff, K., and Blume, A. Interaction of the GM2-activator protein with phospholipid-ganglioside bilayer membranes and with monolayers at the air-water interface. Eur J Biochem. 1999 May; 261(3):650-658.

Guo, X.; MacKay, J. A., and Szoka, F. C. Jr. Mechanism of pH-triggered collapse of phosphatidylethanolamine liposomes stabilized by an ortho ester polyethyleneglycol lipid. Biophys J. 2003 Mar; 84(3):1784-1795.

Haritz, D.; Gabel, D., and Huiskamp, R. Clinical phase-I study of $Na_2B_{12}H_{11}SH$ (BSH) in patients with malignant glioma as precondition for boron neutron capture therapy (BNCT). Int J Radiat Oncol Biol Phys. 1994 Mar 30; 28(5):1175-1181.

Haselsberger, K.; Radner, H.; Gossler, W.; Schlagenhaufen, C., and Pendl, G. Subcellular boron-10 localization in glioblastoma for boron neutron capture therapy with $Na_2B_{12}H_{11}SH$. J Neurosurg. 1994 Nov; 81(5):741-744.

Hatanaka, H. A revised boron-neutron capture therapy for malignant brain tumors. II. Interim clinical result with the patients excluding previous treatments. J Neurol. 1975 Jun 9; 209(2):81-94.

Hawthorne, M. F. The role of chemistry in the development of boron neutron capture therapy of cancer. Angewandte Chemie, International Edition in English. 1993; 32:950-984.

Heerklotz, H. and Seelig, J. Titration calorimetry of surfactant-membrane partitioning and membrane solubilization. Biochim Biophys Acta. 2000 Nov 23; 1508(1-2):69-85.

Hobai, S. and Fazakas, Z. Effect of anion triiodide on the main pahse transition of fully hydrated dipalmitoylphosphatidylcholine bylayers [Web Page]. 1998; Accessed 2006 Jan 8.

Hong, M. S.; Lim, S. J.; Oh, Y. K., and Kim, C. K. pH-sensitive, serum-stable and long-circulating liposomes as a new drug delivery system. J Pharm Pharmacol. 2002 Jan; 54(1):51-58.

Hope, M. J.; Bally, M. B.; Webb, G., and Cullis, P. R. Production of large unimellar

vesicles by a rapid extrusion procedure. Characterization of size distribution, trapped volume and ability to maintain a membrane potential. Biochim Biophys Acta. 1985; 812:55-65.

Huang, C. and Mason, J. T. Geometric packing constraints in egg phosphatidylcholine vesicles. Proc Natl Acad Sci U S A. 1978 Jan; 75(1):308-310.

Huang, C. Studies on phosphatidylcholine vesicles. Formation and physical characteristics. Biochemistry. 1969 Jan; 8(1):344-352.

Huang, S. L. and MacDonald, R. C. Acoustically active liposomes for drug encapsulation and ultrasound-triggered release. Biochim Biophys Acta. 2004 Oct 11; 1665(1-2):134-141.

Huebner, S.; Battersby, B. J.; Grimm, R., and Cevc, G. Lipid-DNA complex formation: reorganization and rupture of lipid vesicles in the presence of DNA as observed by cryoelectron microscopy. Biophys J. 1999 Jun; 76(6):3158-3166.

Johnsson, M. ; Bergstrand, N., and Edwards, K. Optimization of drug loading procedures and characterization of liposomal formulations of two novel agents intended for boron neutron capture therapy (BNCT). J Liposome Res. 1999; 9:53-79.

Johnsson, M. and Edwards, K. Liposomes, disks, and spherical micelles: aggregate structure in mixtures of gel phase phosphatidylcholines and poly(ethylene glycol)-phospholipids. Biophys J. 2003 Dec; 85(6):3839-3847.

Kageji, T.; Nagahiro, S.; Kitamura, K.; Nakagawa, Y.; Hatanaka, H.; Haritz, D.; Grochulla, F.; Haselsberger, K., and Gabel, D. Optimal timing of neutron irradiation for boron neutron capture therapy after intravenous infusion of sodium borocaptate in patients with glioblastoma. Int J Radiat Oncol Biol Phys. 2001 Sep 1; 51(1):120-130.

Kageji, T.; Nakagawa, Y.; Kitamura, K.; Matsumoto, K., and Hatanaka, H. Pharmacokinetics and boron uptake of BSH (Na2B12H11SH) in patients with intracranial tumors. J Neurooncol. 1997 May; 33(1-2):117-130.

Kageji, T.; Otersen, B.; Gabel, D.; Huiskamp, R.; Nakagawa, Y., and Matsumoto, K. Interaction of mercaptoundecahydrododecaborate (BSH) with phosphatidylcholine: relevance to boron neutron capture therapy. Biochim Biophys Acta. 1998 Apr 22;

1391(3):377-383.

Kahl, S. B.; Koo, M. S.; Laster, B. H., and Fairchild, R. G. Boronated porphyrins in NCT: results with a new potent tumor localizer. Strahlenther Onkol. 1989 Feb-1989 Mar 31; 165 (2-3):134-137.

Kennedy, M. T.; Pozharski, E. V.; Rakhmanova, V. A., and MacDonald, R. C. Factors governing the assembly of cationic phospholipid-DNA complexes. Biophys J. 2000 Mar; 78(3):1620-1633.

Kirpotin, D.; Park, J. W.; Hong, K.; Zalipsky, S.; Li, W. L.; Carter, P.; Benz, C. C., and Papahadjopoulos, D. Sterically stabilized anti-HER2 immunoliposomes: design and targeting to human breast cancer cells in vitro. Biochemistry. 1997 Jan 7; 36(1):66-75.

Kong, G.; Anyarambhatla, G.; Petros, W. P.; Braun, R. D.; Colvin, O. M.; Needham, D., and Dewhirst, M. W. Efficacy of liposomes and hyperthermia in a human tumor xenograft model: importance of triggered drug release. Cancer Res. 2000 Dec 15; 60(24):6950-6957.

Kono, K.; Henmi, A., and Takagishi, T. Temperature-controlled interaction of thermosensitive polymer-modified cationic liposomes with negatively charged phospholipid membranes. Biochim Biophys Acta. 1999a Sep 21; 1421(1):183-197.

Kono, K.; Nakai, R.; Morimoto, K., and Takagishi, T. Temperature-dependent interaction of thermo-sensitive polymer-modified liposomes with CV1 cells. FEBS Lett. 1999b Aug 6; 456(2):306-310.

Korlach, J.; Schwille, P.; Webb, W. W., and Feigenson, G. W. Characterization of lipid bilayer phases by confocal microscopy and fluorescence correlation spectroscopy. Proc Natl Acad Sci U S A. 1999 Jul 20; 96(15):8461-8466.

Kozlov, M. M. and Markin, V. S. On the theory of membrane fusion. The adhesion-condensation mechanism. Gen Physiol Biophys. 1984 Oct; 3(5):379-402.

Kozlov, M. M.; Leikin, S. L.; Chernomordik, L. V.; Markin, V. S., and Chizmadzhev, Y. A. Stalk mechanism of vesicle fusion. Intermixing of aqueous contents. Eur Biophys J. 1989; 17(3):121-129.

Lee, R. J.; Wang, S.; Turk, M. J., and Low, P. S. The effects of pH and intraliposomal buffer strength on the rate of liposome content release and intracellular drug delivery. Biosci Rep. 1998 Apr; 18(2):69-78.

Leharne, S. A. and Chowdhry, B. Z. Thermodynamic background to differential scanning calometry. J.E. Ladbury and B.Z. Chowdhry. Biocalorimetry - Applications of Calorimetry in the Biological Sciences. John Wiley & Sons Ltd.; 1998; pp. 5-25.

Leonetti, C.; Scarsella, M.; Semple, S. C.; Molinari, A.; D'Angelo, C.; Stoppacciaro, A.; Biroccio, A., and Zupi, G. In vivo administration of liposomal vincristine sensitizes drug-resistant human solid tumors. Int J Cancer. 2004 Jul 10; 110(5):767-774.

Lim, H. J.; Masin, D.; Madden, T. D., and Bally, M. B. Influence of drug release characteristics on the therapeutic activity of liposomal mitoxantrone. J Pharmacol Exp Ther. 1997 Apr; 281(1):566-573.

Locher, G. L. Biological effects and therapeutic possibilities of neutrons. Am J Roentgenol Radium Ther. 1936; 36:1-13.

Lu, J. Z.; Hao, Y. H., and Chen, J. W. Effect of cholesterol on the formation of an interdigitated gel phase in lysophosphatidylcholine and phosphatidylcholine binary mixtures. J Biochem (Tokyo). 2001 Jun; 129(6):891-898.

Lutz, S.; Neumann, M.; Bellmann, D., and Gabel, D. The interaction of $Na_2B_{12}H_{11}SH$ (BSH) with liposomes; relevance to cellular BSH uptake. Program and abstracts 9th International Symposium on Neutron Capture Therapy. 2000; pp. 69-70.

Mayer, L. D.; Hope, M. J., and Cullis, P. R. Vesicles of variable sizes produced by a rapid extrusion procedure. Biochim Biophys Acta. 1986 Jun 13; 858(1):161-168.

Mayer, L. D.; Hope, M. J.; Cullis, P. R., and Janoff, A. S. Solute distributions and trapping efficiencies observed in freeze-thawed multilamellar vesicles. Biochim Biophys Acta. 1985 Jul 11; 817(1):193-196.

Meerum Terwogt, J. M.; Groenewegen, G.; Pluim, D.; Maliepaard, M.; Tibben, M. M.; Huisman, A.; ten Bokkel Huinink, W. W.; Schot, M.; Welbank, H.; Voest, E. E.; Beijnen, J. H., and Schellens, J. M. Phase I and pharmacokinetic study of SPI-77, a liposomal encapsulated dosage form of cisplatin. Cancer Chemother Pharmacol.

2002 Mar; 49(3):201-210.

Miura, M.; Gabel, D.; Fairchild, R. G.; Laster, B. H., and Warkentien, L. S. Synthesis and in vivo studies of a carboranyl porphyrin. Strahlenther Onkol. 1989 Feb-1989 Mar 31; 165(2-3):131-134.

Mouritsen, O. G. and Jorgensen, K. A new look at lipid-membrane structure in relation to drug research. Pharm Res. 1998 Oct; 15(10):1507-1519.

Mrozek, E.; Rhoades, C. A.; Allen, J.; Hade, E. M., and Shapiro, C. L. Phase I trial of liposomal encapsulated doxorubicin (Myocet; D-99) and weekly docetaxel in advanced breast cancer patients. Ann Oncol. 2005 Jul; 16(7):1087-1093.

Muggia, F. M. Doxorubicin-polymer conjugates: further demonstration of the concept of enhanced permeability and retention. Clin Cancer Res. 1999 Jan; 5(1):7-8.

Nagle, J. F. Lipid bilayer phase transition: density measurements and theory. Proc Natl Acad Sci U S A. 1973 Dec; 70(12):3443-3444.

Nakamura, H.; Miyajima, Y.; Takei, T.; Kasaoka, S., and Maruyama, K. Synthesis and vesicle formation of a nido-carborane cluster lipid for boron neutron capture therapy. Chem Commun (Camb). 2004 Sep 7; (17):1910-1911.

Needham, D. and Dewhirst, M. W. The development and testing of a new temperature-sensitive drug delivery system for the treatment of solid tumors. Adv Drug Deliv Rev. 2001 Dec 31; 53(3):285-305.

Needham, D.; Anyarambhatla, G.; Kong, G., and Dewhirst, M. W. A new temperature-sensitive liposome for use with mild hyperthermia: characterization and testing in a human tumor xenograft model. Cancer Res. 2000 Mar 1; 60(5):1197-1201.

Neumann, M.; Kunz, U.; Lehmann, H., and Gabel, D. Determination of the subcellular distribution of mercaptoundecahydro-closo-dodecaborate (BSH) in human glioblastoma multiforme by electron microscopy. J Neurooncol. 2002 Apr; 57(2):97-104.

New, R. R. C. Preparation of liposomes. R.R.C. New. Liposomes - A Practical Approach. Oxford, UK: Oxford University Press; 1990 (4th printing); pp. 33-104.

Nunes-Correia, I.; Eulalio, A.; Nir, S.; Duzgunes, N.; Ramalho-Santos, J., and Pedroso de Lima, M. C. Fluorescent probes for monitoring virus fusion kinetics: comparative evaluation of reliability. Biochim Biophys Acta. 2002 Mar 19; 1561(1):65-75.

O'Brien, M. E.; Wigler, N.; Inbar, M.; Rosso, R.; Grischke, E.; Santoro, A.; Catane, R.; Kieback, D. G.; Tomczak, P.; Ackland, S. P.; Orlandi, F.; Mellars, L.; Alland, L., and Tendler, C. Reduced cardiotoxicity and comparable efficacy in a phase III trial of pegylated liposomal doxorubicin HCl (CAELYX/Doxil) versus conventional doxorubicin for first-line treatment of metastatic breast cancer. Ann Oncol. 2004 Mar; 15(3):440-449.

O'Leary, T. J.; Ross, P. D.; Lieber, M. R., and Levin, I. W. Effects of cyclosporine A on biomembranes. Vibrational spectroscopic, calorimetric and hemolysis studies. Biophys J. 1986 Apr; 49(4):795-801.

Ono, A.; Takeuchi, K.; Sukenari, A.; Suzuki, T.; Adachi, I., and Ueno, M. Reconsideration of drug release from temperature-sensitive liposomes. Biol Pharm Bull. 2002 Jan; 25(1):97-101.

Otersen, B.; Haritz, D.; Grochulla, F.; Bergmann, M.; Sierralta, W., and Gabel, D. Binding and distribution of Na2B12H11SH on cellular and subcellular level in tumor tissue of glioma patients in boron neutron capture therapy. J Neurooncol. 1997 May; 33(1-2):131-139.

Ott, D.; Hennig, J., and Ernst, T. Human brain tumors: assessment with in vivo proton MR spectroscopy. Radiology. 1993 Mar; 186(3):745-752.

Park, J. W.; Hong, K.; Carter, P.; Asgari, H.; Guo, L. Y.; Keller, G. A.; Wirth, C.; Shalaby, R.; Kotts, C.; Wood, W. I., and et, a. l. Development of anti-p185HER2 immunoliposomes for cancer therapy. Proc Natl Acad Sci U S A. 1995 Feb 28; 92(5):1327-1331.

Pathak, A. P.; Artemov, D.; Ward, B. D.; Jackson, D. G.; Neeman, M., and Bhujwalla, Z. M. Characterizing extravascular fluid transport of macromolecules in the tumor interstitium by magnetic resonance imaging. Cancer Res. 2005 Feb 15; 65(4):1425-1432.

Portis, A.; Newton, C.; Pangborn, W., and Papahadjopoulos, D. Studies on the mechanism of membrane fusion: evidence for an intermembrane Ca^{2+}-phospholipid complex, synergism with Mg^{2+}, and inhibition by spectrin. Biochemistry. 1979 Mar 6; 18(5):780-790.

Pozharski, E. and MacDonald, R. C. Thermodynamics of cationic lipid-DNA complex formation as studied by isothermal titration calorimetry. Biophys J. 2002 Jul; 83(1):556-565.

Rand, R. P. and Parsegian, V. A. The influence of polar group identity on the interactions between phospholipid bilayers. New York: Plenum Press; 1988; pp. 73-81.

Rozycka-Roszak, B.; Przyczyna, A., and Pernak, A. A study on the interaction between 1-decyloxymethyl-3-carbamoylpyridinium salts and model membranes –the effect of counterions. Biophys Chem. 2004 May 1; 109(2):271-279.

Sadzuka, Y.; Hirota, S., and Sonobe, T. Intraperitoneal administration of doxorubicin encapsulating liposomes against peritoneal dissemination. Toxicol Lett. 2000 Jul 27; 116(1-2):51-59.

Sandra, A. and Pagano, R. E. Liposome-cell interactions. Studies of lipid transfer using isotopically asymmetric vesicles. J Biol Chem. 1979 Apr 10; 254 (7): 2244-2249.

Schinazi, R. F. and Prusoff, W. H. Synthesis and properties of boron and silicon substituted uracil of 2'-deoxyuridine. Tetrahedron Lett. 1978; 19(50):4981-4984.

Sessa, G. and Weissmann, G. Phospholipid spherules (liposomes) as a model for biological membranes. J Lipid Res. 1968 May; 9(3):310-318.

Shelly, K.; Feakes, D. A.; Hawthorne, M. F.; Schmidt, P. G. ; Krisch, T. A., and Bauer, W. F. Model studies directed toward the boron neutron-capture therapy of cancer: boron delivery to murine tumors with liposomes. Proc Natl Acad Sci U S A. 1992 Oct 1; 89(19):9039-9043.

Shi, G.; Guo, W.; Stephenson, S. M., and Lee, R. J. Efficient intracellular drug and gene delivery using folate receptor-targeted pH-sensitive liposomes composed of

cationic/anionic lipid combinations. J Control Release . 2002 Apr 23; 80(1-3):309-319.

Siegel, D. P. and Epand, R. M. The mechanism of lamellar-to-inverted hexagonal phase transitions in phosphatidylethanolamine: implications for membrane fusion mechanisms. Biophys J. 1997 Dec; 73(6):3089-3111.

Siegel, D. P. The modified stalk mechanism of lamellar/inverted phase transitions and its implications for membrane fusion. Biophys J. 1999 Jan; 76(1 Pt 1):291-313.

Silvander, M. Steric stabilization of liposomes - a review. Progr Colloid Polym Sci. 2002; 120:35-40.

Silvander, M.; Hansson, P., and Edwards, K. Liposomal surface potential and bilayer packing as affected by PEG - lipid inclusion. Langmuir. 2000; 16:3696-3702.

Slatkin, D.; Micca, P.; Forman, A.; Gabel, D.; Wielopolski, L., and Fairchild, R. Boron uptake in melanoma, cerebrum and blood from Na2B12H11SH and Na4B24H22S2 administered to mice. Biochem Pharmacol. 1986 May 15; 35(10):1771-1776.

Soloway, A. H.; Brownell, G. L. Ojemann R. G., and Sweet, W. H. Boron-slow neutron capture therapy: present status. Proceedings of the International Symposium on the preparation and bio-medical application of labeled molecules; Venice, Italy 23-29 August 1964; pp. 383-403.
Soloway, A. H.; Hatanaka, H., and Davis, M. A. Penetration of brain and brain tumor. VII. Tumor-binding sulfhydryl boron compounds. J Med Chem. 1967 Jul; 10(4):714-717.

Soloway, A. H.; Tjarks, W.; Barnum, B. A.; Rong, F. G.; Barth, R. F.; Codogni, I. M., and Wilson, J. G. The Chemistry of Neutron Capture Therapy. Chem Rev. 1998 Jun 18; 98(4):1515-1562.

Stragliotto, G. and Fankhauser, H. Biodistribution of boron sulfhydryl for boron neutron capture therapy in patients with intracranial tumors. Neurosurgery. 1995 Feb; 36(2):285-92; discussion 292-3.

Stryer, L. Biochemistry. New York, USA: W.H. Freeman & Co. ; 1975 (8th printing); pp. 263-290.

Süleymanoglu, E. Divalent cation induced DNA-zwitterionic vesicle formulation compacted for gene delivery: thermodynamic aspects. Internet Electron J Mol Des. 2004; 3:93-101.

Szollosi, J. ; Nagy, P.; Sebestyen, Z.; Damjanovicha, S.; Park, J. W., and Matyus, L. Applications of fluorescence resonance energy transfer for mapping biological membranes. J Biotechnol. 2002 Jan; 82(3):251-266.

Tame, J. R. H.; O'Brien, R., and Ladbury, J. E. Isothermal titration calorimetry of biomolecules. J.E. Ladbury and B.Z. Chowdhry. Biocalorimetry - Applications of Calorimetry in the Biological Sciences. John Wiley & Sons Ltd.; 1998; pp. 5-25.

Taylor, H. J. and Goldhaber, M. Detection of nuclear disintegration in a photographic emulsion. Nature. 1935; 135:341.

Tseng, Y. L.; Liu, J. J., and Hong, R. L. Translocation of liposomes into cancer cells by cell-penetrating peptides penetratin and tat: a kinetic and efficacy study. Mol Pharmacol. 2002 Oct; 62(4):864-872.

Wymer, N. J.; Gerasimov, O. V., and Thompson, D. H. Cascade liposomal triggering: light-induced Ca^{2+} release from diplasmenylcholine liposomes triggers PLA_2-catalyzed hydrolysis and contents leakage from DPPC liposomes. Bioconjug Chem. 1998 May-1998 Jun 30; 9(3):305-308.

Zheng, J. H.; Chen, C. T.; Au, J. L., and Wientjes, M. G. Time- and concentration-dependent penetration of doxorubicin in prostate tumors. AAPS PharmSci. 2001; 3(2):E15.

Zocchi, E.; Tonetti, M.; Polvani, C.; Guida, L.; Benatti, U., and De Flora, A. Encapsulation of doxorubicin in liver-targeted erythrocytes increases the therapeutic index of the drug in a murine metastatic model. Proc Natl Acad Sci U S A. 1989 Mar; 86(6):2040-2044.

Zschörnig, O.; Richter, W.; Pasche, G., and Arnold, K. Cation-mediated interaction of dextran sulfate with phospholipid vesicles: binding, vesicle surface polarity, leakage and fusion. Colloid Polym Sci. 1992; 278:637-646.

9. Appendices

I

Interaction of $Na_2B_{12}H_{11}SH$ with liposomes: Influence on zeta potential and particle size

Available online at www.sciencedirect.com
SCIENCE DIRECT®
ELSEVIER
Journal of Organometallic Chemistry 690 (2005) 2732 2735
Journal of Organometallic Chemistry
www.elsevier.com/locate/jorganchem

Interaction of $Na_2B_{12}H_{11}SH$ with liposomes: Influence on zeta potential and particle size

Doaa Awad [a,*], Irene Tabod [a], Silke Lutz [a,1], Holger Wessolowski [b], Detlef Gabel [a]

[a] Department of Chemistry, University of Bremen, D-28334 Bremen, Germany
[b] Institute of Environmental Process Engineering, University of Bremen, D-28334 Bremen, Germany

Received 13 September 2004; accepted 11 January 2005
Available online 25 February 2005

Abstract

The interaction of $Na_2B_{12}H_{11}SH$ (BSH) with liposomes has been studied. BSH is a compound used clinically in boron neutron capture therapy of glioblastoma, and is known to enter tumor cells. Liposomes were used as a model for studying the interaction of BSH with cell membranes. BSH led to changes in the zeta potential of liposomes consisting of DODAB (dioctadecyldimethylammonium bromide) alone or with DOPC (dioleylphosphatidylcholine) or DOPE (dioleylphosphatidylethanolamine). It also led to changes of the size of DODAB liposomes, with a maximum size at small zeta potentials. A firm binding of BSH with the head groups of the lipid must be assumed.

Keywords: BSH; Liposomes; Liposome size; Zeta potential

1. Introduction

BSH ($Na_2B_{12}H_{11}SH$, also known as mercaptoborate sodium) has long been used for therapy of brain tumors with BNCT (boron neutron capture therapy) [1,2]. We have investigated the pharmacokinetics of BSH in patients [3,4] and could determine that the pharmacokinetics is linear. The initial volume of distribution V_1 is 0.3 L/kg [3]. With a dose of 1 g BSH per kg body weight, the initial concentration of BSH in V_1 is about 5 mM. In tumor material of glioma patients who had been infused with BSH, boron persists for long periods of time [5], but is distributed in a heterogeneous manner. Uptake of BSH was mostly in cells of the tumor positively staining for glial fibrillary acidic protein (GFAP) [6]. BSH could not be removed by fixation with aqueous formaldehyde nor by washing during histochemical staining [7]. The subcellular localization of boron in tumor tissue could be determined with both electron energy loss spectroscopy and electron microscopy following immunohistochemical staining [8]; boron was found to be associated with electron-dense material in the intercellular space, with the cell membrane, and with the nuclear membrane and the chromatin. The pathway by which the very hydrophilic boron cluster compound is taken up into the cells, and nature of the binding to structures within the cells, remains unclear. One hypothesis [7] is that the boron cluster initially interacts with quaternary ammonium groups on the cell surface. We have shown that the hydrophilic cluster can dissolve in organic solvents in the presence of phospholipids [9]. Tetramethylammonium ions usually lead to precipitation of cluster compounds from aqueous solutions [10]. The firmly bound BSH could then be internalized, and redistributed within the cell after degradation of the lipids. It is

* Corresponding author. Tel.: +49 421 2182841; fax: +49 421 2182871.
E-mail address: doaaelsayed363@hotmail.com (D. Awad).
[1] Present address: novosom AG, D-06120 Halle, Germany.

0022-328X/$ - see front matter © 2005 Elsevier B.V. All rights reserved.
doi:10.1016/j.jorganchem.2005.01.013

interesting to note that the prevalence of choline in brain tumors exceeds those of the healthy brain by a factor of 4 [11].

In order to further explore the hypothesis, we investigated the interaction of BSH with liposomes of different composition, by determining the zeta potential and the size of the particles as a function of the BSH concentration. The zeta potential is a function of the overall charge of a particle, and changes in size reflect aggregation or fusion.

2. Materials and methods

DODAB (dioctadecyldimethylammonium bromide) was a gift of Dr. Radmacher, DOPE (dioleylphosphatidylethanolamine) and DOPC (dioleylphosphatidylcholine) were a gift of Lipoid GmbH. BSH ($Na_2B_{12}H_{11}SH$) was prepared according to the literature procedures [12].

Liposomes were prepared by sonication alone or in combination with extrusion through polycarbonate membranes with a pore diameter of 100 nm (Avestin, Mannheim, Germany). The liposomes consisted of either pure DODAB, or a mixture of 37.5 mol% DODAB and 31.5 mol% each of DOPC and DOPE, or a mixture of 50 mol% DODAB and 50 mol% DOPE and DOPC, respectively. The liposomes were prepared in 1 mM Tris buffer pH 7.4. Lipid contents was determined with the Stewart assay [13], taking into account the different color intensity of each of the lipids. Liposomes were stored up to one week at 4 °C; their size was not found to change during this period.

The size distribution and the zeta potential of the liposomes were measured with a Malvern Zetamaster. For zeta potential measurements, 5–10 individual determinations were averaged. The liposome suspension was 1 mM in Tris–HCl pH 7.4. BSH was added in different concentrations. Measurements were started after a few minutes. The BSH concentration required to achieve a zeta potential of 0 mV was determined by interpolation of the data.

3. Results and discussion

The liposomal suspensions investigated and selected measurements are listed in Table 1. BSH showed a strong and concentration-dependent effect on the average size of the particles in solutions containing DODAB liposome. A maximum size of 5 μm was found when BSH was added to the liposome solution at slightly more than a 1:2 concentration ratio BSH: DODAB (see Fig. 1). At both higher and lower concentrations of BSH, the particle sizes were smaller (in the absence of BSH, 57 nm, in the presence of 500 μM BSH, 105 nm for liposomes present at a lipid concentration of 70 μM). At intermediate concentrations, the solution contained aggregates visible to the naked eye. The size of the liposomes in the presence of high concentrations of BSH was almost twice of that in the absence, indicating that the cluster increases the effective size of the liposome. The same behavior was found for both pure DODAB liposomes and liposomes prepared from DODAB and other lipids (Table 1).

The zeta potential of DODAB liposomes was found to be strongly dependent on the amount of BSH added (Fig. 1). The initially positive value went to neutral and then negative values with increasing BSH concentrations. We interpret this as a firm binding of BSH to the positively charged head groups of the lipid, effectively first neutralizing and then overcompensating the surface charge of the liposome and thereby reducing its electrophoretic mobility. When the zeta potential of the DODAB liposomes passed from positive to neutral values (concentration of BSH around 70 μM, i.e., equimolar to the concentration of the lipid), the colloidal solution turned instable (indicated by the appearance of very large aggregates). This would be expected, when the initial repulsion between the positively charged liposomes is reduced by the firm interaction of the positively charged head groups of the lipid with the negatively charged BSH. With a further decrease of the zeta potential to negative values (−40 mV in the presence of 500 μM BSH), large aggregates were no longer seen, probably by the repulsion of the liposomes now carrying

Table 1
Liposomes prepared and their zeta potentials in the absence or presence of BSH

DODAB (μM)	DOPE (μM)	DOPC (μM)	Zeta potential (mV) w/o BSH	C_{BSH} for zeta potential = 0 (μM)	Zeta potential (mV) at BSH concentration (μM)
35			n.d.	23	−31.0/500
70			43.7	70	−36.9/500
140			n.d.	90	−43.8/1000
200			56.0	120	−34.2/500
500			n.d.	290	−48.1/1000
70	70		48.0	100	−9.8/700
70		70	57.2	130	−19.9/700
53	44	44	41.6	55	−21.5/470

Concentrations are given in μM, zeta potentials in mV. n.d., not determined.

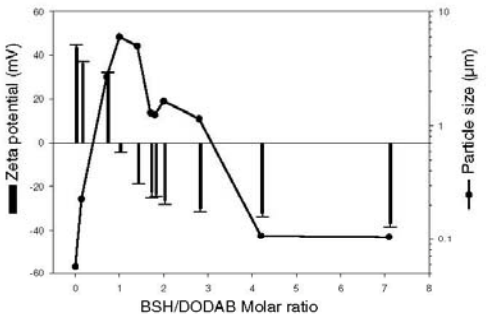

Fig. 1. Zeta potential (including the standard deviation) and particle size for DODAB liposomes as a function of the molar ratio between BSH and the lipid. Lipid concentration was 70 μM in 1mM Tris HCl pH 7.4.

an overall negative charge, as indicated by the zeta potential.

Maximum particle sizes and minimal absolute values of the zeta potential of DODAB liposomes were observed when BSH was added in concentrations about half of that of the lipid, except for the DODAB/DOPE and DODAB/DOPC liposomes, where more than equimolar amounts of BSH to DODAB yielded the maximum size and a zeta potential of 0 mV (Fig. 2).

As the absolute BSH concentrations were low (between 10 and 500 μM, depending on the lipid concentration used), a rather small dissociation constant (below around 20 μM) for the ion pairs from the quaternary ammonium salt and the cluster would have to be assumed. This assumption is based on the observation that also at low concentrations of lipid and BSH, the concentration ratio for yielding a zeta potential of 0 mV does not change. This is in agreement with the observation that the cluster can be isolated from aqueous solutions by adding tetraalkylammonium ions [10], and indicates that the boron cluster cannot be considered a weakly coordinating anion [14] for quaternary ammonium salts.

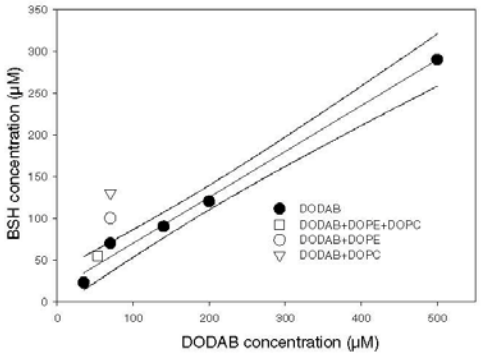

Fig. 2. Concentrations of BSH required for reaching a zeta potential of 0 mV for DODAB liposomes. Liposomes consisted of either pure DODAB (filled circles) or DODAB and additional lipids as indicated. For mixtures of lipids, the DODAB concentration is given.The lines are the linear regression line and the 95% confidence intervals.

Effective neutralization of the charge caused by DODAB would require one molecule of BSH for every two molecules of DODAB on the surface, or every four molecules of DODAB in bigger vesicles (where the curvature of the vesicle and the resulting decrease of the inner surface in comparison to the outer surface can be neglected). It was found that for pure DODAB liposomes, the concentration ratio of BSH to DODAB required for reaching a zeta potential of 0 mV was independent of the concentration of the lipid. The amount of BSH required was 55% of that of the total DODAB concentration; for the lipid molecules on the outside of the liposome, and taking into account the curvature of the membrane, a 1:1 molar ratio between BSH and DODAB present on the surface can be assumed. This represents a formal excess of BSH by a factor of 2.

When the DODAB liposomes contained DOPE or DOPC the concentration of BSH required for a zeta potential of 0 mV were generally higher than those required for the same amount of DODAB of pure DODAB liposomes.

Neutralization of the surface charge of DODAB liposomes was achieved at absolute concentrations of BSH well below the initial concentration reached by BSH following its infusion into patients [3]. The neutralization is an effect associated with BSH and not merily of the presence of divalent anions, as neither a substantial reduction of zeta potential, nor an increase in size, of the liposomes was observed when sulfate anions were added at equal or higher concentrations.

The interaction of negatively charged ions with positively charged liposomes has been observed before [15]. In that case, however, nucleic acids were used as polyanions. To our knowledge, it is the first time that an interaction of liposomes with small divalent anions is observed and quantified.

Acknowledgement

The gift of lipids from Lipoid GmbH, Ludwigshafen, Germany, is gratefully acknowledged.

References

[1] Y. Nakagawa, H. Hatanaka, J. Neuro-Oncol. 33 (1997) 105.
[2] K. Hideghety, W. Sauerwein, A. Wittig, C. Gotz, P. Paquis, F. Grochulla, K. Haselsberger, J. Wolbers, R. Moss, R. Huiskamp, H. Fankhauser, M. de Vries, D. Gabel, J. Neuro-Oncol. 62 (2003) 145.

[3] D. Gabel, D. Preusse, D. Haritz, F. Grochulla, K. Haselsberger, H. Fankhauser, C. Ceberg, H.-D. Peters, U. Klotz, Acta Neurochir. 139 (1997) 606.
[4] T. Kageji, S. Nagahiro, K. Kitamura, Y. Nakagawa, H. Hatanaka, D. Haritz, F. Grochulla, K. Haselsberger, D. Gabel, Int. J. Radiat. Oncol. Biol. Phys. 51 (2001) 120.
[5] D. Haritz, D. Gabel, R. Huiskamp, Int. J. Radiat. Oncol. Biol. Phys. 28 (1994) 1175.
[6] M. Neumann, M. Bergmann, D. Gabel, Acta Neurochir. 145 (2003) 971.
[7] B. Otersen, D. Haritz, F. Grochulla, M. Bergmann, W. Sierralta, D. Gabel, J. Neuro-Oncol. 33 (1997) 131.
[8] M. Neumann, U. Kunz, H. Lehmann, D. Gabel, J. Neuro-Oncol. 57 (2002) 97.
[9] T. Kageji, B. Otersen, D. Gabel, R. Huiskamp, Y. Nakagawa, K. Matsumoto, Biochim. Biophys. Acta 1391 (1998) 377.
[10] D. Gabel, D. Moller, S. Harfst, J. Rösler, H. Ketz, Inorg. Chem. 32 (1993) 2276.
[11] D. Ott, J. Hennig, T. Ernst, Radiology 186 (1993) 745.
[12] M. Komura, K. Aono, K. Nagasawa, S. Sumimoto, Chem. Exp. 2 (1987) 173.
[13] J.C.M. Stewart, Anal. Biochem. 104 (1959) 10.
[14] I. Krossing, I. Raabe, Angew. Chem., Int. Ed 43 (2004) 2066.
[15] M.R. Almofti, H. Harashima, Y. Shinohara, A. Almofti, Y. Baba, H. Kiwada, Arch. Biochem. Biophys. 410 (2003) 246.

II

Triggered release of liposome content by $B_{12}H_{11}SH(2-)$: The anionic boron cluster $B_{12}H_{11}SH(2-)$ (BSH) as a novel means to trigger release of liposome contents

Triggered release of liposome content by $B_{12}H_{11}SH(2-)$

DOI: 10.1002/anie.200123456

The anionic boron cluster $B_{12}H_{11}SH(2-)$ (BSH) as a novel means to trigger release of liposome contents[**]

Detlef Gabel, Doaa Awad, Tanja Schaffran, Diana Radovan, Daniel Dărăban, Luminita Damian, Mathias Winterhalter, Göran Karlsson, Katarina Edwards*

Liposomes are novel carriers for pharmaceutical agents. For example, in cancer treatment liposomes serves for administration of doxorubicin (DOX). DOX is slowly released and can maintain a threshold level. The systemic toxicity is reduced when compared to the free drug. Liposomal drugs can therefore be administered in higher concentrations before dose-limiting side effects are met. Further, they often show longer retention times in the body and sometimes also accumulate to a larger extent in target tissue. They are, however, frequently less active for a given dose when compared to the free agent, as the drug cannot easily escape from the liposome to reach its target. Since liposomes must be designed to avoid premature release of their content, a trigger for controlled release is needed

A number of solutions have been suggested to trigger release of liposomal drugs. These include the use of pH-sensitive liposomes,[1] enzyme-susceptible liposomes,[2] thermosensitive liposomes,[3] or ultrasound-responsive liposomes.[4] So far, none of these approaches are in clinical use and there is a well-recognised need for effective triggered release.

In this study we show that liposomes consisting of dipalmitoyl phosphatidylcholine (DPPC) release their contents upon addition of the negatively charged boron cluster $Na_2B_{12}H_{11}SH$ (BSH).

BSH is already in clinical use for the treatment of glioblastoma with boron neutron capture therapy (BNCT),[5,6] and has been administered in concentrations of 100 mg/kg body weight without provoking any adverse reaction.[7] The blood concentration of BSH surpasses 2 mM at the end of an intravenous infusion of 100 mg/kg, and declines with an initial half life of around 4.5 h.[6] Concentrations in brain tumour and several other tissues are similar to that of blood.[7] Repeated administration is possible and leads to higher blood concentration.[8]

BSH triggers release of liposome content in a dose-dependent manner. Concentrations of 1 mM BSH suffice to increase noticeably the release rate of carboxyfluorescein (CF) encapsulated in liposomes prepared from DPPC, either as such or supplemented with 2 mol% 1,2-disteaoryl-sn-glycero-3-phosphatidyl-ethanolamine-N[methoxypoly(ethyleneglycol)] (DSPE-PEG2000) (see Fig. 1). At higher BSH concentrations, leakage is complete within minutes. At low BSH concentrations, inclusion of PEG lipids leads to more pronounced sigmoidal release curves and higher leakage rates, whereas at higher BSH concentrations the rate is lower. DOX leaks with about the same kinetics as CF (correcting for the quenching of DOX fluorescence by BSH) (results not shown).

Differental scanning calorimetry (DSC) reveals that 10 mM BSH shifts the main transition of DPPC from 41.6°C to 40.9°C, and the pretransition from 35.7°C to 34.1°C (see Fig.2).

Cryo-transmission electron microscopy (cryoTEM) reveals that DPPC liposomes aggregate and increase in apparent size upon incubation with BSH at 37°C, and that they change their morphology drastically after incubation at 45°C (Fig. 3). No structural effects of BSH on PEG-containing liposomes were seen, although they leak similarly fast as the non-PEGylated liposomes, as shown in Fig. 1.

---

[*] Prof. Dr. D. Gabel, D. Awad, MSc, Dipl.-Chem. T. Schaffran, D. Radovan, MSc, D. Balaban, MSc
Department of Chemistry
University of Bremen
D-28334 Bremen, Germany
Fax: (+)49 421 2812871
E-mail: gabel@chemie.uni-bremen.de

Prof. Dr. M. Winterhalter, Dr. L. Damian
School of Engineering and Science
International University Bremen
D-28725 Bremen, Germany

Prof. Dr. K. Edwards, G. Karlsson
Department of Physical and Analytical Chemistry
University of Uppsala
S-751 23 Uppsala, Sweden

[**] D. Awad acknowledges a stipend from the Egyptian government, D. Radovan support from the Erasmus program of the EU. K. Edwards gratefully acknowledges financial support from the Swedish Research Council and the Swedish Cancer Society. Gift of lipids from Lipoid, Ludwigshafen, is gratefully acknowledged.

When adherently growing cells are exposed to DOX-filled DPPC-PEG liposomes in combination with BSH their survival is significantly lower than when the cells are exposed to DOX-filled liposomes or BSH alone (see Fig. 4). BSH does not influence the toxicity of free DOX.

Ions are known to influence the structure of phospholipid bilayers. Ca^{2+} and La^{3+} ions bring about fusion of (acidic) phosphatidylserine liposomes at concentrations as low as 10^{-5} and 10^{-3} M, respectively.[9] The poly-anion DNA gives rise to major structural rearrangements, and formation of so-called lipoplexes, when mixed with positively charged liposomes.[10] At concentrations up to 0.1 M, small anions have little effects on neutral liposomes.[12] We confirmed this for Na_2SO_4. The effect must therefore lie in a more specific interaction of BSH with the lipid.

It might be speculated that BSH interacts with the membrane head groups of DPPC, interaction with the hydrophobic part of the bilayer being more improbable due to the ionic nature of the cluster.

The mechanism by which BSH interacts with the membrane head group is not evident from our results. As most tetramethylammonium salts of derivatives of $B_{12}H_{12}^{2-}$, including BSH, are insoluble in water [11], the quaternary ammonium group of the choline unit might be involved. Our observation that already small concentrations of BSH change the DSC behaviour in the pretransition region, where changes in the arrangement of the head groups and the formation of ripple phases are believed to take place[12] support this view. The molecular events leading to a transient or permanent increase in permeability of the liposome membrane are equally unclear. Although strong aggregation and (at higher temperatures very marked) change in morphology of DPPC liposomes is induced by BSH, this cannot be responsible for the release, as PEGylated liposomes are not aggregated by BSH, and yet release their content equally well. Rather, the observed gross morphological changes of DPPC liposomes might be secondary to alterations in the properties of the isolated liposomes.

Investigation of the mechanism by which BSH interacts with DPPC, elucidation of the nature of the phase transitions observed, study of the structure of the phases and their composition, understanding of the sigmoidal release kinetics, and experiments with other lipids should help to clarify the nature of the phenomena observed.

Medical application of the release of liposome-encapsulated chemotherapeutic agents by BSH appears obvious. The consecutive administration of suitable liposomes and BSH, which is well tolerated by patients, might open new perspectives for the treatment of diseases with liposome-encapsulated drugs.

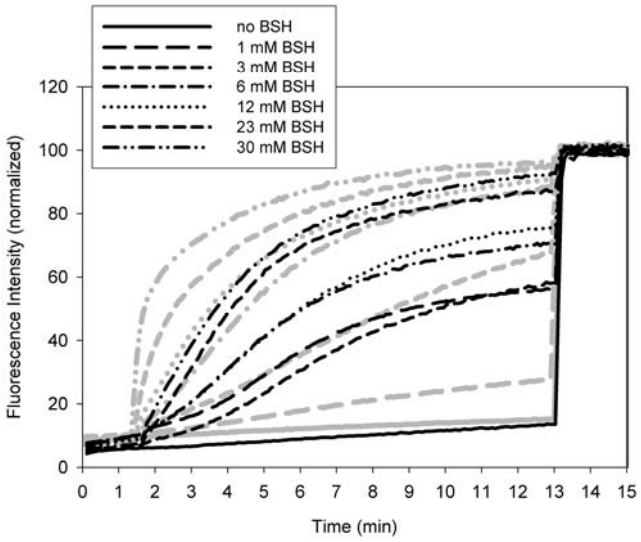

Figure 1. Release of CF (measured as increase of fluorescence) from DPPC (grey lines) and DPPC+2mol% DSPE-PEG (black lines) liposomes in the presence of the indicated concentrations of BSH at 37°C. The concentrations of BSH were (lines from bottom to top) 0, 1, 3, 6, 12, 23, and 30 mM, added at 90 s. At 13 min, Triton X-100 was added to 0.1% for lysis of all liposomes. Lipid concentration was 10 µM.

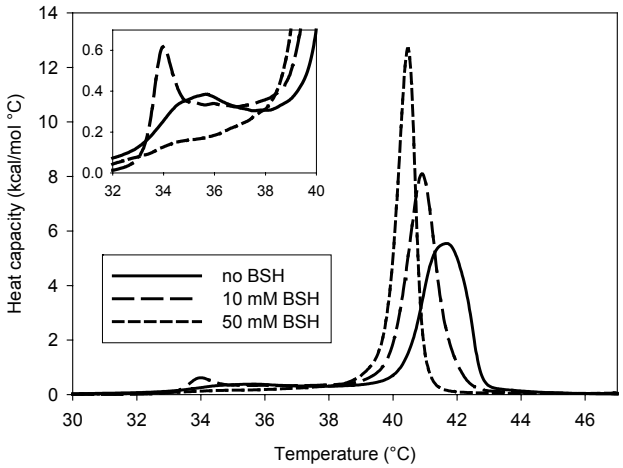

Figure 2. DSC of DPPC (concentration 5 mM) in the absence and the presence of 10 and 50 mM BSH. Inset: Enlargement of the pre-transition area.

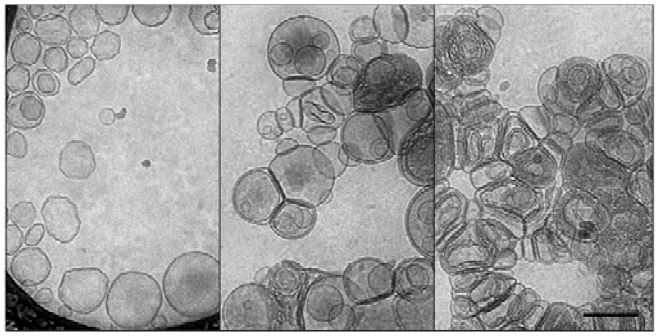

Figure3. Cryo-TEM pictures of DPPC liposomes (left) incubated with 10 mM BSH at 37°C (center) and 45°C (right), prepared at the incubation temperatures. Lipid concentration 10 mM.

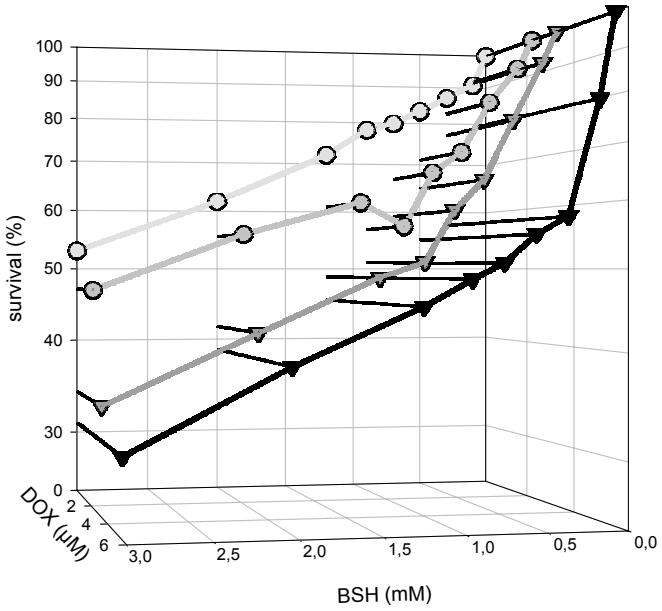

Figure 4. Cell survival of V79 Chinese hamster cells exposed to BSH or to increasing amounts of DOX-containing liposomes of DPPC with 2 mol% DSPE-PEG2000 in the presence of BSH. The curves are normalized to 100% when no BSH was present .The concentrations of DOX increase with increasing blackness of the lines, and were 0, 2.2, 3.3, and 5.5 μM, respectively. In order to guide the eye, drop lines to the BSH/survival plane are shown. The LD_{50} for free DOX in the absence of BSH was 0.85 μM, and was not changed significantly by the addition of BSH up to the highest concentration tested (10 mM).

Experimental Section

DPPC and DSPE-PEG_{2000} were from Lipoid, Ludwigshafen, Germany. DOX was from Polymed Therapeutics, Houston, TX. CF was from Kodak.

Liposomes were prepared by film hydration and extrusion through a 100-nm polycarbonate membrane.[13] DOX was loaded by published procedures.[14] Encapsulated DOX was determined by fluorescence following lysis with Triton X-100. CF was encapsulated passively at a concentration of 100 mM.

Lipid concentration was measured by the Stewart assay.[15]

Leakage of liposomes was followod through the increase of fluorescence of liberated CF (excitation 490 nm, emission 515 nm) or DOX (excitation 470 nm, emission 555 nm). Triton X-100 was added at the end to measure the value for 100% release. The values for DOX were corrected for quenching by BSH (about 30%).

V79 Chinese Hamster cells were grown in F10 medium and 5% newborn calf serum at 37°C and 5% CO_2. They were seeded into 96-well plates at 11.000 cells per well, and grown for 24 hours prior to exposure to the drug, and the exposed for 24 hours at 37°C and 5% CO_2. The supernatant was replaced with a WST-1 solution (1:4 diluted with PBS) and incubated for 4-6 hours. The absorbance at 450 nm was read. Appropriate controls were set to 100%.

CryoTEM and sample preparation was carried out as described before.[16] Liposomes were incubated in Eppendorf cups at the temperatures indicated, and cryoTEM samples were prepared at the incubation temperature.

DSC was carried out in a Microcal VP-DSC instrument at a lipid concentration of 5 mM in phosphate buffered saline. Heating rates were 60°/h.

Received: ((will be filled in by the editorial staff))
Published online on ((will be filled in by the editorial staff))

Keywords: liposomes · boranes · calorimetry · leakage · cellular toxicity

[1] G. Shi, W. Guo, S. M. Stephenson, R. J. Lee, *J. Controlled Release* **2002**, *80* 309-19.
[2] T. L. Andresen, S. S. Jensen, K. Jorgensen, *Prog. Lipid Res.* **2005**, *44* 68-97.
[3] D. Needham, G. Anyarambhatla, G. Kong, M. W. Dewhirst, *Cancer Res.* **2000**, *60* 1197-201.
[4] S. L. Huang, R. C. MacDonald, *Biochim. Biophys. Acta* **2004**, *1665* 134-41.
[5] H. Hatanaka, Y. Nakagawa, *Int. J. Radiation Oncol. Biol. Phys.* **1994**, *28* 1061-1066.
[6] T. Kageji, S. Nagahiro, K. Kitamura, Y. Nakagawa, H. Hatanaka, D. Haritz, F. Grochulla, Haselsberger K, D. Gabel, *Int. J. Radiation Oncol. Biol. Phys.* **2001**, *51* 120-130.
[7] D. Gabel, D. Preusse, D. Haritz, F. Grochulla, K. Haselsberger, H. Fankhauser, C. Ceberg, H.-D. Peters, U. Klotz, *Acta Neurochir.* **1997**, *139* 606-612.
[8] K. Hideghéty, W. Sauerwein, K. Haselsberger, F. Grochulla, H. Fankhauser, R. Moss, R. Huiskamp, D. Gabel, M. de Vries, *Strahlenther. Onkol.* **1999**, *175* 111-114.
[9] S. A. Tatulian, V. I. Gordeliy, A. E. Sokolova, A. G. Syrykh, *Biochim Biophys Acta* **1991**, *1070* 143-51.
[10] S. Weisman, D. Hirsch-Lerner, Y. Barenholz, Y. Talmon, *Biophys J* **2004**, *87,* 609-14.
[11] D. Gabel, D. Moller, S. Harfst, J. Rösler, H. Ketz, *Inorg. Chem.* **1993**, *32* 2276-2278.
[12] T. Kaasgaard, C. Leidy, J. H. Crowe, O. G. Mouritsen, K. Jorgensen, *Biophys. J.* **2003**, *85* 350-60.
[13] S. A. Abraham, K. Edwards, G. Karlsson, S. MacIntosh, L. D. Mayer, C. McKenzie, M. B. Bally, *Biochim. Biophys. Acta* **2002**, *1565* 41-54.
[14] N. Dos Santos, K. A. Cox, C. A. McKenzie, F. van Baarda, R. C. Gallagher, G. Karlsson, K. Edwards, L. D. Mayer, C. Allen, M. B. Bally, *Biochim. Biophys. Acta* **2004**, *1661* 47-60.
[15] J. C. Stewart, *Anal. Biochem.* **1980**, *104* 10-4.
[16] M. Almgren, K. Edwards, G. Karlsson, *Colloids Surf., A* **2000**, *174* 3-21.

((Subject Heading))

Detlef Gabel*, Doaa Awad, Tanja Schaffran, Diana Radovan, Daniel Dărăban, Luminita Damian, Mathias Winterhalter, Göran Karlsson, Katarina Edwards

The anionic boron cluster $B_{12}H_{11}SH(2-)$ (BSH) as a novel means to trigger release of liposome contents

Triggered release. Liposomes can be triggered to release their contents by the addition of millimolar concentrations of $B_{12}H_{11}SH(2-)$, a compound in clinical use. This observation can be of great value in the therapy of diseases by liposome-encapsulated drugs.

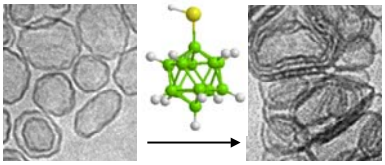

((Insert TOC Graphic here))

III

Interaction of $Na_2B_{12}H_{11}SH$ with dimyristoyl phosphatidylcholine liposomes

Interaction of $Na_2B_{12}H_{11}SH$ with dimyristoyl phosphatidylcholine liposomes

Doaa Awad[a], Luminita Damian[b], Mathias Winterhalter[b], Göran Karlsson[c], Katarina Edwards[c], Detlef Gabel[a]

[a] Department of Chemistry, University of Bremen, D-28334 Bremen, Germany

[b] School of Engineering and Science, International University Bremen, D-28725 Bremen, Germany

[c] Department of Physical and Analytical Chemistry, University of Uppsala, S-75123 Uppsala, Sweden

Abstract

The interaction of $Na_2B_{12}H_{11}SH$ (BSH) with dimyristoyl phosphatidylcholine (DMPC) liposomes has been investigated. BSH is an established boron carrier for boron neutron capture therapy (BNCT). Liposomes synthesized from DMPC were used to explore the interaction of BSH with cell membranes. The effect of BSH on DMPC liposomes has been investigated using differential scanning calorimetry. Changes in transition temperature by BSH have been observed. The partition coefficient and the enthalpies for the binding of BSH to the liposomes were determined by isothermal titration calorimetry. Cryo-transmission electron microscopy showed aggregation and fusion which includes the formation of thicker liposome walls. The extent of the decrease in resonance energy transfer between N-(7-nitrobenz-2-oxa-1,3-diazol(-4-yl)-1,2-di-hexadecanoyl-sn-glycero-3-phospho-ethanolamine (NBD-PE) and rhodamine B 1,2-dihexadecanoyl-sn-glycero-3-phospho-ethanolamine (Rh-PE), embedded in the liposomes bilayer, has been monitored in the absence and presence of BSH. Carboxyfluorecein leakage from DMPC liposomes has also been observed. A decrease in the surface dielectric constant of the liposomes surface has been found. When choline has been used in excess over BSH, its presence had a small influence on the interaction of BSH with the liposomes.

1. Introduction

BSH is used in medicine for the treatment of tumors in a technique named boron neutron capture therapy (BNCT) (Hatanaka 1994). BSH is firmly bound to the glioma tissue sections of several patients having received BSH prior to surgery (Otersen 1997 and Neumann 2002). It is strongly associated with extracellular structures, the

cell membrane and with the chromatin. The negatively charged BSH would not be expected to pass through the cell membrane which is also negatively charged. For this reason we interested in this phenomenon which is most probably due to the lipid composition of the cell membrane because it has been found that glioblastoma tissue is rich in choline (Ott 1993). BSH is water insoluble in the presence of tetramethylammonium as a counter ion (Gabel 1993). In our estimation, this indicates a strong interaction between the negatively charged BSH and the positively charged ammonium group. Therefore, we suppose that the quaternary ammonium groups of the liposomes and subsequently of the membranes are necessary in order that BSH achieve an effect. We have investigated the interaction of BSH with liposomes of different composition by determining the zeta potential and the size of the particles as a function of the BSH concentration. A firm binding of BSH with the head group has been assumed (Awad 2005). In order to further investigate this phenomenon, we determined the changes induced in DMPC liposomes by BSH using DSC, ITC, cryo-TEM, FRET experiments, Leakage experiments and dielectric constant measurements. The changes indicate aggregation and fusion of liposomes which could be due to an interaction of BSH with the choline headgroups of the liposomes. According to this hypothesis, presence of choline should prevent or weaken the effect of BSH. We have tried to investigate this hypothesis by performing experiments using BSH which is preincubated with choline and comparing the results with those obtained from experiments carried out using only BSH.

2. Materials and methods

2.1. Materials

DMPC (dimyristoyl phosphatidylcholine) was gift of Lipoid GmbH. BSH ($Na_2B_{12}H_{11}SH$) was from Boron Biologicals. Carboxyfluorescein (CF) was obtained from Aldrich. NBD-PE (N-(7-nitrobenz-2-oxa-1,3-diazol(-4-yl)-1,2-di-hexadecanoyl-sn-glycero-3-phospho-ethanolamine, riethylammonium salt) and Rh-PE (rhodamine B 1,2-dihexadecanoyl-sn-glycero-3-phospho-ethanolamine,trimethylammonium salt) were from Molecular Probes (Eugene, OR, USA). DPE (Dansylphosphatidylethanolamine) and choline were from Sigma Chemical (St. Louis, Mo, USA). Unless stated, all experiments were carried out in 1 mM Hepes, 150 mM NaCl, pH 7.4.

2.2. Liposomes preparation

DMPC was dried from chloroform and methanol (2:1) then hydrated in buffer. The DMPC liposomes were prepared by 10 freeze-thaw cycles and extruded 21-times through a 100-nm polycarbonate membrane at 40°C.

DMPC liposomes containing the water soluble fluorophore CF (carboxyfluorescein) were prepared by extrusion. The lipid film was hydrated with 100 mM aqueous solution (pH 7.4) of CF to give a final lipid concentration of 80 mM. Free CF was removed by passing the extruded suspension through a column of Sephadex G-25. CF-containing vesicles were obtained in the void volume, whereas free CF was retarded.

2.3. Cryo-transmission electron microscopy (cryo-TEM)

The liposomal suspension (final concentration 10 mM) was applied to polymer-coated grid. The sample was shock-frozen in liquid ethane. The vitrified sample was mounted and examined in a Zeiss EM 902 A electron microscope, operating at an accelerating voltage of 80 keV in filtered bright field image mode at $\Delta E = 0$ eV. The stage temperature was kept below 108 K and images were recorded at defocus settings between 1 and 3 µm. Several negatives were taken to ensure the reproducibility of the results (Almgren 2000). DMPC liposomes were incubated overnight with 10 mM BSH at three different temperatures (4, 25, 37°C), then images were taken.

2.4. Differential scanning calorimetry (DSC)

DSC measurements were carried out on a VP-DSC microcalorimeter from Microcal (Northampton, MA, USA) adding buffer in the reference cell. Samples were degassed under vacuum prior the measurement. Upscans and downscans were recorded at temperature range between 15 and 40°C with a scan rate of 90 K/h. As the lipids phase transition is fast a filtering period of 2s was chosen. A background scan collected with buffer in both cells was substracted from each scan. The final lipid concentration was 10 mM. The appropriate amounts of BSH were added to the DMPC liposomes to give final concentrations of 5, 10, 50, 100, 200, 300 and 400 mM BSH. The liposomes were incubated with BSH for 2h at 4°C before scanning.

An experiment was performed using 100 mM BSH which had been preincubated with 400 mM choline to compare the results with those obtained from experiments carried out using only BSH.

For data analysis the software package ORIGIN (Microcal) was used. The temperatures of the transitions are given at the maximum heat flow. Enthalpies are the sums of the enthalpies of components obtained through peak fitting (often resulting in more than one component for each peak).

2.5. Isothermal titration calorimetry (ITC)

The ITC experiments were performed with a VP-ITC microcalorimeter (MicroCal Northampton, MA, USA). The sample cell (1.4371 ml) was filled with the liposomes while the titration syringe (296 µl) was loaded with a BSH solution. Liposomes (3, 6, 9 and 12 mM) were titrated with 4 mM BSH. The binding was monitored at 15°C. The total enthalpy (ΔH) of BSH-DMPC interaction was calculated after an injection of a total volume ΔV (in successive steps) of 4 mM BSH. By applying Schwarz et al.' theory to the ITC data, the partition coefficient and the stoichiometry of the reaction were determined (Schwarz et al. submitted article).

2.6. Lipid mixing

For measurements of lipid mixing, a mixture of 1 mol% each of the fluorescence energy transfer donor and acceptor lipid probes NBD-PE and Rh-PE was added to the DMPC lipid. 2.4 mM of labeled DMPC liposomes were mixed with 17.6 mM of unlabeled DMPC liposomes in absence and presence of different concentrations of BSH (150-400 mM) overnight at three different temperatures (15, 24, 41°C). The final volume for each assay was 20 µl and diluted with 2 ml buffer just before the measurements. The fluorescence measurements were carried out by exciting NBD at 460 nm and recording the fluorescence emission of both NBD and Rh in emission spectra ranging from 500 to 600 nm. Triton was then added to a final concentration of 1% to determine the maximum fluorescence of NBD achievable.

2.7. Leakage experiments

The incubation medium contained 100 µM CF-containing vesicles in 150 mM NaCl, 10 mM Hepes, pH 7.4. The experiments were carried out at 15, 23 and 37°C. Cuvettes containing a stirring bar were placed in thermostated cuvette holder. Different concentrations of BSH (0.5, 0.75, 2, 3, 4, 5, 6, 7, 10 mM) were added and the changes in the fluorescence intensity were recorded for 5 min. Finally 5 µl of 10% (v/v) Triton X-100 was added in order to measure the maximum fluorescence

intensity corresponding to the total trapped dye. Leakage percentages were calculated using the following equation:

$$percentage\_leakage = \frac{Ft - F0}{F\max - F0} \cdot 100 \quad [1]$$

where Fmax is the fluorescence intensity after addition of Triton X-100, Ft is the fluorescence intensity after addition of BSH and F0 is the fluorescence intensity before BSH addition. Measurements were made in a Perkin-Elmer LS-50B Fluorometer at an excitation wavelength of 490 nm and an emission wavelength of 515 nm.

2.8. Surface dielectric constant

For the vesicle surface polarity assays, 1 mol% dansylphosphatidylethanolamine (DPE) was incorporated into the DMPC lipid, then liposomes were prepared as described above (Ohki 2003). 6 mM DMPC-DPE was incubated overnight at 24°C with different concentrations of BSH (0, 200, 400, 600, 1000 mM) in a final volume of 50 µl which was diluted to 1.5 ml before the measurements. The fluorescence signal of DPE was recorded between 350 and 600 nm (excitation at 340 nm). The surface dielectric constant ε was calculated using an empiric formula from measurements in standard organic solvents (Ohki 2003).

$\lambda_{max} = 462.8 + 31.4\ (\log \varepsilon)$ [2]

2.9. Zeta potential and size experiments

All sizing and zeta potential measurements were made on Malvern Zetasizer Nano ZS (Malvern Instruments Ltd., Malvern, U.K.). Liposomes were incubated with different concentrations of either BSH or mixture of BSH and choline (1:4) overnight at 23°C. The final lipid concentration in the incubation mixture was 10 mM. The final BSH concentrations were 2.5, 5, 10, 20, 40, 80, 100, 200, 300 and 400 mM. Before the measurements, the liposomes were diluted 60 times with 1 mM HEPES buffer (pH 7.4). For zeta potential measurements 15 individual determinations were averaged. For size measurements 10 individual determinations were averaged.

3. Results

3.1. Cryo-transmission electron microscopy (cryo-TEM)

The morphology of the liposomes in absence and presence of BSH was determined by cryo-TEM. Fig.1 reveales a certain degree of heterogeneity in the preparation.

Unilamellar liposomes of various sizes co-exist with a few bi- and multilamellar liposomes.

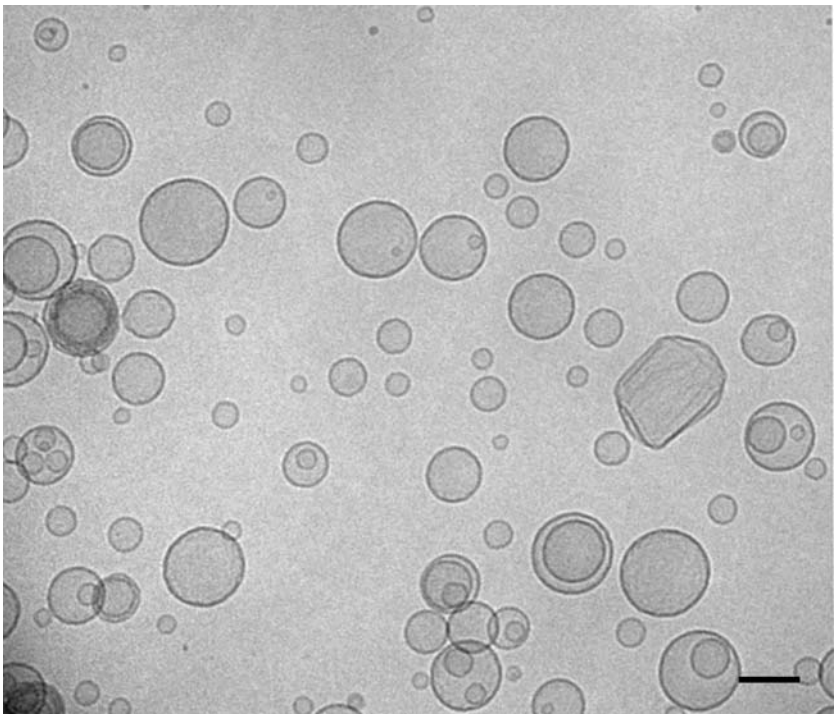

Fig. 1 Cryo-TEM of 10 mM DMPC liposomes. Scale bar 100 nm.

The effects seen by BSH were dependent upon the temperature of incubation and preparation of the samples. Figs. 2 and 3 show that liposomes aggregate and flatten by the action of BSH already at equimolar concentrations of lipid and BSH and 4°C, well below the phase transition temperature. Some thicker membranes, and membranes wrapping around liposomal structures, are seen (Fig. 2).The flattening of liposomes appears to be the most dominant change.

Fig. 2 DMPC liposomes (10 mM lipid) incubated with 10 mM BSH overnight at 4°C. The white arrow indicates compact multilamellar structure. The black arrow aggregate of unilamellar liposomes which are flattened in the contact region. The arrowheads indicate lipid bilayers built around another liposomal structures.

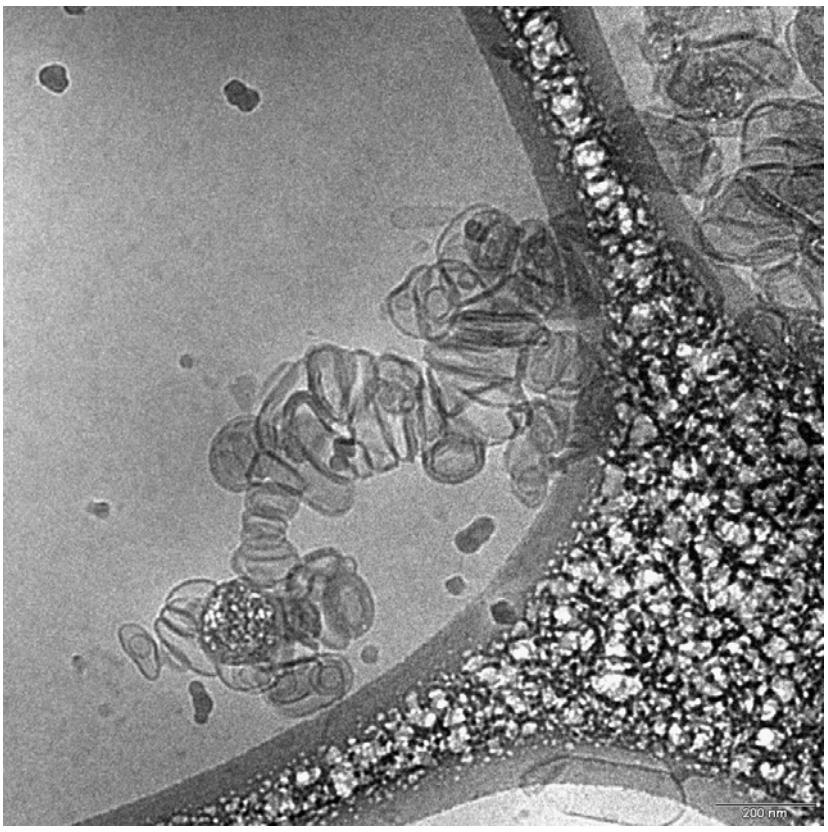

Fig. 3 DMPC liposomes (10 mM lipid) incubated with 100 mM BSH overnight at 4°C.

At 25°C, near the phase transition temperature, extensive aggregation and rearrangement take place when liposomes are incubated with BSH (Figs. 4 and 5). Pronounced is the appearance of thick membrane structures (which have a considerable sensitivity to the electron beam, resulting in the radiation damage visible) when the BSH concentration was equimolar to that of the lipid (10 mM) (Fig. 4). Several of these structures (thickness several tens of nm) end abruptly. A definite layering can be seen in some of the thick structures. At 100 mM BSH, much less very thick structures are seen, but many structures contain thickened membranes (Fig. 5). In general, the appearance of the preparation at high BSH concentration shows more flattened, thin-walled liposomes resembling the structures seen at 4°C, than the preparation with 10 mM BSH.

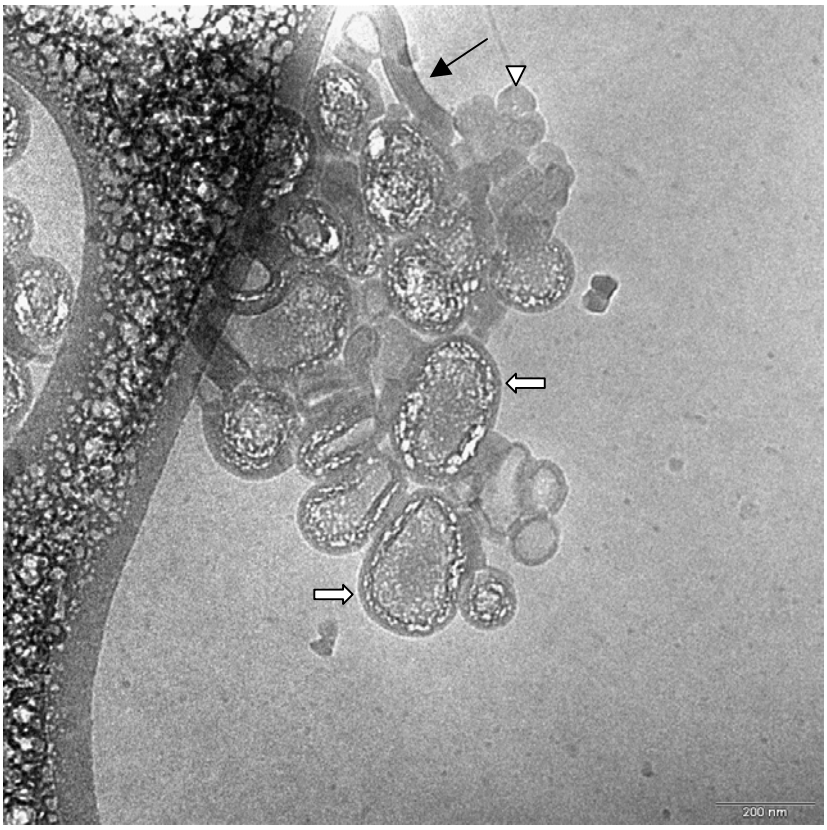

Fig. 4. DMPC liposomes (10 mM lipid) incubated with 10 mM BSH overnight at 25°C. The black arrow indicates stack of tightly associated lipid bilayers which are not closed. The arrowhead indicates aggregated multilamellar liposomes. The white arrows mark multilamellar complexes containing lipid structures (most probably hexagonal phases). A rather radiation damage can be noticed (white spots).

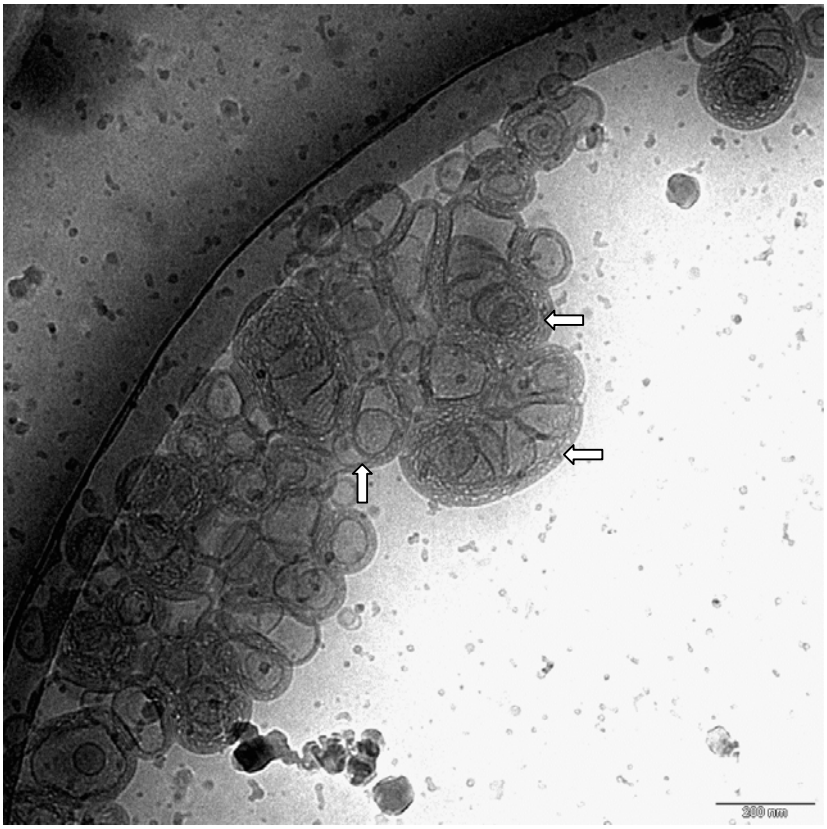

Fig. 5 DMPC liposomes (10 mM lipid) incubated with 100 mM BSH overnight at 25°C. The arrows mark multilamellar structures enclosing either deformed or multilamellar liposomes.

When the temperature of incubation and preparation is raised to 37°C, equimolar concentrations of lipid and BSH show an even increased thickness of the membranes, with a few open structures. At 100 mM BSH, many more open structures appear, and the general appearance of the vesicles shows considerably thinner membranes than the sample incubated at 10 mM BSH.

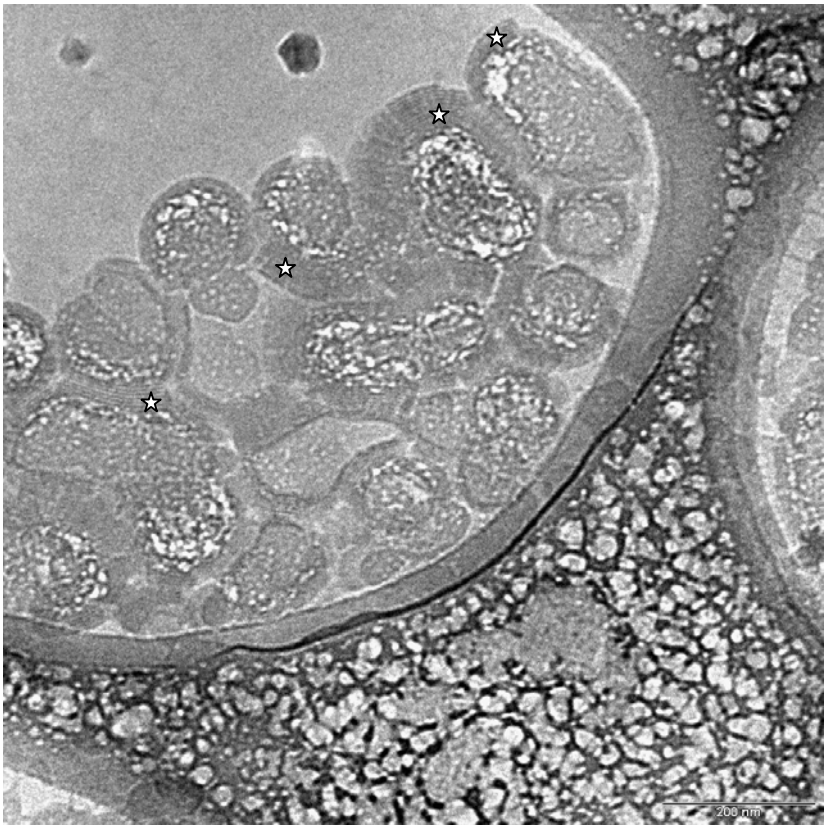

Fig. 6 DMPC liposomes (10 mM lipid) incubated with 10 mM BSH overnight at 37°C. The asterisks indicate incomplete outer bilayers.

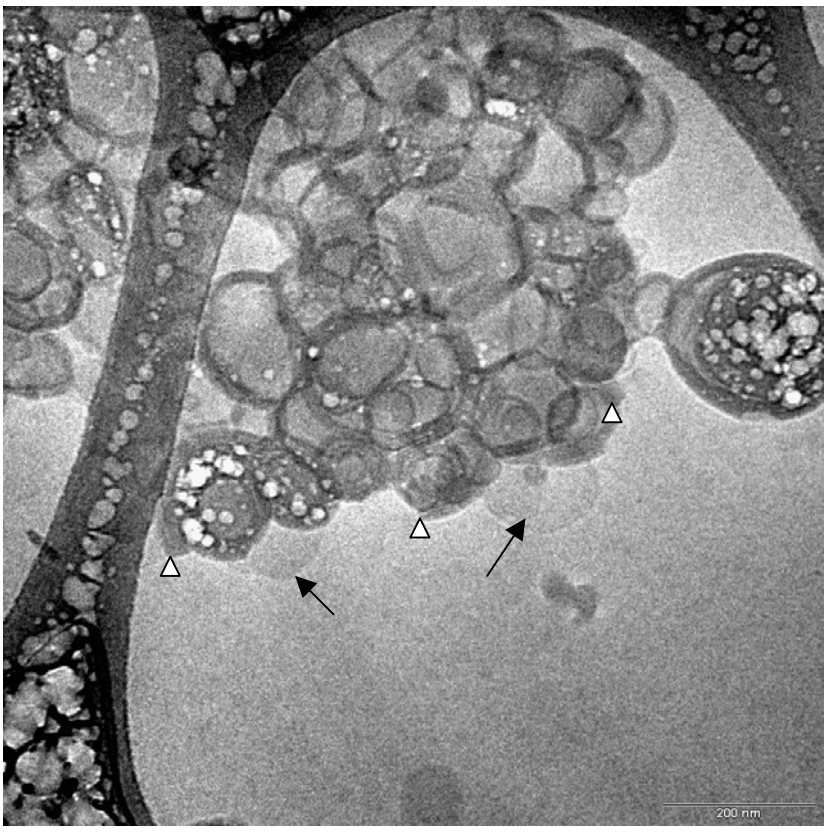

Fig. 7 DMPC liposomes (10 mM lipid) incubated with 100 mM BSH overnight at 37°C. The arrowheads mark unclosed bilayer, whereas the arrows indicate open bilayer sheets.

Heterogeneity of all samples was considerable, with many large aggregates filling one or more openings in the polymer lattice of the grid.

The presence of choline at room temperature (fourfold or fourtyfold excess over BSH and lipid) represses the appearance of thick membrane structures. At 40 mM choline (10 mM each of BSH and lipid) many open structures are seen, which are virtually absent without choline. At 400 mM choline, most structures consisted of individually visible vesicles, closely packed and flattened, resembling the structures seen at 4°C without choline.

a

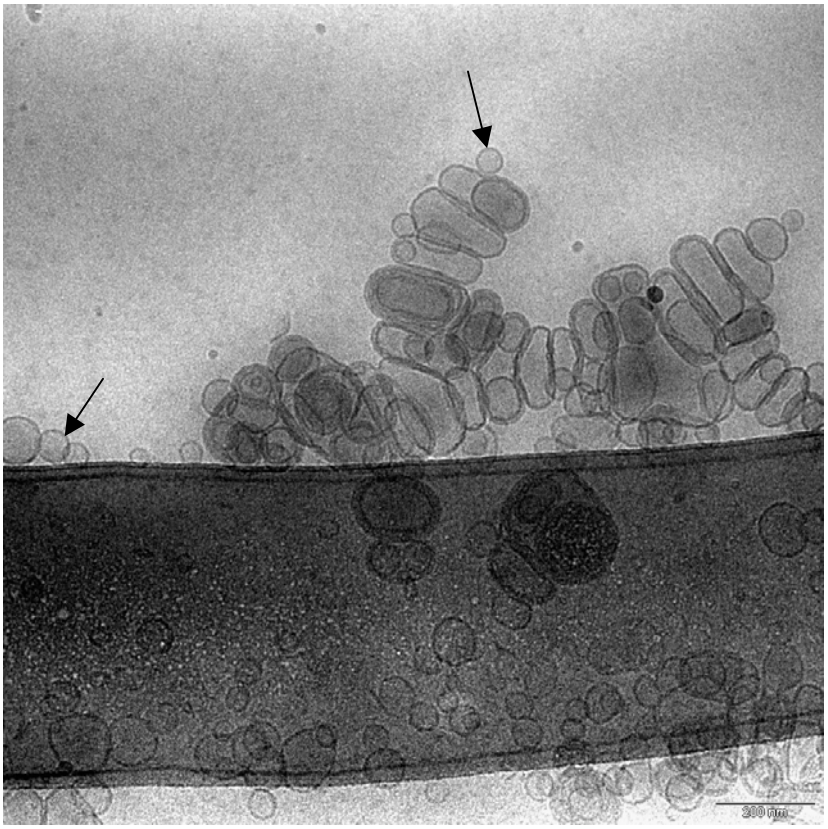

b

Fig. 8 DMPC liposomes incubated with a mixture of (a) 10 mM BSH and 40 mM choline or a mixture of (b) 10 mM BSH and 400 mM choline overnight at room temperature. The arrows indicate the presence of original liposomes.

When Na_2SO_4 was taken as source of divalent anions, the appearance of the resulting liposomes were indistinguishable from the original preparation (Fig. 9).

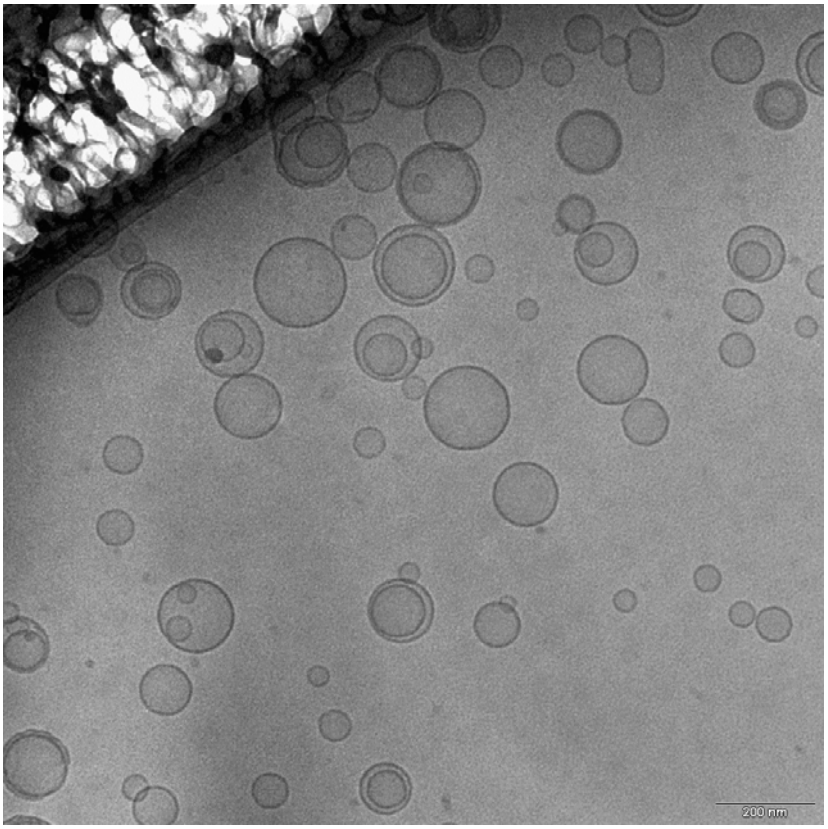

Fig. 9 DMPC liposomes (10 mM lipid) incubated with 100 mM sodium sulfate overnight at 25°C.

3.2. Differential scanning calorimetry (DSC)

Heating thermograms for DMPC and different DMPC:BSH mixtures (1:0.5 to 1:40) are shown in Fig. 10 and 11. In the absence of BSH a small pretransition peak can be seen at 14.95°C. The maximum heat flow (main transition) is observed at 24.3°C, which can be resolved by data analysis to three transitions at 23.9, 24.2 and 24.6°C, respectively. BSH has a major influence on the shape and temperature of the transition peak. The pretransition peak completely disappears already when little BSH (2.5 mM) is added (data not shown). With inreasing BSH concentrations, the transition temperature drops a minimum value (21°C) at 100 mM BSH and then slightly increases with further increasing the BSH concentration. When the liposomes are incubated with 50 mM BSH, a new transition peak appears in the DSC thermograms. Interestingly, the transition temperature of this peak is shifted by more than 10 degrees to higher temperatures when increasing the BSH concentration from 50 to 300 mM. The change in total enthalpy of the main transition does not change significantly up to BSH concentrations of 100 mM, but then increases with higher concentrations of BSH (Fig. 12).

When heating the sample, we found that the main phase transition of DMPC occurs at 24.3°C; when cooling the transition occurs at 23.6°C (Fig. 13). With increasing concentrations of BSH the transition exhibits considerably increased hysteresis, which is about 7°C at 300 mM BSH (Fig. 14); this is not very much influenced by the scan rate (data not shown).

The DSC scans of DMPC liposomes incubated with mixture of BSH and choline (Fig. 15) show that the presence of choline weakens the effect of BSH; that is, the presence of 400 mM choline with 100 mM BSH leads to a transition pattern which corresponds to an effective BSH concentration of 50 mM.

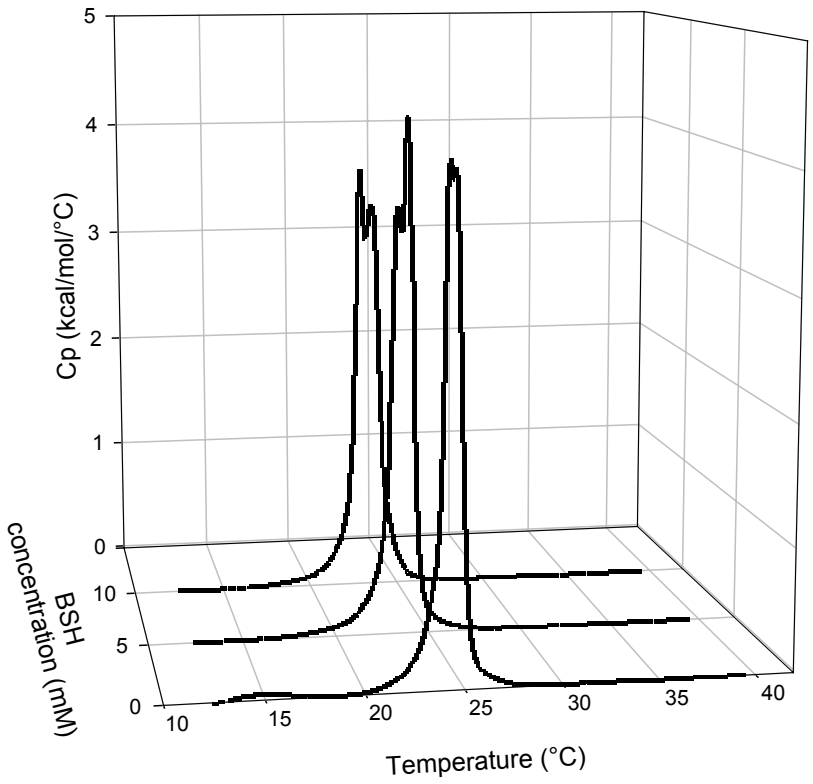

Fig. 10 DSC scans of 10 mM DMPC liposomes without and with small concentrations of BSH.

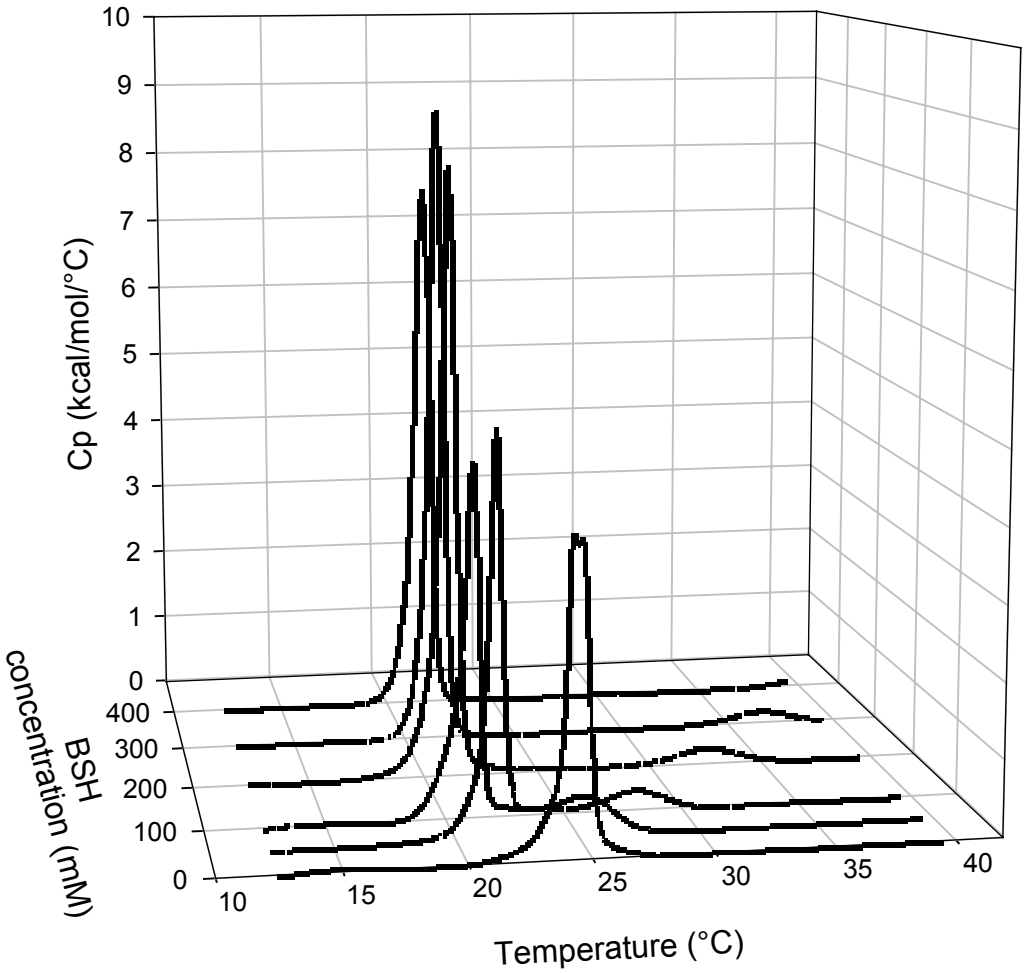

Fig. 11 DSC scans of 10 mM DMPC liposomes with varying concentrations of BSH.

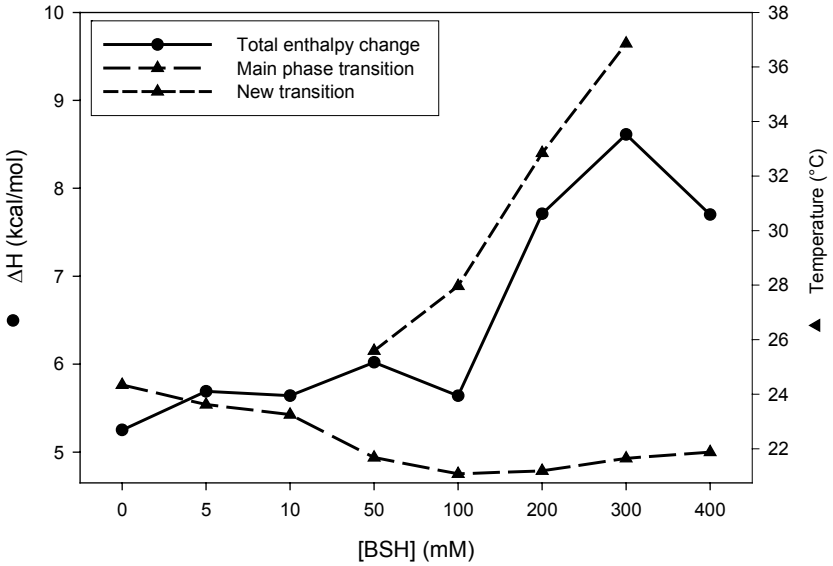

Fig. 12 Phase transition temperatures and total enthalpy change of DMPC liposomes as a function of BSH concentrations. 10 mM DMPC liposomes are incubated with different concentrations of BSH for 2h at 4°C before the start of the scan.

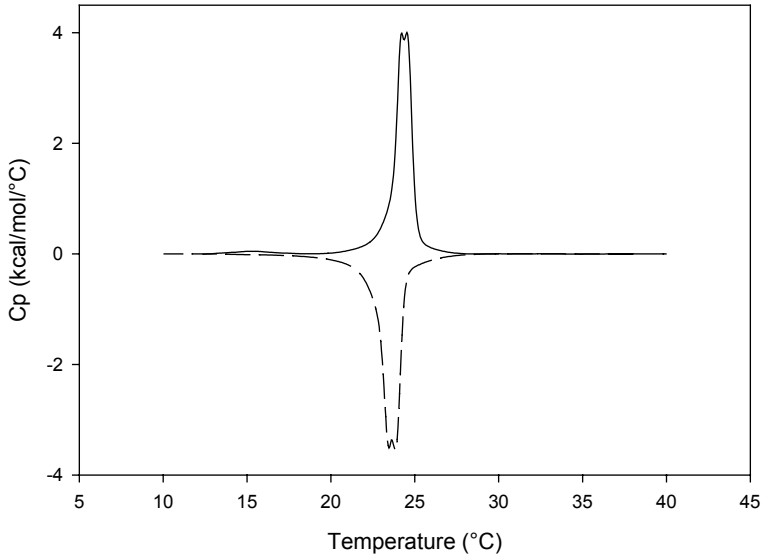

Fig. 13 DSC upscan (whole line) and downscan (dashed line) of DMPC liposomes without BSH. Lipid concentration is 10 mM. Scan rate is 90°C/h.

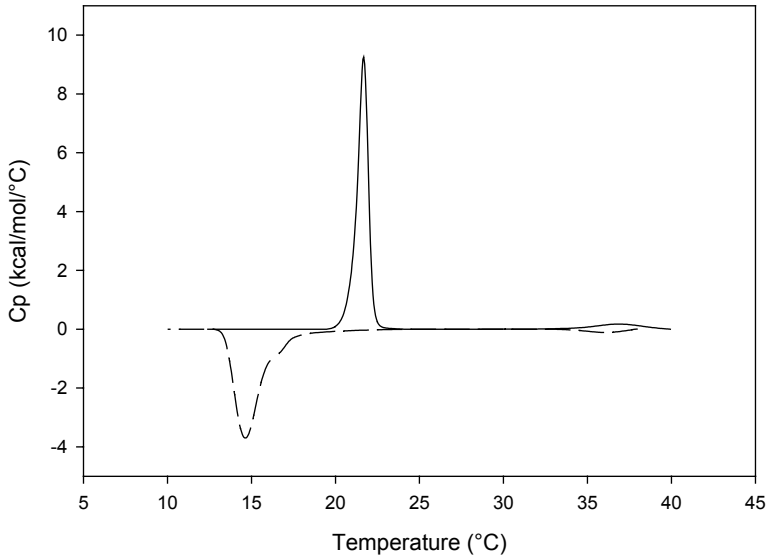

Fig. 14 DSC upscan (whole line) and downscan (dashed line) of DMPC liposomes incubated with 300 mM BSH for 2h at 4°C. Lipid concentration is 10 mM. Scan rate is 90°C/h.

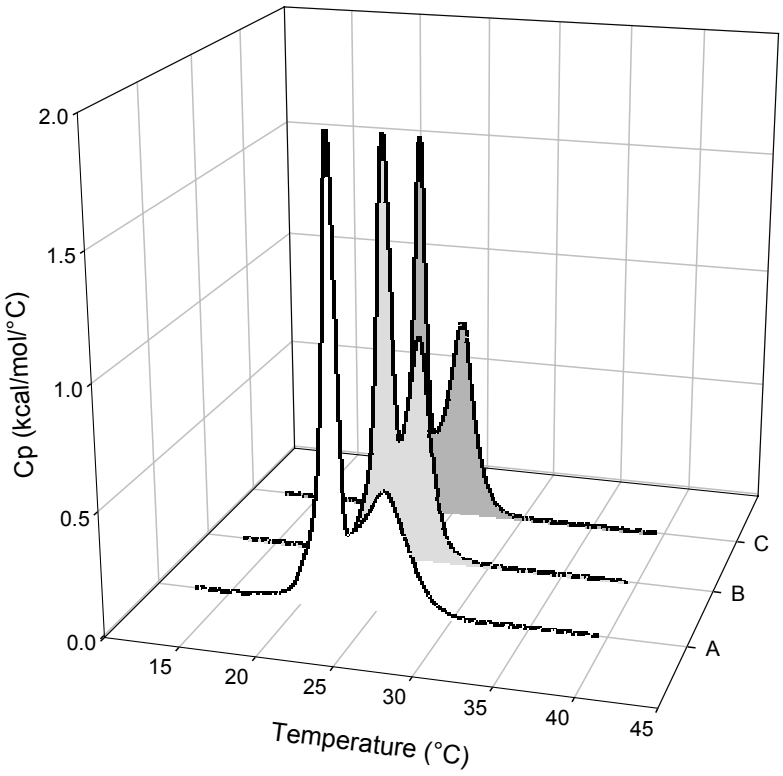

Fig. 15 DSC scans of DMPC liposomes preincubated with BSH and choline. A: 10 mM DMPC liposomes incubated overnight with 100 mM BSH. B: 10 mM DMPC liposomes incubated overnight with 50 mM BSH. C: 10 mM DMPC liposomes incubated overnight with a mixture of 100 mM BSH and 400 mM choline.

3.3. Isothermal titration calorimetry (ITC)

There is an initially linear course through the origin which may be attributed to an ideal partitioning isotherm, namely $r = K_p \cdot C_f$, where K_p is a partition coefficient, C_f the concentration of the free ligand, and r the ratio of bound BSH and the total concentration of lipid. K_p is calculated from the slope of the first part of the curve of Fig. 16 and found to be 43 M^{-1}. This corresponds to a weak binding, in the same order as association constants of enzyme-substrate interactions.

At higher binding ratios, the binding curve bends upward, meaning that further BSH is bound more avidly, or that a larger number of binding sites become available. A more avid binding would correspond to a cooperative binding.

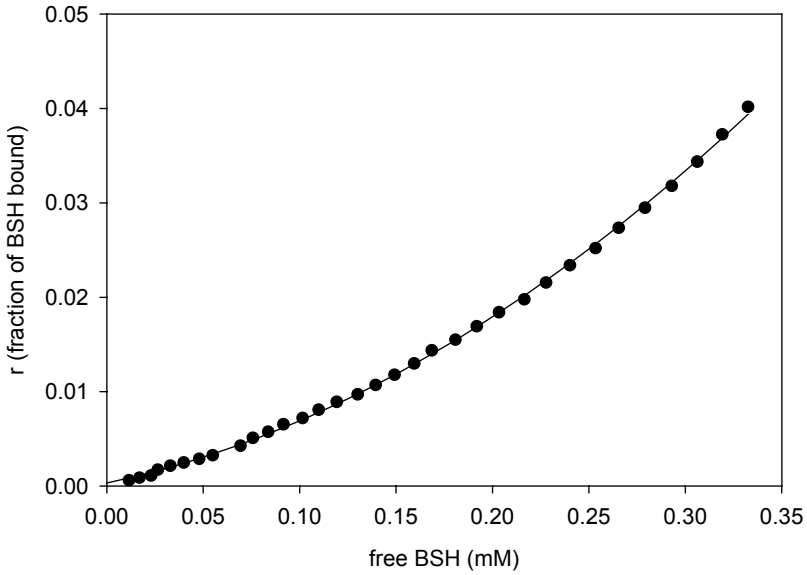

Fig. 16 Apparant association isotherm (binding ratio versus free BSH concentration).

3.4. Lipid mixing experiments

Lipid mixing occurs only with high concentrations of BSH, well beyond the concentrations which are required to induce the considerable structurals changes shown in Figs. 2 to 7. The extent of lipid mixing is maximal (but staying at only 20%) when the liposomes are incubated with 300 mM BSH overnight at 24°C which is the phase transition temperature of DMPC. The extent of fusion is even less (5%) in case of incubation with 250 mM BSH overnight at 15°C whereas no fusion is recorded in case of incubation overnight at 41°C. Concentrations below or above 250-300 mM BSH result in a decrease in fusion.

The low extent of lipid mixing is surprising in view of the appearance of thick membrane structures induced by BSH.

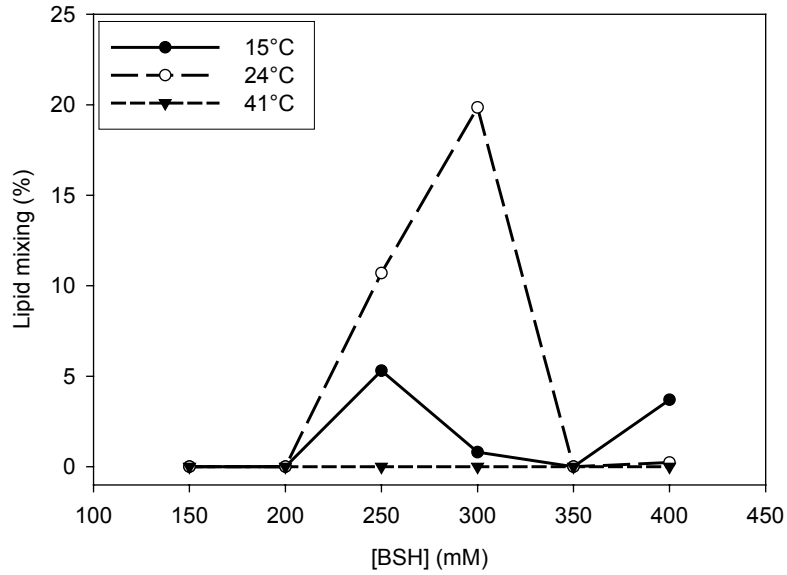

Fig. 17 Percentage of lipid mixing versus BSH concentration.

3.5. Leakage experiments

The results obtained from the leakage experiments confirm that the BSH-induced changes in DMPC liposomes are leaky. Leakage of aqueous contents is found to be a function of the BSH concentration. The release percentages are recorded 5 min after the addition of BSH. The experiments are performed at 15, 23 and 37°C. Spontaneous leakage of CF from DMPC vesicles after BSH addition is found. In contrast, no leakage is found after addition of sodium sulfate.

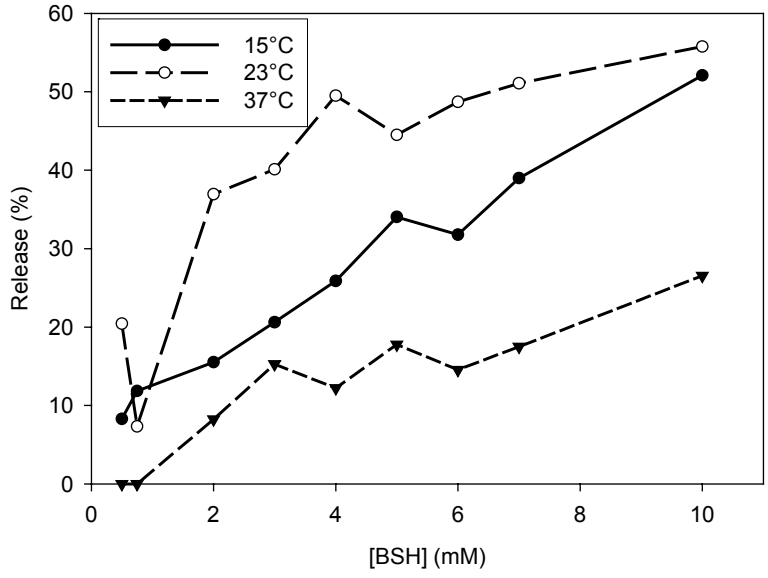

Fig. 18 Extent of leakage of CF from DMPC liposomes, expressed in release percentages after 3 minutes incubation, as a function of BSH concentration, at 15, 23 and 37°C.

3.6. Surface dielectric constant

The dielectric constant value is decreased from 14 to 6 but in presence of a very high BSH concentration (1 M). It should be noted that the sample must be 30 times diluted before the measurements and accordingly a certain degree of dissociation of bound BSH from the liposomal structures is expected.

3.7. Zeta potential and size experiments

Changes in zeta potential of the DMPC liposomes at different BSH/liposome mixing ratios are observed (Fig. 19). Already in the presence of BSH in molar ratios well below 1:1, a large drop of the initial value (-5 mV) is observed, and a plateau value of around –35 mV is reached at concentration ratios of BSH to lipid of bigger than 2:1. The presence of choline (4-fold molar excess over BSH) changes the level of the plateau to the less negative value of –30 mV, but appears not to change the concentration of BSH where 50% of the total change occurs (being around a molar ratio of BSH to lipid of 1:2 in both cases).

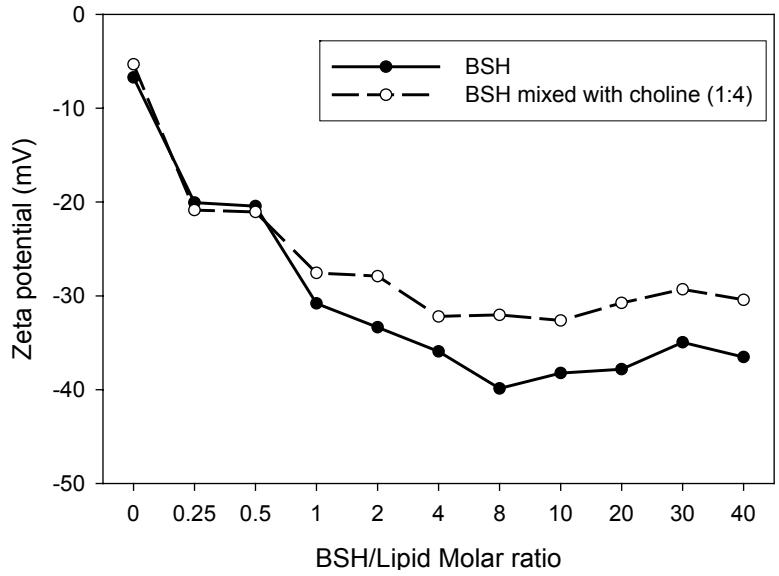

Fig. 19 Zeta potential as a function of the concentration of either BSH or of a mixture of BSH and choline.

The average particle size indicates that DMPC liposomes have a diameter of 154 nm in the absence of BSH. In the presence of BSH, the complex mixture of structures, aggregated etc. produced, as visualized by cryoTEM, makes size measurements very unreliable. The multimodal evaluation of the appropriate scatter experiments might therefore not be appropriate. For this reason, the numerical values obtained are probably of little relevance, and are therefore not given here.

4. Discussion

Cryo-TEM

Several new structures appear in cryo-TEM images of liposomes incubated overnight with BSH. Aggregates of liposomes which are deformed and flattened at the contact region predominate at low temperature, whereas compact multilamellar complexes, as well as complexes that possess open bilayers are abundant at higher temperatures.

Similar morphology changes were observed previously when the interaction of cationic liposomes with either DNA or single-strand oligodeoxynucleotides (ODN) was investigated (Huebner 1999 and Weisman 2004). Huebner et al. explain the formation of multilamellar complexes by a mechanism that involves the rupture of an approaching vesicle and subsequent adsorption of its membrane to a template vesicle or a lipid-DNA complex. Similarly, we think that an extensive aggregation of the liposomes may lead to their rupture. The extremely thick membranes may be due to stacks of ruptured bilayers that cover another liposomes. Sometimes the ruptured bilayer stacks cover only parts of inner liposomes producing unclosed bilayers. Moreover, lipid bilayer sheets may fuse with original vesicles in suspention or with vesicles that have already fused leading to formation of unilamellar liposomes that are larger than the original liposomes. Huebner and his group discussed the strong deformation of the DNA-coated unilamellar vesicles. They suggest that an asymmetry in packing pressure induced by an asymmetry in the lipid-DNA interaction is the reason. They think that this is due to a reduction in the effective headgroup area of the cationic lipids, when charges are partially compensated by the oppositely charged DNA on one side of the bilayer, and when the hydrophilicity of polar headgroup is reduced by the presence of adsorbed DNA. This is probably an explanation of our results taking into consideration that both the surface polarity results and the

hysteresis observed in the DSC scans indicate that BSH leads to dehydration of the liposomes.

The electrostatic repulsion would be expected to prevent the rearrangement of DMPC liposomes into multilayer structures. This could point to a role of BSH molecules acting as adhesion points between the bilayers. The cryo-TEM micrographs also show that DMPC liposomes incubated with mixtures of BSH and choline 1:4 and 1:40 aggregate, fuse and change their morphology but to a lesser extent when compared with the images of DMPC and BSH, indicating that BSH is less effective in the presence of choline.

DSC

Until now only few DSC experiments report the phase transition temperature behavior of unilamellar DMPC vesicles while most of the articles are concerned with the multilamellar ones. We report here the change in phase behavior of unilamellar DMPC vesicles in absence and presence of different BSH concentrations.

It is observed that the main transition peak is split into two peaks. Although the splitting of the main transition peak of extruded unilamellar DMPC liposomes has been recorded by several authors (Jin 1998, Halstenberg 1998, Heimburg 1998 and Heerklotz 2002), the exact reason of its occurrence is not yet known.

The pretransition is abolished by small BSH concentrations. There are two explanation for the nature of pretransition (Frye 1985 and Heimburg 2000). Frye et al. determined the cross polarization P-31 nuclear magnetic resonance of phospholipids; they found a dramatic change in the rate of headgroup rotation at the pretransition of dipalmitoylphosphatidylcholine. Furthermore, they suggest a more ordered director for the headgroup rotation of phosphatidylethanolamine, which does not display a pretransition, than for phosphatidylcholine headgroup rotation. On the other hand, Heimburg does not consider the pretransition and main transition as independent events. He presents a model that is based on the assumption that these two transitions are caused by the same physical effect, namely chain melting. Our experiments cannot determine if the BSH-induced disappearance of the pretransition is due to the influence of BSH on the headgroup behavior or due to perturbation of acyl chain packing, but what we observe that the pretransition is influenced by smaller BSH concentrations than the main transition.

The temperature of the main transition decreases up to 100 mM BSH by more than 3 degrees, indicating that the fluid phase is favored thermodynamically in the presence

of BSH. The main transition is not only shifted to lower temperatures but also becomes narrower, which might be indicative of the presence of multilamellar structures (Heimburg 1998 and Heerklotz 2002).

Interestingly, a new transition peak is observed at BSH concentration of 50 mM and more. Increasing BSH concentrations result in a shift of this peak to higher temperatures. It is probable that this peak belongs to much more stable structures (such as those observed in cryo-TEM images) with low water content, consisting of a multilayer complex enclosing BSH molecules in between. Similar results are obtained by Süleymanoglu who investigated the interaction of DNA with phosphatidylcholine liposomes in the presence of Mg^{2+} ions using DSC (Süleymanoglu 2004). An increased thermal stability of DNA-mediated ternary complex is confirmed by a shift in lipid-DNA nanocondensate transition toward higher temperatures. Giehl et al. observed a shoulder at higher temperatures in their DSC thermograms; their interpretation is that a partial dehydration of the headgroup region leads to an increase of the gel to liquid-crystalline phase transition temperature (Giehl 1999).

There is a marked hysteresis (~7°C) between the heating and cooling scans of liposomes incubated with 300 mM BSH which is most probably due to a modification of the structured water associated to the phosphocholine headgroup region (Hobai 1998). Hysteresis is recorded for liposomes composed of lipid mixtures and explained by formation of dehydrated components which need long time to rehydrate (Epand 2000).

The ΔH value does not increase significantly with BSH concentrations ranging from 5 to 100 mM; it increases, however, with BSH over 100 mM. We think that the increase is due an ordering effect exerted by BSH molecules (Ali 2000). In other words, accumulation of BSH molecules at the bilayer surface increases the electrostatic interactions between DMPC bilayers producing DMPC-BSH-DMPC structures.

In DSC, preincubation of 100 mM BSH with 400 mM choline leads to a change of transition which corresponds to an effective BSH concentration of 50 mM. On possible interpretation is that the quaternary ammonium salt of DMPC is required for an interaction with BSH, and that this interaction can be perturbed by the addition of similar non-liposomal ammonium salts. The cryo-TEM pictures with choline support the notion that choline changes the interaction between BSH and liposomal surface.

ITC

The binding between BSH and DMPC liposomes which we try to investigate is an unspecific association since there are no specific binding sites. Such process should be described in terms of a partitioning equilibrium of the substrate (BSH) between lipid and aqueous phases which can be regarded as a partition constant. The low value of binding (partition) constant (K_p = 43 M^{-1}) indicates a weak BSH-liposome interaction. This value represent the binding of BSH at the very beginning of the reaction where K_p can be determined from the initially linear part of the curve. The upward curvature indicates a cooperativity of binding of BSH molecules to the liposomes. This might be due to BSH-induced structural changes in the liposomes, or to a change in partition coefficient upon binding of the first BSH molecules. New structures may have more sites available to BSH, or sites with a higher affinity for BSH, than an unperturbed lipid bilayer has. Although maximum effect of BSH is determined near the phase transition (~23°C), the BSH binding to DMPC liposomes is monitored at 15°C. When we tried to carry out the partition experiment at 25, the obtained heat flow data were peculiar due to the interference of the exothermic binding process with the endothermic process that accompany the phase transition; by the BSH-induced change temperature of the phase transition considerable heat is required which masks the heat released by the binding.

Lipid mixing

The extent of lipid mixing seems very restricted compared to the dramatic changes detected by cryo-TEM indicating that the new structures formed do not mix their membranes to a large extent. 20% lipid mixing is detected around the temperature of the main phase transition and at the same time at high BSH concentrations.

Leakage

In the cryo-TEM pictures, thickening of the membranes and membrane surface association reveal that leakage must have occurred. It is confirmed through leakage experiments that BSH leads to an immediate leakage. Below and above phase transition, leakage percentages over 5 min depend linearly on BSH concentration. There is pronounced dependence on BSH concentration around the phase transition where smaller concentrations are relatively more effective. Leakage at 23°C occurs to larger extend which is consistent with the results of lipid mixing and can be interpreted through cryo-TEM pictures. At 15°C, many closed structures are still

present, whereas at 37°C, new stable structures might have formed very rapidly, preventing extensive leakage. Around the phase transition temperature, processes are slow enough to allow for both lipid mixing and leakage before the new structures are formed.

No leakage was found after addition of sodium sulfate. This is consistent with cryo-TEM results showing no change in the liposomal morphology after overnight incubation with sodium sulfate. Sodium sulfate is used to prove that BSH effect is due to a specific feature of BSH and cannot be achieved by another divalent anions.

Dielectric constant

The interaction of BSH with the DMPC liposomes is accompanied by a decrease in the surface polarity of the liposomes indicated by a shift of the maximum of the emission spectrum of DPE to a shorter wavelength which means that BSH leads to a decrease in the water content in the gap between the opposing phospholipid bilayers.

Zeta potential

The negative zeta potential values indicate firm binding of BSH molecules to DMPC liposomes. It is worth noting that the negatively charged liposomes do not repel each other but they tend to stick under the effect of BSH, forming structures shown in cryo-TEM images. Such structures are most probably stabilized by the counter ions available in the reaction medium.

Nature and way of formation of new phases

Altogether, these results indicate that BSH is able to trigger several changes in DMPC liposomes. BSH effect takes place, according to our hypothesis, in several steps as illustrated in the diagram (Fig.20).

Step 1: A fast electrostatic interaction between BSH molecules (symbolized as negative circles) and choline groups (symbolized by +-signs) of the liposomes (indicated by DSC, zeta potential and choline experiments).

Step 2: Extensive electrostatic interactions between the liposomes induced by BSH molecules leads to their aggregation. The forces involved are strong enough to maximize the contact surface between the liposomes, leading to their flattening (not shown in Fig. 20).

Step 3: Step 3 is slow at lower temperatures (cryo-TEM pictures at low temperature), and thus is less likely to occur. At higher temperature, a strong adherence between the liposomes leads to a rupture of some of them which then wrap around another

intact liposomes. Repetition of step 3 results in formation of concentric bilayers of multilamellar liposomes sandwiching the BSH molecules between the lamellas. Open bilayers can be produced, if the ruptured bilayer stacks cover only parts of inner liposomes (cryo-TEM images). Structures obtained in step 3 or its repetition are most probably without much water (DSC scans, surface dielectric constant and hysteresis). Since the intact liposomes wrapped up in a bilayer are unable to leak, the proposed structures in step 3 can explain the results of leakage experiments.

Step 4: At higher temperature and much BSH, opening of the liposomes into bilayer sheets occurs (cryo-TEM at high temperature and high BSH concentration).

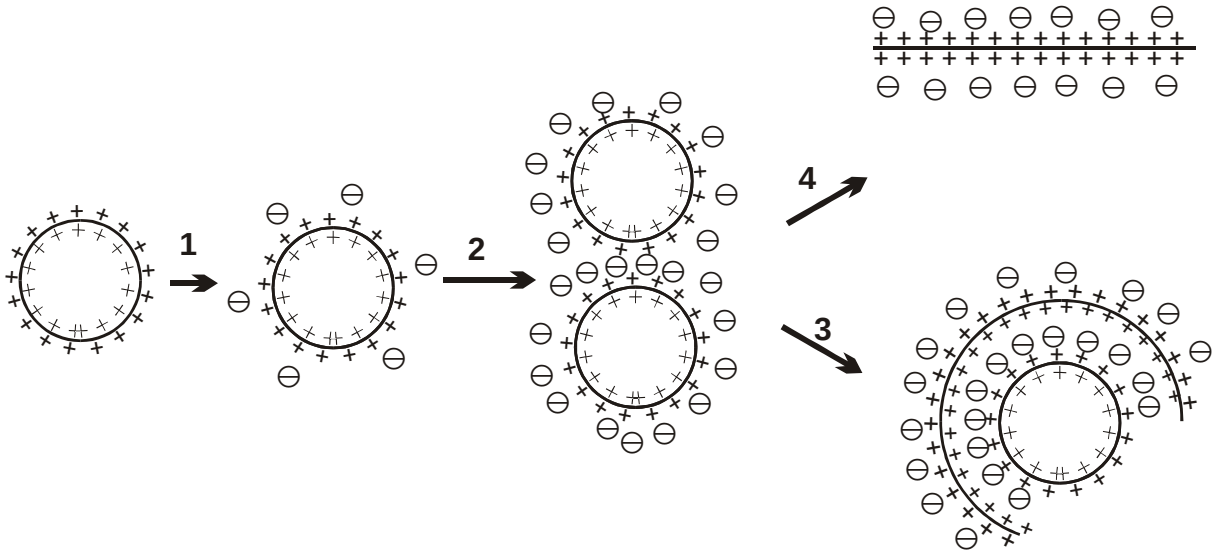

Fig. 20 Schematic diagram illustrating the hypothesized mechanism of action of BSH. See text for explanation

References

1. . Research needs for neutron capture therapy. Workshop summary minutes of a strategic planning workshop, Williamsburg, Virginia, May 9-12, 1995. US Department of Energy, Office of Health and Environmental Research ; 1995.

2. Ali, S.; Minchey, S.; Janoff, A., and Mayhew, E. A differential scanning calorimetry study of phosphocholines mixed with paclitaxel and its bromoacylated taxanes. Biophys J. 2000 Jan; 78(1):246-56.

3. Asuncion-Punzalan, E.; Kachel, K., and London, E. Groups with polar characteristics can locate at both shallow and deep locations in membranes: the behavior of dansyl and related probes. Biochemistry. 1998 Mar 31; 37(13):4603-11.

4. Bayerl, T. M.; Kochy, T., and Bruckner, S. On the modulation of a high-enthalpy pretransition in binary mixtures of DMPC and DMPG by polar headgroup interaction. Biophys J. 1990 Mar; 57(3):675-80.

5. Epand, R. M.; Bach, D.; Borochov, N., and Wachtel, E. Cholesterol crystalline polymorphism and the solubility of cholesterol in phosphatidylserine. Biophys J. 2000 Feb; 78(2):866-73.

6. Frye, J.; Albert, A. D.; Selinsky, B. S., and Yeagle, P. L. Cross polarization P-31 nuclear magnetic resonance of phospholipids. Biophys J. 1985 Oct; 48(4):547-52.

7. Giehl, A.; Lemm, T.; Bartelsen, O.; Sandhoff, K., and Blume, A. Interaction of the GM2-activator protein with phospholipid-ganglioside bilayer membranes and with monolayers at the air-water interface. Eur J Biochem. 1999 May; 261(3):650-8.

8. Halstenberg, S.; Heimburg, T.; Hianik, T.; Kaatze, U., and Krivanek, R. Cholesterol-induced variations in the volume and enthalpy fluctuations of lipid bilayers. Biophys J. 1998 Jul; 75(1):264-71.

9. Heerklotz, H. and Seelig, J. Application of pressure perturbation calorimetry to lipid bilayers. Biophys J. 2002 Mar; 82(3):1445-52.

10. Heimburg, T. Mechanical aspects of membrane thermodynamics. Estimation of the mechanical properties of lipid membranes close to the chain melting transition from calorimetry. Biochim Biophys Acta. 1998 Dec 9; 1415(1):147-62.

11. ---. A model for the lipid pretransition: coupling of ripple formation with the chain-melting transition. Biophys J. 2000 Mar; 78(3):1154-65.

12. Hobai, S. and Fazakas, Z. Effect of anion triiodide on the main phase transition of fully hydrated dipalmitoylphosphatidylcholine bilayers [Web Page]. 1998; Accessed 2006 Jan 8.

13. Holopainen, J. M.; Lemmich, J.; Richter, F.; Mouritsen, O. G.; Rapp, G., and Kinnunen, P. K. Dimyristoylphosphatidylcholine/C16:0-ceramide binary liposomes studied by differential scanning calorimetry and wide- and small-angle x-ray scattering. Biophys J. 2000 May; 78(5):2459-69.

14. Jin, A. J.; Mudd, C. P., and Gershfeld, N. L. Unusual structural transformations in large unilamellar vesicle suspensions of DMPC by Cpλ-1 calorimetry. Biophys J. 1998; 74:A312.

15. McMullen, T. P.; Lewis, R. N., and McElhaney, R. N. Comparative differential scanning calorimetric and FTIR and 31P-NMR spectroscopic studies of the effects of cholesterol and androstenol on the thermotropic phase behavior and organization of phosphatidylcholine bilayers. Biophys J. 1994 Mar; 66(3 Pt 1):741-52.

16. Nunes-Correia, I.; Eulalio, A.; Nir, S.; Duzgunes, N.; Ramalho-Santos, J., and Pedroso de Lima, M. C. Fluorescent probes for monitoring virus fusion kinetics: comparative evaluation of reliability. Biochim Biophys Acta. 2002 Mar 19; 1561(1):65-75.

17. O'Leary, T. J.; Ross, P. D.; Lieber, M. R., and Levin, I. W. Effects of cyclosporine A on biomembranes. Vibrational spectroscopic, calorimetric and hemolysis studies. Biophys J. 1986 Apr; 49(4):795-801.

18. Ohki, S. and Arnold, K. Determination of liposome surface dielectric constant and hydrophobicity . J Membr Biol. 1990; 114:253-273.

19. Szollosi, J.; Nagy, P.; Sebestyen, Z.; Damjanovicha, S.; Park, J. W., and Matyus, L. Applications of fluorescence resonance energy transfer for mapping biological membranes. J Biotechnol. 2002 Jan; 82(3):251-66.

20. Süleyman, E. Divalent cation induced DNA-zwitterionic vesicle formulation compacted for gene delivery: thermodynamic aspects. Internet Electron J Mol Des. 2004; 3:93-101.

21. Zschörnig, O.; Richter, W.; Pasche, G., and Arnold, K. Cation-mediated interaction of dextran sulfate with phospholipid vesicles: binding, vesicle surface polarity, leakage and fusion. Colloid Polym Sci. 1992; 278:637-646.

IV

Synthesis and liposomal preparation of two novel dodecaborate cluster lipids for boron neutron capture therapy

Synthesis and liposomal preparation of two novel dodecaborate cluster lipids for boron neutron capture therapy

Eugen Justus[1], Doaa Awad[1], Michaela Hohnholt[1], Katarina Edwards[2], Göran Karlsson[2], Luminita Damian[3], Detlef Gabel[1*]

[1] Department of Chemistry, University of Bremen, PO Box 330440, D-28334 Bremen.

[2] Department of Physical Chemistry, Uppsala University, Box 579, S-75123 Uppsala.

[3] School of Science and Engineering, International University Bremen, PO Box 750561, D-28725 Bremen

* Tel. +49 421 2182200, e-mail gabel@chemie.uni-bremen.de

Abstract

A new class of lipids, containing the *closo*-dodecaborate cluster, has been synthesized. Two lipids, S-(N,N-(2-dimyristoyloxyethyl)-acetamido)-thioundecahydro-closo-dodecaborate (2-) (**B-6-14**) and S-(N,N-(2-dipalmitoyloxyethyl)-acetamido)-thioundecahydro-closo-dodecaborate (2-) (**B-6-16**) are described. Both of them have a double-tailed lipophilic part and a headgroup carrying a double negative charge. Differential scanning calorimetry show that **B-6-14** and **B-6-16** bilayers have main phase transition temperatures of 18.8 and 37.9°C, respectively. Above the transition temperature of 18.8°C, **B-6-14** can form liposomal vesicles. Upon cooling below the transition temperature, stiff bilayers are formed. When incorporated into liposomal formulations with equimolar amounts of distearoyl phosphatidylcholine (DSPC) and cholesterol, stable liposomes are obtained. The zeta potential measurements indicate that both **B-6-14**- and **B-6-16**-containing vesicles are negatively charged, with the most negative potential described of any liposome so far. The liposomes are of high potential value as transporters of boron to tumor cells in treatments beased on boron neutron capture therapy (BNCT).

Introduction

In boron neutron capture therapy of tumors (BNCT), successful treatment requires a selective delivery of boron-10 to tumor tissues to maximize damage to the tumor and to minimize damage to surrounding normal tissue.[1] However, relatively large intracellular accumulations of boron (approximately 20-30 µg of boron-10 per gram of tumor) are necessary to produce cell death.[2] Several means of selective targeting of boron-10 to tumors were investigated. In 1964 Soloway suggested that antibodies might be used for delivering boron-10 to cancer cells.[3] Assuming an antigen site density of 10^6 per tumor cell, this would require approximately 1000 boron-10 atoms per antibody molecule to attain 10^9 boron atoms per cell (approximately 20-50 µg boron-10/gram of tumor). By linking 1000 boron atoms to a molecule of antibody, the resulting structures failed to find their antigenic target.[4] The increased rate of mitosis of malignant cells has led to synthesis of boron-containing precursors of nucleic acid.[5] Porphyrin derivatives that contain boron were synthesized as capture agents for BNCT.[6] However, significant normal tissue uptake of the boronated porphyrins [7], [8]} may limit their use in BNCT.

Liposomes show selective localization in tumors due to the increased microvascular permeability of tumors.[9], [10] Liposomes extravasate through the highly permeable microvessels of tumors and remain locked in the interstitial fluid compartment due to a lack of functional lymphatic drainage.[11] They might therefore be useful agents for transporting boron to the tumor site. The targeting of boron-10 to tumors using drug carriers such as liposomes has recently been investigated[12], [13], [14], [15], [16], [17]

Two approaches are possible for using liposomes in boron delivery: encapsulation of a boron compound into the entrapped volume of liposomes, and incorporation of boron-containing lipids into liposomes. Encapsulation of a boron compound in liposomes has been described by, e.g. Hawthorne,[14] Mehta[18] and Maruyama.[19] Problems might arise by the encapsulation of these compounds into the liposomes through, e.g., low encapsulation efficiency and changes in the physical-chemical behavior through the presence of the boron compounds, and leakage upon storage and in contact with serum. The amount of boron which can be encapsulated in liposomes depends on the maximal concentration of the boron compound which is compatible with stability. For liposomes of 100 nm diameter, the encapsulated volume is about 2.5 L per mol lipid.[20] With concentrations of the encapsulated agent of 0.1 M, about 0.25 mol can be encapsulated per mol of lipid. The alternative approach, incorporation of boron-containing amphiphilic molecules into liposomes, has been described by, e.g. Hawthorne,[15] Nakamura,[21] and Rossi.[22] Many of the problems encountered in the encapsulation approach can be avoided. It is, in principle, not even necessary to prepare closed vesicles, as long as tumor accumulation is possible.

For the preparation of boron-containing liposomal vesicles, boron-containing lipids are required. A few approaches toward the synthesis of lipids intended for incorporation into liposomes have been described in the literature.

Synthesis of a nido-carborane lipid with a one-tailed moiety (Fig. 1, compound **1**) has been described, and the liposomal boron delivery using this compound and DSPC has been examined in mice.[15], [23] Later, Nakamura designed a nido-carborane lipid with a double-tailed moiety for the purposes of high

boron accumulation into liposomes [21] (Fig.1, compound **2**). More recently, Hawthorne et al. described a very similar lipid (differing only in the number of methylene groups of the sidechain) and investigated the in vivo toxicity of liposomes formed from the boron-containing lipid and helper lipids (DSPC, cholesterol (CHO)). They found that the liposomes were very toxic already at dosages of 6 mg boron per kg body weight.[24] Nidocarborane lipids might therefore be problematic as agents for boron delivery in BNCT.

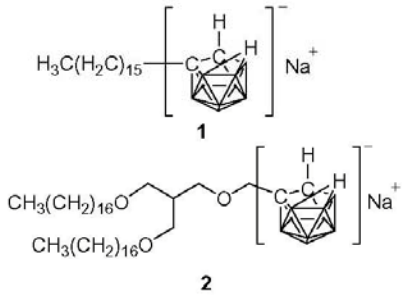

Figure 1. Structures of the boron cluster lipids **1** and **2**.

Our target was the preparation of $(B_{12}H_{11}S)^{2-}$-containing lipids since mercaptoundecahydrododecaborate ($B_{12}H_{11}SH^{2-}$, BSH) is the only acceptable boron cluster compound that can be used at the present time in clinical trials in Japan, Europe, or the USA. Other suitable target species are under rapid development, but $B_{12}H_{11}SH^{2-}$ will probably remain as the baseline compound for clinical studies conducted in the immediate future.[25] Soloway found that $B_{12}H_{11}SH^{2-}$ was sufficiently nontoxic (LD_{50} 73 $\pm$ 4 mg of boron per kg body weight in male CD1 Swiss mice by intraperitoneal injection) to be used clinically.[26] Absence of toxicity in patients has later been proven in clinical trials[27] The boron compounds that are used as capture agents for BNCT should be nontoxic when administered in amounts required to obtain sufficient tumor concentrations to sustain a lethal $^{10}B(n,\alpha)^{7}Li$ reaction.

Results

Chemistry

In this work, two different dodecaborate cluster-containing lipids, **B-6-14** and **B-6-16**, were synthesized according to Scheme 1. The structures are similar to those of DC-6-14 (*O,O'*-ditetradecanoyl-*N*-(a-trimethylammonioacetyl)diethanolamine chloride, described by Almofti et al.[28]) and are named accordingly. The synthesis followed either the work of Trowbridge and Falk (Method A),[29] or through the *O*-protected diethanolamine (Method B). The introduction of the boron cluster was achieved by alkylation with *S*-cyanoethylmercaptoundecahydrododecaborate **10** and subsequent alkaline removal of the cyanoethyl protecting group.[30]

In method A, two equivalents of the chloroanhydride of the fatty acids were allowed to react with diethanolamine. The resulting products *N,N*-(2-dimyristoyloxyethyl)- and *N,N*-(2-dipalmitoyloxyethyl)-

amine **3 a,b** were reacted with chloroacetylchloride in the presence of triethylamine, to obtain. **4 a,b** in 87% yield. The reaction between the chloroacetamides **4 a,b** and the tetramethylammonium salt of 2-cyanoethyl-mercaptoundecahydro-closo-dodecaborate (2-) produced sulfonium salts **5 a,b** in 60% yield. The end products **B-6-14** and **B-6-16** were obtained from the reaction of sulfonium salts **5 a,b** with tetramethylammonium hydroxide in acetone. The yield of lipids **B-6-14** and **B-6-16** is 48-55% (overall yield from diethanolamine 25-28%).

The lipids can also be obtained through method B. Here, the introduction of the fatty acid chain occurs later, and the intermediate **9** is therefore a suitable synthon when aiming at a variety of fatty acid derivatives. Two equivalents of chlorotrimethylsilane are reacted with diethanolamine in the presence of triethylamine. The trimethylsilyloxy derivative **7** is reacted with chloroacetylchloride in the presence of triethylamine to give **8** in 84% yield. **8** can react in analogy to path 1 with *S*-cyanoethylmercaptuundecahydrododecaborate. Starting from **9**, the yield of **B-6-14** was 76% (overall yield from diethanolamine 46%).

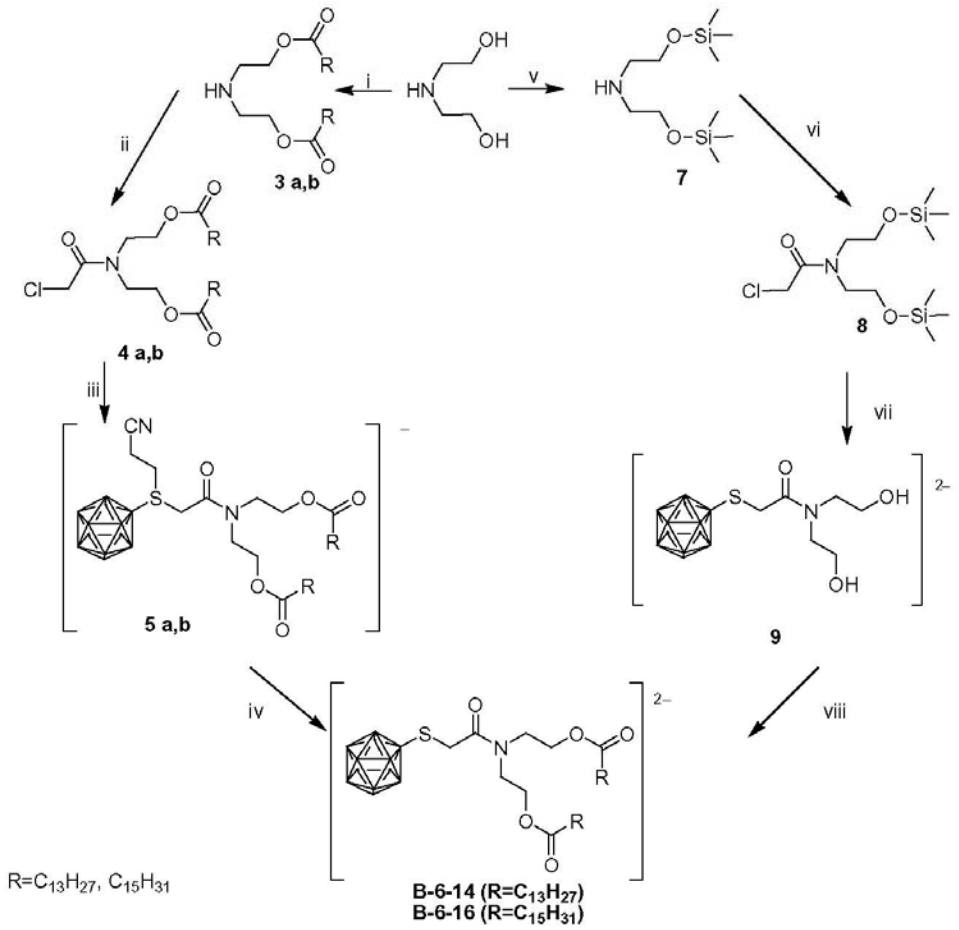

Scheme 1. Synthesis of boron lipids. i) 1.HCl, $CHCl_3$ 2. RCOCl, $CHCl_3$ 3. KOH, $CHCl_3$; ii) $ClCH_2COCl$, $(C_2H_5)_3N$, C_6H_6; iii) $[(CH_3)_4N]_2^+[B_{12}H_{11}SCH_2CH_2CN]^{2-}$, acetonitrile; iv) $(CH_3)_4NOH$, acetone; v) $(CH_3)_3SiCl$, $(C_2H_5)_3N$, $CHCl_3$; vi) $ClCH_2COCl$, $(C_2H_5)_3N$, THF; vii) 1. $[(CH_3)_4N]^+[B_{12}H_{11}SCH_2CH_2CN]^-$, acetonitrile 2. $(CH_3)_4NOH$, acetone; viii) 1. NaH, acetonitrile 2. RCOCl.

The synthesized compounds have two negative charges due to the presence of the undecahydro-*closo*-dodecaborate(2-) cluster in the head group. They are one of the examples of amphiphilic lipids which carry two negative charges in the part that would be in direct contact with water when incorporated into mixed lipid films; phosphatidylglycerol lipids being the other example.

Physical characterization and liposome preparation

DSC results demonstrated that **B-6-14** and **B-6-16** alone exhibit a main phase transition at 18.8 and 37.9°C, respectively (Fig. 2). These results are quite comparable to the transition temperatures of

dimyristoyl- and dipalmitoylphosphatidylcholine (DMPC resp. DPPC), which are 24.3 and 41°C, resp.[31] Phase transition data for the lead structure DC-6-14 are not reported in the literature. Liposomes containing 33.3 mol% of either **B-6-14** or **B-6-16**, as well as the same mol% of DSPC and CHO, exhibit broad phase transitions, and the enthalpy of transition was low (data not shown). It had been found previously that 10 mol% CHO is sufficient to significantly decrease the main enthalpy, cooperativity and lipid chain melting of DPPC and 1-palmitoyl phosphatidylcholine (16:0LPC) binary mixtures.[32] In the presence of an increasing CHO concentration, the phase transition broadens, and the transition enthalpy decreases before it is finally totally abolished. Lippert and Peticolas suggested that addition of CHO decreases the interaction between adjacent side chains of lipid, causing a change from a cooperative to a noncooperative gel-liquid crystal transition.[33]

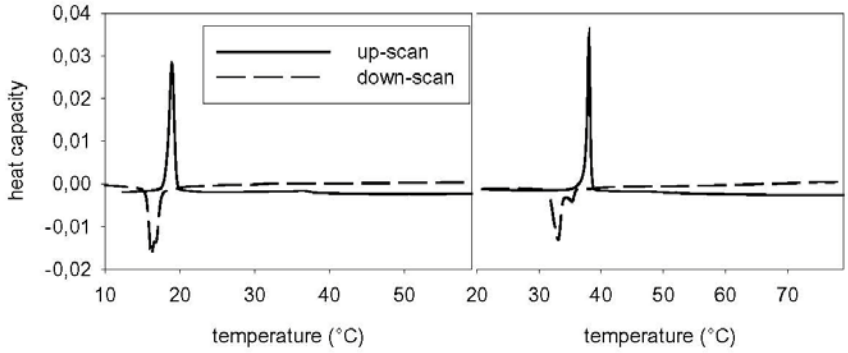

Figure 2. DSC of pure films of **B-6-14** (left) and **B-6-16** (right) (the first upscan and the first downscan are shown). Lipid concentration 5 mM.

Liposomes from pure **B-6-14** can be prepared by lipid film hydration and extrusion above the phase transition temperature if the samples are not cooled below the phase transition temperature of 18.8°C (Fig. 3a). The vesicles are heterogeneous in size, with many of them well below the 100-nm size of the extrusion membrane. When kept in the refrigerator for some period, only large open bilayers are found (Fig 3b). The equipment used in the present study did not allow vitrification from temperatures safely above the phase transition temperature for **B-6-16** (37.6°C), and therefore no conclusion about the possible formation of liposomes is possible. As is the case for **B-6-14**, open bilayers are obtained when the sample is stored for some time at 4°C (Fig 3c). Some of the large bilayer sheets of both lipids covered more than one of the holes in the supporting polymer net.

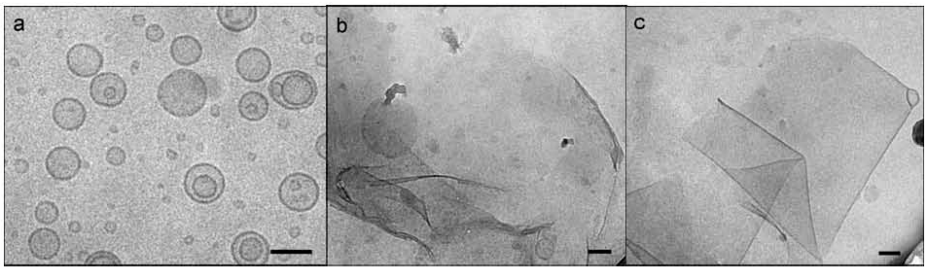

Figure 3. Cryo-TEM pictures of a preparation of **B-6-14** prepared by extrusion at 50°C and vitrification from 30°C(a), prepared by extrusion at 50°C, storage at 4°C for one week and vitrification from 25°C (b) and **B-6-16** prepared as sample b (c). Scale bare 100 nm.

B-6-14 represents the first boron-containing lipid which can form liposomes without the addition of helper lipids. Nakamura [21] obtained vesicles only in combination with helper lipids.

From x-ray crystal analysis (see, e.g.[34]), the van der Waals radius of the dodecaborate cluster can be determined to approximately 4 Å, giving an unsolvated cross-section area of the head group of about 0.5 nm^2. This is very close to the area occupied by lipids with saturated fatty acid chains in the gel phase.[31] This might be one of the reasons why the liposomes formed above the phase transition temperature are converted to open bilayers upon cooling.

Liposomes consisting of either a mixture of 33.3 mol% **B-6-14**, 33.3 mol% DSPC and 33.3 mol% CHO or a mixture of 33.3 mol% **B-6-16**, 33.3 mol% DSPC and 33.3 mol% CHO were successfully prepared (Fig. 3) by thin film hydration and extrusion.

The mean diameter of the liposomes containing **B-6-14** and **B-6-16** in combination with DSPC and CHO was found to be 135 nm and 123 nm, respectively, when measured by dynamic light scattering. This value is corroborated by the results from cryo-TEM (see below). The liposomes containing 33.3 mol% of either **B-6-14** or **B-6-16** had zeta potentials of –67 and –63 mV, respectively, reflecting the double negative charge of the headgroup. Liposomes prepared by extrusion from neat **B-6-14** at 50°C and analyzed at 30°C hat a zeta potential of –63 mV and a broad size distribution centered at 129 nm, which was, however, not stable with time.

The pictures obtained from cryo-TEM (Fig. 4) showed formation of boron cluster-containing liposomes when an equimolar mixture of the boron lipid, DSPC and CHO was used for liposome preparation. The micrographs confirm a size of approximately 100 nm as measured by the dynamic light scattering. Cryo-TEM also revealed a certain degree of heterogeneity in the preparation. A few open structures were observed (see Fig. 4b), but most of the material was present as closed liposomes.

It had been found that liposomes composed of DSPC/CHO (60/40 molar ratio) and prepared by extrusion through 100 nm filters have a strong tendency to aggregate.[35] As a consequence of the attractive interaction the liposomes adapt a non-spherical, more elongated shape. The spherical shape of the liposomes displayed in Fig. 4 is likely due to the presence of the boron-containing lipid and the repulsion caused by the negatively charged headgroups.

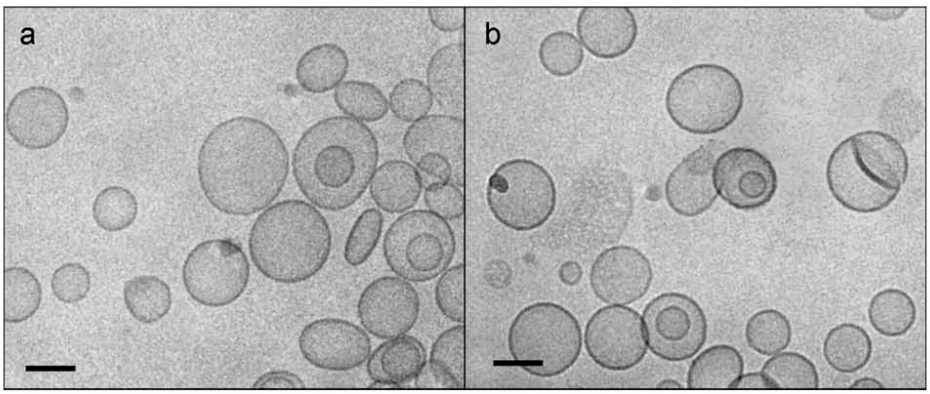

Figure 4 Cryo-TEM pictures of liposomes prepared from an equimolar mixture of DSPC, CHO and **B-6-14** (a), or **B-6-16** (b), resp. Scale bar 100 nm.

Conclusions

Synthesis of two closo-dodecaborate cluster-containing lipids has been achieved. Liposomes containing these lipids can prepared which are stable above the phase transition temperature. Liposomes stable below the phase transition temperature can be obtained by preparing bilayers containing equimolar amounts of the boron lipid, DSPC, and CHO. The liposomes containing the pure lipid are among the most boron-rich units prepared to date for BNCT. The structure of the liposomes provides two modes of delivery: encapsulation of boron, and transport of boron-containing lipids. Previously, liposomes have been used to encapsulate concentrated aqueous solutions of water-soluble polyhedral borane anion salts [14], [18], [19] or to incorporate lipophilic boron-containing moieties embedded within the bilayer membrane.[15], [21], [23], [24].

The use of a boron-containing lipid circumvents problems with the possible leakage of encapsulated material. The liposomes prepared here can most probably be tagged with tumor-seeking entities,[36] and thereby possibly achieve a selective accumulation for successful BNCT. Due to their high contents of boron, and the known procedures by which liposomes can be targeted, they appear to be of great potential value for BNCT.

Experimental

General

NMR spectra were recorded on a Bruker DPX 200 spectrometer. IR spectra of KBr pellet were collected on a BioRad FTS 155 spectrometer. Electrospray mass spectra were measured with a Bruker Esquire spectrometer. Charge was determined through isotope satellite peaks. For B-containing compounds, the peak with highest intensity is given. Melting points were measured on a Büchi 512 melting point apparatus.

Chemistry

N,N-Bis-(2-dimyristoyloxyethyl)-2-chloracetamide (4a) N,N-Bis-(2-myristoyloxyethyl)amin (**3a**) (5.23 g, 0.01 mol) and (1.11g, 0.011 mol) triethylamine were dissolved in $CHCl_3$ (50 mL) and cooled to -10°C. While stirring, chloroacetylchloride (1.24 g, 0.011mol) was added dropwise. After stirring the reaction mixture for 2-3 hours, hexane was added until a precipitate (triethylamine hydrochloride) formed. The precipitate was removed by filtration, and acetone (50 mL) were added and the solution was kept at +4°C overnight, whereupon the product precipitated. It was filtered off, dried, and recrystallized from $CHCl_3$. Yield 5.11 g (85%), m.p. 52-54°C. IR (KBr): ν=2956-2850 (C-H), 1732 (C=O), 1661 (-N-C=O), 1179 (C-O), 720 cm^{-1} (C-Cl). ^{1}H NMR (200MHz, $[D_1]CDCl_3$, 25°C, TMS): δ=0.89 (t, J(H,H)=3.0 Hz, 6H, $C\underline{H}_3$-CH_2-), 1.27 (s, 40H, CH_3-$(C\underline{H}_2)_{10}$-CH_2-), 1.51-1.69 (m, 4H, -CO-CH_2-$C\underline{H}_2$-), 2.23-2.38 (m, 4H, -CO-$C\underline{H}_2$-), 3.57-3.76 (m, 4H, -O-$C\underline{H}_2$-), 4.19 (s, 2H, Cl-$C\underline{H}_2$-CO-), 4.12-4.32ppm (m, 4H, -N-$C\underline{H}_2$-). MS (ESI, methanol, m/z): negative 636 $[M+Cl^-]^-$; positive 624 $[M+Na^+]^+$, 640 $[M+K^+]^+$.

N,N-Bis-(2-dipalmitoyloxyethyl)-2-chloracetamide (4b) Similar to **4a**. Yield 5.72 g (87%), m.p. 80-82 °C (hexane). IR (KBr): ν=2917-2851 (C-H), 1732 (C=O), 1661 (-N-C=O), 1179 (C-O), 720 cm^{-1} (C-Cl). ^{1}H NMR (200MHz, $[D_1]CDCl_3$, 25°C, TMS): δ=0.89 (t, J(H,H)=3.0 Hz, 6H, $C\underline{H}_3$-CH_2-), 1.26 (s, 48H, CH_3-$(C\underline{H}_2)_{12}$-CH_2-), 1.52-1.67 (m, 4H, -CO-CH_2-$C\underline{H}_2$-), 2.26-2.37 (m, 4H, -CO-$C\underline{H}_2$-), 3.60-3.73 (m, 4H, -O-$C\underline{H}_2$-), 4.17 (s, 2H, Cl-$C\underline{H}_2$-CO-), 4.23-4.33 ppm (m, 4H, -N-$C\underline{H}_2$-). MS (ESI, methanol, m/z): negative 692 $[M+Cl^-]^-$; positive 680 $[M+Na^+]^+$, 696 $[M+K^+]^+$.

S-(2-Cyanoethyl)-S-(N,N-(2-dimyristoyloxyethyl)-acetamido)-sulfonioundecahydro-*closo*-dodecaborate (1-) tetramethylammonium salt (5a) Bis- tetramethylammonium 2-cyanoethyl-thioundecahydro-closo-dodecaborate (2-) (**10**) (0.375 g, 1.0 mmol) and (1.2 g, 2.0 mmol) N,N-bis-(2-dimyristoyloxyethyl)-2-chloracetamide (**4a**) were suspended in acetonitrile (40 ml) for 24 h and then heated to 70°C for 3 h. The mixture was cooled and the solid was removed by filtration. The solvent was evaporated and the product was dried at the oil pump. Yield 0.485 g (56%). IR (KBr): ν=2923-2853 (C-H), 2487 (B-H), 1739 (C=O), 1651 (-N-C=O), 1175 cm^{-1} (C-O). ^{1}H NMR (200MHz, $[D_3]CD_3CN$, 25°C, TMS): δ=0.88 (t, J(H,H)=3.2 Hz, 6H, $C\underline{H}_3$-CH_2-), 1.27 (s, 40H, CH_3-$(C\underline{H}_2)_{10}$-CH_2-), 1.48-1.63 (m, 4H, -CO-CH_2-$C\underline{H}_2$-), 2.21-2.38 (m, 4H, -CO-$C\underline{H}_2$-), 2.96-3.48 (m, 2H -S-$C\underline{H}_2$-), 3.12 (s, 12H, $(C\underline{H}_3)_4N$), 3.24-3.37 (m, 2H, -$C\underline{H}_2$-CN), 3.52-3.64 (m, 4H, -O-$C\underline{H}_2$-), 4.12-4.20 (m, 4H, -N-$C\underline{H}_2$-), 4.25 (s, 2H, S-$C\underline{H}_2$-CO), 0.1-2.3 ppm (m, 11H, B-$\underline{H}$). ^{11}B NMR (200MHz, $[D_6]$DMSO, 25°C): δ=-5.86 (1B), -14.56 ppm (11B). MS (ESI, acetonitrile, m/z): negativ 794 $[A]^-$; positive 74 $[Kat]^+$, 942 $[A^- +2Kat^+]^+$.

S-(N,N-(2-Dimyristoyloxyethyl)-acetamido)-thioundecahydro-*closo*-dodecaborate (2-) ditetramethylammonium salt (B-6-14). Method A: To a solution of **5a (**0.867 g, 1.0 mmol) in acetone 1 eq of a 25 % solution of tetramethylammonium hydroxyde in methanol was added dropwise. The white precipitate of the product formed immediately. The precipitate was filtered off and dried. Yield 0.434 g (49%), m.p. 165°C (decomp.). IR (KBr,): ν=2922-2853 (C-H), 2487 (B-H), 1739 (C=O), 1651 (-N-C=O), 1175 cm^{-1} (C-O). ^{1}H NMR (200MHz, $[D_3]CD_3CN$, 25°C, TMS): δ=0.85 (t, J(H,H)=3.2 Hz, 6H, $C\underline{H}_3$-CH_2-), 1.25 (s, 40H, CH_3-$(C\underline{H}_2)_{10}$-CH_2-), 1.44-1.61 (m, 4H, -CO-CH_2-$C\underline{H}_2$-), 2.21-2.37 (m, 4H, -

CO-C$\underline{H}_2$-), 3.11 (s, 24H, (C$\underline{H}_3$)$_4$N), 3.16 (s, 2H, S-C$\underline{H}_2$-CO), 3.38-3.62 (m, 4H, -O-C$\underline{H}_2$-), 4.10-4.27 (m, 4H, -N-C$\underline{H}_2$-), 0.2-2.3 ppm (m, 11H, B-$\underline{H}$). ^{11}B NMR (200MHz, [D$_6$]DMSO, 25°C): δ=-8.70 (1B), -13.23 (5B), -15.31 (5B), -18.80 ppm (1B). ^{13}C NMR (400MHz, [D$_3$]CD$_3$CN, 25°C, TMS): δ=174.16, 64.18, 62.39, 56.25, 56.19, 56.13, 48.80, 46.24, 36.25, 34.72, 34.66, 32.59, 30.31, 30.17, 30.03, 29.77, 27.59, 23.32, 14.33ppm. MS (ESI, acetonitrile, m/z): negative 738 [A^--H^-+H^+]$^-$; positive 74 [Kat]$^+$, 963 [A^{2-}+3Kat$^+$]$^+$.

Method B: To a solution of **9** (0.331 g 0.7 mmol) in dry CH$_3$CN (30 mL), a 60% suspension of NaH in mineral oil (0.051 g, 1.8 mmol) was added. The mixture was stirred under N$_2$ for 30 min at RT, then for 30 min at 70°C, and cooled to 25°C. To the stirred mixture, myristoyl chloride (0.493 g, 2.0 mmol) was added dropwise at RT, and stirred for 24 h. The solvent was evaporated. The remaining oil was crystallized from 2-3 mL acetone. Yield 0.48 g (76%).

S-(2-Cyanoethyl)-S-(N,N-(2-dipalmitoyloxyethyl)-acetamido)-sulfonioundecahydro-*closo*-dodecaborate (1-) tetramethylammonium salt (5b). Similar to **5a**. Yield 0.554 g (60%). IR (KBr): ν=2935-2887 (C-H), 2491 (B-H), 1732 (C=O), 1651 (-N-C=O), 1175 cm^{-1} (C-O). ^{1}H NMR (200MHz, [D$_3$]CD$_3$CN, 25°C, TMS): δ=0.88 (t, J(H,H)=3.1 Hz, 6H, C$\underline{H}_3$-CH$_2$-), 1.27 (s, 48H, CH$_3$-(C$\underline{H}_2$)$_{12}$-CH$_2$-), 1.45-1.62 (m, 4H, -CO-CH$_2$-C$\underline{H}_2$-), 2.23-2.35 (m, 4H, -CO-C$\underline{H}_2$-), 2.93-3.04 (m, 2H -S-C$\underline{H}_2$-), 3.07 (s, 12H, (C$\underline{H}_3$)$_4$N), 3.22-3.36 (m, 2H, -C$\underline{H}_2$-CN), 3.57-3.63 (m, 4H, -O-C$\underline{H}_2$-), 4.12-4.20 (m, 4H, -N-C$\underline{H}_2$-), 4.25 (s, 2H, S-C$\underline{H}_2$-CO), 0.1-2.3 ppm (m, 11H, B-$\underline{H}$). ^{11}B NMR (200MHz, [D$_6$]DMSO, 25°C): δ=-5.86 (1B), -14.56 ppm (11B). MS (ESI, acetonitrile, m/z): negative 850 [A]$^-$; positive 74 [Kat]$^+$.

S-(N,N-(2-Dipalmitoyloxyethyl)-acetamido)-thioundecahydro-*closo*-dodecaborate (2-) ditetramethylammonium salt (B-6-16) Similar to **B-6-14**, Method A. Yield 0.518 g (55%), m.p. 179°C (decomp). IR (KBr): ν=2935-2867 (C-H), 2487 (B-H), 1732 (C=O), 1651 (-N-C=O), 1175 cm^{-1} (C-O). ^{1}H NMR (200MHz, [D$_3$]CD$_3$CN, 25°C, TMS): δ=0.88 (t, J(H,H)=3.1 Hz, 6H, C$\underline{H}_3$-CH$_2$-), 1.27 (s, 48H, CH$_3$-(C$\underline{H}_2$)$_{12}$-CH$_2$-), 1.47-1.63 (m, 4H, -CO-CH$_2$-C$\underline{H}_2$-), 2.23-2.33 (m, 4H, -CO-C$\underline{H}_2$-), 3.10 (s, 24H, (C$\underline{H}_3$)$_4$N), 3.16 (s, 2H, S-C$\underline{H}_2$-CO), 3.47 (t, J(H,H)=3.1Hz, 2H, -N-C$\underline{H}_2$-), 3.79 (t, J(H,H)=2.8Hz, 2H, -N-C$\underline{H}_2$-), 4.08 (t, J(H,H)=3.1, 2H, -O-C$\underline{H}_2$-), 4.22 (t, J(H,H)=2.8Hz, 2H, -O-C$\underline{H}_2$-), 0.2-2.3 ppm (m, 11H, B-$\underline{H}$). ^{11}B NMR (200MHz, [D$_6$]DMSO, 25°C): δ=-8.70 (1B), -13.23 (5B), -15.31 (5B), -18.80 ppm (1B). ^{13}C NMR (400MHz, [D$_3$]CD$_3$CN, 25°C, TMS): δ=174.60, 166.63, 64.63, 62.80, 56.57, 56.51, 49.20, 46.69, 36.68, 35.15, 35.06, 33.03, 30.78, 30.63, 30.48, 30.21, 26.02, 23.77, 14.78ppm. MS (ESI, acetonitrile, m/z): negative 796 [A^{2-}-H^-+H^+]$^-$; positive 74 [Kat]$^+$.

N,N-Bis-(2-trimethylsilyloxyethyl)-2-chloracetamide (8). A mixture of N,N-Bis-(2-trimethylsilyloxyethyl)amine **7** (23.23 g, 0.093 mol) (prepared by reacting diethanolamine with 1 eq of bis(trimethylsilyl)disilazan without solvent) and triethylamine (13.0 mL 0.093 mol) in THF (125 mL) was added dropwise to a solution of chloroacetylchloride (7.42 mL, 0.093 mol) in THF (60 mL) at –20°C. The precipitated (triethylammonium chloride) was removed by filtration and the solvent was evaporated. The remaining oil was distilled in vacuo at 1.4·10^{-2} mbar (130-131°C). Yield 28.5 g (94%). IR (KBr): ν=2959-2875 (C-H), 1651 (C=O), 655 cm^{-1} (C-Cl). ^{1}H NMR (200MHz, [D$_1$]CDCl$_3$, 25°C, TMS): δ=0.087 (s, 18H, C$\underline{H}_3$-Si-), 3.43 (t, J(H,H)=2.9 Hz, 2H, N-C$\underline{H}_2$), 3.52 (t, J(H,H)=2.9 Hz 2H, N-C$\underline{H}_2$-), 3.57-3.73 (m, 4H, -O-C$\underline{H}_2$-), 4.21ppm (s, 2H, Cl-C$\underline{H}_2$-CO-). MS (70eV, EI): m/z: 325 [M].

S-(N,N-(2-Diethanol)-acetamido)-thioundecahydro-*closo*-dodecaborat (2-) ditetramethylammonium salt (9). 10 (1.87 g 5.0 mmol) and **8** (2.44 g 7.5 mmol) were stirred in CH_3CN (40 mL) at RT and then heated to 70°C for 2 hours. The mixture was cooled, and tetramethylammonium chloride was removed by filtration. The solvent was evaporated. The residue was dissolved in acetone and treated with 1 eq of a 25% solution of tetramethylammonium hydroxide in MeOH. The precipitate of **9** formed immediately, was removed by filtration and dried. Yield 1.5 g (65%). IR (KBr): ν=3400 (O-H), 3036-2875 (C-H), 2484 (B-H), 1622 cm^{-1} (C=O). ^{1}H NMR (200MHz, [d_6]DMSO, 25°C, TMS): δ=2.99 ppm (s, 2H, S-CH_2-), 3.08 (s, 24H, (CH_3)$_4$N), 3.19-3.32 (m, 2H, -N-CH_2-), 3.33-3.44 (m, 2H, -N-CH_2-), 3.45-3.57 (m, 4H, -O-CH_2-), 4.50-4.90 (m, 2H, -CH_2-OH), 0.2-2.3 ppm (m, 11H, B-H). ^{11}B NMR (200MHz, [d_6]DMSO-d_6, 25°C): δ= -8.70 (1B), -13.23 (5B), -15.31 (5B), -18.80 ppm (1B). MS (ESI, acetonitrile, m/z): negative 160 $[A]^{2-}$; positive 74 $[Kat]^+$, 542 $[A^{2-}+3Kat^+]^+$.

Preparation of liposomes

Each lipid mixture was dissolved in a mixture of acetonitrile and chloroform (2:1). The solution was dried to a thin film in a round-bottom flask. The dried lipid film was then hydrated and dispersed by vortexing in 10 mM HEPES buffer saline, pH 7.4 (150 mM NaCl, 10 mM HEPES buffer) to achieve a lipid concentration of 10 mg/ml. The resulting suspension was subjected to 10 cycles of freezing and thawing, then extruded through a polycarbonate membrane with a pore diameter of 100 nm (Avestin, Mannheim, Germany) at a temperature of 50°C.

For preparation of liposomes in the absence of helper lipids, 20 mg of lipid were dissolved in acetonitrile and dried to a film. The film was then hydrated with 4 ml of 10 mM HEPES buffer saline, pH 7.4. The lipid suspension was subjected to 10 freeze-thaw cycles, and then extruded as described previously.

Lipid contents was measured by the Stewart assay,[37] using appropriate standard curves for the individual lipids.

cryo-TEM

The liposomal suspension was applied to a polymer-coated grid either at room temperature or (in the case of Fig. 5a) at 30°C. The sample was shock-frozen in liquid ethane. The vitrified sample was mounted and examined in a Zeiss EM 902 A electron microscope, operating at an accelerating voltage of 80 keV in filtered bright field image mode at ΔE = 0 eV. The stage temperature was kept below 108 K and images were recorded at defocus settings between 1 and 3 µm. A large number of areas were examined in order to ensure the reproducibility of the results.[38]

Zeta potential and size measurements

Zeta potential and size were measured at 25°C using Malvern Zetasizer Nano ZS, Malvern Instruments Ltd., Malvern, U.K. The liposomes were diluted to a concentration of about 1 mg lipid per mL with 1mM HEPES buffer (pH 7.4). For zeta potential measurements 15 individual determinations were averaged. For size measurements 10 individual determinations were averaged.

Differential scanning calorimetry measurements

DSC measurements were carried out on a VP-DSC microcalorimeter from Microcal (Northampton, MA, USA), using a lipid concentration of 5 mM. Samples were degassed under vacuum prior to the measurements. The upscans and downscans were recorded at a temperature range between 10 and 60°C, a scan rate of 90°C/h, and a filtering period of 2 s. A background scan collected with buffer in both cells was subtracted from each scan. For data analysis the software package ORIGIN (Microcal) was used.

Acknowledgment

E.J. acknowledges the support of Otto Benecke Stiftung. We are grateful for a gift of lipids from Lipoid GmbH, Ludwigshafen, Germany. K.E. gratefully acknowledges financial support from the Swedish Research Council and the Swedish Cancer Society.

References

[1] R. F. Barth, A. H. Soloway, R. G. Fairchild, *Cancer Res.* **1990,** *50,* 1061-1070.

[2] R. F. Barth, A. H. Soloway, R. G. Fairchild, R. M. Brugger, *Cancer* **1992,** *70,* 2995-3008.

[3] A. H. Soloway, H. Hatanaka, M. S. Davis, *J. Med. Chem.* **1967**, *10*, 714-717.

[4] F. Alam, R. F. Barth, A. H. Soloway, *Antibody, Immunoconjugates and Radiopharmaceuticals* **1989,** *2,* 145-163.

[5] R. F. Schinazi, W. H. Prusoff, *Tetrahedron Lett.* **1978,** *50,* 4981-4984.

[6] R. G. Fairchild, S. B. Kahl, B. H. Laster, J. Kalef-Ezra, E. A. Popenoe, *Cancer Res.* **1990,** *50,* 4860-4865.

[7] M. Miura, D. Gabel, R. G. Fairchild, B. H. Laster, L. S. Warkentien, *Strahlenther. Onkol.* **1989,** *165,* 131.

[8] S. B. Kahl, B. H. Laster, M.-S. Kood, L. S. Warkentien, R. G. Fairchild, in *Clinical Aspects of Neutron Capture Therapy*, (Eds. R. G. Fairchild, V. P. Bond, A. D. Woodhead) **1989**, pp. 205-211.

[9] A. P. Pathak, D. Artemov, B. D. Ward, D. G. Jackson, M. Neeman, Z. M. Bhujwalla, *Cancer Res.* **2005,** *65,* 1425-32.

[10] M. R. Dreher, W. Liu, C. R. Michelich, M. W. Dewhirst, F. Yuan, A. Chilkoti, *J. Natl. Cancer Inst.* **2006,** *98,* 335-44.

[11] F. M. Muggia, *Clin. Cancer Res.* **1999,** *5,* 7-8.

[12] M. Johnsson, N. Bergstrand, K. Edwards, *J. Liposome Res.* **1999,** *9,* 53-79.

[13] K. Shelly, D. A. Feakes, M. F. Hawthorne, P. G. Schmidt, T. A. Krisch, W. F. Bauer, *Proc. Natl. Acad. Sci. U. S. A.* **1992,** *89,* 9039-9043.

[14] D. A. Feakes, K. Shelly, C. B. Knobler, M. F. Hawthorne, *Proc. Natl. Acad. Sci. U. S. A.* **1994,** *91,* 3029-3033.

[15] D. A. Feakes, K. Shelly, M. F. Hawthorne, *Proc. Natl. Acad. Sci. U. S. A.* **1995,** *92,* 1367-1370.

[16] N. Bergstrand, E. Bohl, J. Carlsson, K. Edwards, H. Ghaneolhosseini, L. Gedda, M. Johnsson, M. Silvander, S. Sjöberg, in *Contemporary Boron Chemistry*, (Eds. M. Davidson, A. K. Hughes, T. B. Marder, K. Wade), **2000**, pp. 131-134

[17] M. F. Hawthorne, K. Shelly, *J. Neuro-Oncol.* **1997,** *33,* 53-58.

[18] S. C. Mehta, J. C. Lai, D. R. Lu, *J. Microencapsul.* **1996,** *13,* 269-79.

[19] K. Maruyama, O. Ishida, S. Kasaoka, T. Takizawa, N. Utoguchi, A. Shinohara, M. Chiba, H. Kobayashi, M. Eriguchi, H. Yanagie, *J. Control. Rel.* **2004,** *98,* 195-207.

[20] V. P. Torchilin, V. Weissig, *Liposomes, Second Edition*, Oxford University Press, Oxford, UK **2003**, p. 64.

[21] H. Nakamura, Y. Miyajima, T. Takei, S. Kasaoka, K. Maruyama, *Chem. Commun.* **2004,** 1910-1.

[22] S. Rossi, G. Karlsson, G. Martini, K. Edwards, *Langmuir* **2003,** *19,* 5608-5617.

[23] R. A. Watson-Clark, M. L. Banquerigo, K. Shelly, M. F. Hawthorne, E. Brahn, *Proc. Natl. Acad. Sci. U. S. A.* **1998,** *95,* 2531-2534.

[24] T. Li, J. Hamdi, M. F. Hawthorne, *Bioconjug. Chem.* **2006,** *17,* 15-20.

[25] M. F. Hawthorne, *Angewandte Chem. Intern. Ed.* **1993,** *32,* 950-984.

[26] A. H. Soloway, H. Hatanaka, M. S. Davis, *J. Med. Chem.* **1967,** *10,* 714-717.

[27] D. Gabel, D. Preusse, D. Haritz, F. Grochulla, K. Haselsberger, H. Fankhauser, C. Ceberg, H.-D. Peters, U. Klotz, *Acta Neurochir.* **1997,** *139,* 606-612.

[28] M. R. Almofti, H. Harashima, Y. Shinohara, A. Almofti, Y. Baba, H. Kiwada, *Arch. Biochem. Biophys.* **2003,** *410,* 246-53.

[29] J. R. Trowbridge, R. A. Falk, I. J. Krems, *J. Org. Chem.* **1955,** *20,* 990-995.

[30] D. Gabel, D. Moller, S. Harfst, J. Rösler, H. Ketz, *Inorg. Chem.* **1993,** *32,* 2276-2278.

[31] J. F. Nagle, S. Tristram-Nagle, *Biochim. Biophys. Acta* **2000,** *1469*, 159-95.

[32] J. Z. Lu, Y. H. Hao, J. W. Chen, *J. Biochem. (Tokyo)* **2001,** *129,* 891-8.

[33] J. L. Lippert, W. L. Peticolas, *Proc. Natl. Acad. Sci. U. S. A.* **1971,** *68,* 1572-6 .

[34] Y. A. Azev, E. Lork, T. Duelcks, D. Gabel, *Tetrahedron Lett.* **2004,** *45,* 3249-3252.

[35] K. Edwards, M. Johnsson, G. Karlsson, M. Silvander, *Biophys. J.* **1997,** *73,* 258-66.

[36] O. Ishida, K. Maruyama, H. Tanahashi, M. Iwatsuru, K. Sasaki, M. Eriguchi, H. Yanagie, *Pharm. Res.* **2001,** *18,* 1042-8.

[37] J. C. Stewart, *Anal. Biochem.* **1980,** *104,* 10-4.

[38] M. Almgren, K. Edwards, G. Karlsson, *Colloids Surf A Physicochem. Engin. Asp.* **2000,** *174,* 3-21.

Keywords

Lipids, liposomes, boranes, neutron capture therapy

Graphical abstract

Liposomes from new boron-containing lipids have great potential in boron neutron capture therapy

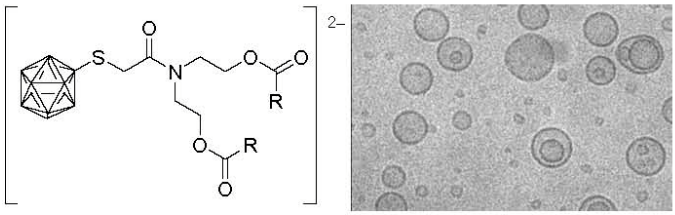

Declaration

The work described in this thesis is my own work, unless otherwise stated or mentioned in the references. The thesis was written by myself and nobody else.

_____

Doaa Elsayed Mohammed Osman Awad

Bremen, the 4th of October